

Received May 3, 2022, accepted May 29, 2022, date of publication June 1, 2022, date of current version June 9, 2022.

Digital Object Identifier 10.1109/ACCESS.2022.3179589

Soft Pneumatic Actuators: A Review of Design, Fabrication, Modeling, Sensing, Control and Applications

MATHEUS S. XAVIER^{1,2,5}, (Graduate Student Member, IEEE), CHARBEL D. TAWK³,
ALI ZOLFAGHARIAN⁴, JOSHUA PINSKIER⁵, (Member, IEEE),
DAVID HOWARD⁵, (Member, IEEE), TAYLOR YOUNG¹, (Student Member, IEEE),
JIEWEN LAI⁶, (Graduate Student Member, IEEE), SIMON M. HARRISON^{5,7},
YUEN K. YONG¹, (Member, IEEE), MAHDI BODAGHI⁸,
AND ANDREW J. FLEMING¹, (Member, IEEE)

¹Precision Mechatronics Laboratory, School of Engineering, The University of Newcastle, Callaghan, NSW 2308, Australia

²Department of Electrical and Electronic Engineering, The University of Melbourne, Melbourne, VIC 3010, Australia

³Faculty of Engineering and Computer Science, University of Wollongong in Dubai, Dubai, United Arab Emirates

⁴School of Engineering, Deakin University, Geelong, VIC 3217, Australia

⁵Data61, CSIRO, Pullenvale, QLD 4069, Australia

⁶Department of Mechanical Engineering, The Hong Kong Polytechnic University, Hong Kong

⁷Data61, CSIRO, Clayton, VIC 3168, Australia

⁸Department of Engineering, School of Science and Technology, Nottingham Trent University, Nottingham NG11 8NS, U.K.

Corresponding authors: Matheus S. Xavier (matheus.xavier@uon.edu.au) and Charbel D. Tawk (charbeltawk@uowdubai.ac.ae)

ABSTRACT Soft robotics is a rapidly evolving field where robots are fabricated using highly deformable materials and usually follow a bioinspired design. Their high dexterity and safety make them ideal for applications such as gripping, locomotion, and biomedical devices, where the environment is highly dynamic and sensitive to physical interaction. Pneumatic actuation remains the dominant technology in soft robotics due to its low cost and mass, fast response time, and easy implementation. Given the significant number of publications in soft robotics over recent years, newcomers and even established researchers may have difficulty assessing the state of the art. To address this issue, this article summarizes the development of soft pneumatic actuators and robots up until the The scope of this article includes the design, modeling, fabrication, actuation, characterization, sensing, control, and applications of soft robotic devices. In addition to a historical overview, there is a special emphasis on recent advances such as novel designs, differential simulators, analytical and numerical modeling methods, topology optimization, data-driven modeling and control methods, hardware control boards, and nonlinear estimation and control techniques. Finally, the capabilities and limitations of soft pneumatic actuators and robots are discussed and directions for future research are identified.

INDEX TERMS Soft robotics, soft pneumatic actuator, design, modeling, sensing, control.

I. INTRODUCTION

Conventional robots are constructed from rigid links connected through joints with a single degree of freedom (DoF) and have been employed in industrial applications with excellent speed and accuracy [1], [2]. However, these robots have limited dexterity and are not effective in unstructured or constrained workspaces [3], [4] as these may require a level of versatility that is difficult to achieve using hard materials [5]. In contrast, soft robots are made of highly deformable

The associate editor coordinating the review of this manuscript and approving it for publication was Guilin Yang¹.

materials and are generally characterized by high dexterity and safety; therefore, they are ideal for applications where the environment is highly dynamic, sensitive to physical interaction, or constrained with restricted access [6], [7]. Soft robots usually follow a bioinspired design [8], [9], including snakes [10]–[13], worms [14], [15], fish [16]–[19], manta rays [20], [21] and tentacles [22]–[24].

A comparison of the main actuation modes used in soft robotics is provided in Table 1, where a relative comparison of features from each of these modes is presented. For fluid-driven actuation, gas or liquid is used to control the chamber deformation [25]–[27]. For cable-driven actuation,

TABLE 1. Comparison of popular actuation methods for soft robots. Legend: ★★★ easy/high, ★★ average/medium, and ★ difficult/low.

Actuation	Displacement/Force	Speed	Fabrication	Sensing	Control	Efficiency	Miniaturization	Biocompatibility	Applications
Pneumatic	★★★	★★★	★★★	★★	★★	★	★★	★★	★★★
Hydraulic	★★★	★★★	★★★	★★	★★★	★	★★	★★★	★★
Cable-driven	★★★	★★★	★★	★★	★★	★★	★	★★	★★
EAP	★	★★★	★★	★★★	★★	★★★	★★★	★★	★
SMM	★	★★	★★	★★★	★★★	★★	★★★	★★	★
Electromagnetic	★★	★★★	★★	★★★	★★★	★★★	★★★	★★★	★★
TCA	★★	★	★★	★★★	★★★	★★	★★★	★★	★

pull and release cables embedded in the soft actuator are used to control the deformation [28]–[30]. For shape-memory materials (SMM), temperature changes are used to control phase change and deformation [31], [32]. For electroactive polymers (EAP), such as dielectric elastomers, an electric potential is applied between two electrodes to deform a soft dielectric [33], [34]. For twisted-and-coiled actuators (TCA), motion is achieved with temperature changes due to thermal expansion and their spring-like structures [35]–[37]. For further details on soft robotic actuation technologies, including their respective advantages and limitations, the reader is referred to [38]–[42].

Pneumatic actuation remains the dominant technology in soft robotics due to its light weight, fast response time, and easy implementation [38], [43], [44]. In addition, pneumatic systems can be developed using low-cost components such as diaphragm pumps and on/off solenoid valves [45]–[47]. Pneumatic soft robots offer high dexterity and safety, large deformations, good power-to-weight ratio and low manufacturing cost [43], [48]. These soft robots are fabricated from Soft Pneumatic Actuators (SPAs), including pneumatic network and fiber-reinforced actuators [27]. SPAs can be actuated using positive or negative pressures. Negative pressure actuation provides a fail-safe feature, improved lifetime, and durability. Vacuum actuators are suitable for constrained volume applications since they shrink under actuation [39], [43]. In addition, the performance of SPAs can be improved using a combination of both positive and negative pressure [49], [50].

Soft pneumatic actuators exhibit a variety of motions, such as bending, extension, contraction, and twisting [25], [26], [51]. They can be fabricated using a molding process [52], [53] or directly 3D-printed using flexible filaments or elastomeric resins [54], [55]. Pneumatic soft robots are used in applications such as minimally invasive surgery [56], [57], rehabilitation [58], [59], elderly assistance [60], safe human-robot interaction [61], [62] and handling of fragile materials [63], [64]. Despite recent breakthroughs, soft pneumatic actuators and robots experience challenges and limitations related to autonomy, portability, scalability, noise, repeatability, reproducibility, durability, accessibility, impact, complex modeling, integrated sensing and intelligent control.

A significant number of review papers have been published in the last five years due to the rapid advancement of soft robotics. While these papers cover specific aspects of soft robotics, they are not tailored to pneumatic-driven soft robots.

A list of review articles focusing on fluid-driven soft robots is presented in Table 2. The design, fabrication, and control of soft pneumatic actuators and robots are reviewed in [25], [26], [68]. However, these articles only address actuation with positive pressure. On the other hand, [27], [65] have focused on material characterization and modeling of soft fluidic actuators, while [43], [67] only address 3D/4D-printed SPAs.

Considering the large number of recent publications on pneumatic-driven soft robotics, newcomers and even established researchers have difficulty assessing the state of the art. This article provides readers with a comprehensive overview of pneumatic soft robots with a holistic approach covering all aspects from design, modeling, fabrication, actuation, characterization, sensing, control and applications. Moreover, this review includes recent developments in pneumatic-driven soft robotics such as

- novel soft pneumatic actuator designs,
- novel simulators, such as DiffAqua, SoMo, Sorotoki, ChainQueen, Elastica, SoRoSim,
- recent analytical, numerical, and data-driven modeling developments, such as dynamic/transient FEM and FSI for soft actuators,
- evolutionary design and reality gap,
- pneumatic hardware control boards for soft robotics, such as FlowIO, PneuSoRD, ProgrammableAir, Pneuduino, and pneumatic parameter analysis and selection,
- low and high-level model-based nonlinear controllers, nonlinear estimation, observer-based nonlinear controllers, and energy-based modeling and control.

The remainder of this article is organized as follows. Section II introduces the various soft pneumatic actuator designs with a classification based on their motion types. Fabrication methods for these actuators using molding procedures and direct 3D-printing are presented in Section III. Section IV discusses the analytical and numerical modeling of SPAs. This section also includes a discussion on computational design and topology optimization. Section V deals with pneumatic systems used for actuation, including parameter analysis and selection, novel pneumatic control boards, stiffening mechanisms, and untethered actuation. Section VI describes the proprioceptive and exteroceptive sensing technologies available for soft robots. Control methods used for SPAs, such as model-based and data-driven controllers are discussed in Section VII. Section VIII reviews

TABLE 2. Recent review articles on fluid-driven soft robots.

Year	Design	Modeling		Fabrication		Energy Sources	Sensing	Control	Applications	Ref.
		Analytical	Simulation	Molding	3D-Printing					
2021	✓	✓	✓	✓						[27]
2021	✓	✓	✓	✓	✓		✓			[65]
2021	✓		✓		✓		✓		✓	[43]
2021	✓			✓	✓		✓	✓	✓	[66]
2020	✓	✓	✓		✓		✓	✓		[67]
2020	✓	✓	✓	✓	✓		✓	✓	✓	[68]
2017	✓	✓	✓	✓	✓			✓	✓	[25]
2017	✓	✓	✓	✓	✓	✓	✓	✓	✓	[26]

the main applications for SPAs in the literature. Section IX discusses the capabilities and limitations of pneumatic-driven soft robots and identifies directions for future research. Finally, Section X concludes this article.

II. SOFT ACTUATOR DESIGNS

Using specifically-engineered anisotropic structures, soft actuators can be made to display four different types of motion: extension, contraction, bending, and twisting [25], [26]. The two most popular categories of SPAs are the fiber-reinforced and pneumatic network (PneuNet) actuators, which are discussed below for each motion category. We also present a range of unconventional and novel designs for SPAs, as shown in Fig. 1.

A. EXTENDING AND CONTRACTION ACTUATORS

Pneumatic artificial muscles, also known as McKibben actuators [66], [69], [70], were one of the first soft pneumatic actuators. They are made of a flexible inner tube covered with a helical braided shell [71]. On pressurization, the muscle is inflated to generate a contractile force between the two ends [72]. More recent designs for planar fluidic muscles include Peano muscles or pouch motors, which provide capabilities similar to McKibben actuators but in a slimmer form [73], [74].

Symmetrical single chamber actuators can be used to achieve extension motion. Fibers are wrapped around the chamber to prevent the ballooning effect [75] and high radial expansion [76]–[78]. Inspired by the McKibben actuators, fiber reinforcements with a double helical wrapping restrict the ballooning effect in soft actuators and increase stroke [45] (Fig. 1a-2). With single fiber wrapping, maximum axial extension occurs for fiber angles at 0° , while maximum radial expansion with no axial extension occurs for wrapping at 90° . Fiber-reinforced actuators show enhanced extension, require lower amounts of input flow, and minimize the energy lost in radial expansion of the rubber [76], [79], [80]. Dense reinforcements generally require higher input air pressure [76] but also improve linearity, reliability, and durability [76], [81]. A circular cross-section is recommended for extending actuators as this improves linearity and reduces wear [81].

Extension and contraction can also be achieved using a structure with bellow chambers, which has a high radial stiffness and confines ballooning effects [82]. Linear bellow actuators can be obtained off-the-shelf [83], using 3D-printing [84], [85] or silicone molding techniques [86]. A 3D-printed linear soft vacuum actuator with a 6.49 Hz bandwidth, 27 N output force, and 21500 cycle lifetime was described in [87]. A vacuum SPA with an inextendable tubular membrane over a series of ring-like (annular) reinforcing elements is described in [88]. Vacuum linear SPAs can also be created using reversible buckling in assemblies of elastomeric beams [89] or origami-inspired structures [90], [91].

Other novel designs include: (i) a scissor-mechanism-based artificial muscle described in [92] (Fig. 1a-5), which has a blocked force of 300 N, contraction ratio of 80% under negative pressure, and 40000 cycle lifetime. (ii) a 3D-printed origami vacuum-driven pneumatic artificial muscle with low vacuum pressure requirements, 62% contraction ratio and capability to lift 200 times its self-weight [93]. (iii) a 3D-printed extension actuator with expandable pouches that can achieve an extension ratio up to 600% [94]. (iv) pneumatic actuators with contractile units arranged in parallel in a flexible matrix inspired by ultrasonic measurements on skeletal muscle [95] (Fig. 1a-3).

B. BENDING ACTUATORS

Bending actuators are typically based on an asymmetric geometry such as (i) an inflatable void, (ii) multi-material fabrication, or (iii) corrugated membrane [25]. In (i), the inflatable void is placed off center, which creates layers of differing thickness [109]. Bending is maximized when one of the layers is two to three times thicker than the other [25], [52], [109]. Optimal force is obtained when the ratio of length to width of the inflatable void is approximately 10 [25]. In multi-material fabrication (ii), the actuator utilizes different rubber compositions; for example, a silicone rubber with high stiffness is used for the bottom layer of the actuator. This bottom layer may also have a larger thickness or a strain limiting layer [110]. The third technique is the multi-chambered or PneuNet actuator, whereby folds (fins) on one side of the actuators expand under pressure generating bending. PneuNet bending actuators are one of the most

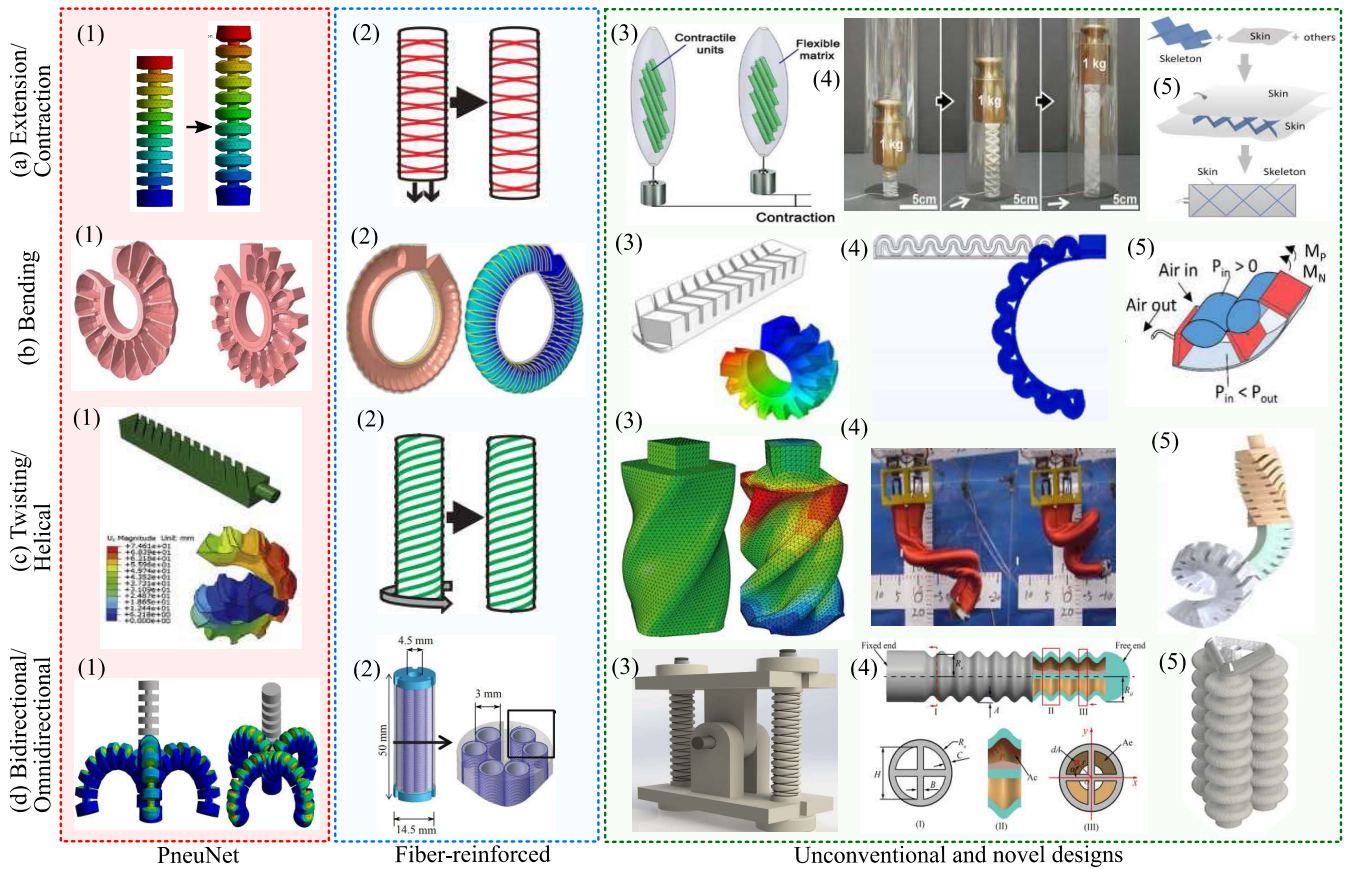


FIGURE 1. Soft pneumatic actuator designs. (a) Extension and contraction SPAs: (1) [47], (2) [96], (3) [95], (4) [97] and (5) [92]. (b) Bending SPAs: (1) [98], (2) [78], (3) [99], (4) [100] and (5) [101]. (c) Twisting and helical SPAs: (1) [102], (2) [96], (3) [103], (4) [104] and (5) [105]. (d) Bidirectional and Omnidirectional SPAs: (1) [47], (2) [106], (3) [107], (4) [108] and (5) [49]. All figures are reproduced with permission.

investigated designs in the literature [58], [98], [111], which consist of an elastic top layer and a bottom layer which is free to bend but not extend. Slow PneuNets use a block of silicone rubber with embedded air chambers [110], [111], while the fast PneuNets contain gaps between the inside walls of each chamber [98] (Fig. 1b-1).

The most significant factors affecting the bending angle of PneuNet actuators are the: bottom layer thickness, wall thickness, and gap size. In general, smaller gaps result in higher bending but may damage the channels [112]. For rapid actuation and low radial expansion, the internal walls should be thinner and have a larger surface area than the other exterior walls [58], [98]. For a fixed length, more chambers enable greater bending at lower pressures [98], [113], [114], and thicker chamber walls result in lower bending and lower output force [58], [98], [110], [114]. The force output can be increased by increasing the chamber height [58]. Another advantage of bending PneuNet actuators is that actuation can be achieved with positive, negative, or combined positive and negative pressures [43], [49].

Fiber-reinforcement techniques can also be used in bending actuators to limit the radial expansion and maximize performance [77], [81]. For pure bending motion,

double helical wrapping is usually added to the actuator (Fig. 1b-2). Fiber-reinforced bending actuators are usually achieved using a semi-circular cross-section with an additional strain limiting layer at the bottom of the actuator [78], [80], [115]. They are also referred to as PneuFlex actuators [64], [116], [117]. For these actuators, larger bending levels can be achieved with reduced wall thickness, or increased length or radius [78]. Furthermore, fiber-reinforced SPAs with a greater difference between braided angles on opposite sides provide higher bending angles and force at the same pressure level [118]. Combining fiber angles of 70° and 35° in a single actuator was shown to produce the highest bending angle in [119].

Novel actuator designs include: (i) free bottom pneumatic network actuators [114], where the outer sides of the actuator are bonded to the bottom layer, which results in approximately 20% greater bending and 40% higher force compared to conventional PneuNet actuators. (ii) high output force actuators fabricated using embedded core casting, which consist of an airbag reinforced by fiber layers (actuating core) and an elastic holder made of silicone rubber [120]. (iii) a soft bending actuator using combined positive and negative pressures to achieve blocked forces

up to 150 N [101] (Fig. 1b-5). (iv) a 3D-printed fold-based SPA with a sine-wave shape (Fig. 1b-4) and an internal channel across the entire length of the actuator [121], which provides 120° bending at 25 psi and lifts more than twice its own weight [100]. (v) PneuNet actuators with a herringbone chamber design (Fig. 1b-3) to facilitate simultaneous bending deformations in both longitudinal and transverse directions, which improves conformance in soft gripping [99].

C. HELICAL AND TWISTING ACTUATORS

Twisting and extending actuators can be obtained with a single fiber wrapping around a symmetrical single chamber (Fig. 1c-2), where a maximum twist is obtained for fiber angles around 30° [122]. Twisting and bending actuators can be obtained using one of the bending actuator designs discussed above with a single helical wrapping. Similar to pure bending actuators, this is commonly achieved using semi-circular actuators with a strain limiting layer.

Helical pneumatic network actuators can achieve programmable bending and twisting motions [102] by adjusting the chamber angles (Fig. 1c-1). More specifically, as the chamber angle increases, the bending decreases and twisting increases [102]. 3D-printed SPAs with helical motion have also been proposed [18], [123]. According to [123], the angular displacement increases with pressure and the inclination angle, while the internal radius of the helix decreases with both pressure and inclination angle. Increased chamber angle results in lower bending and higher twisting, while the length of the helical actuator only influences the number of loops that are created [18]. These actuators were also shown to have higher mechanical blocking force than other bending actuators in [18].

Novel designs include: (i) torsional SPAs developed by [103] (Fig. 1c-3), which achieve a torsion angle of 1.94 deg/mm and an output torque of 26 N·mm. (ii) a modular actuator system presented in [124], which is capable of multi-modal extension up to 70 mm, compression up to 24 mm, two-axis bending up to 115°, and twisting motion up to 240°. (iii) a tube-type pneumatic helical actuator inspired by the molecular structure of DNA (Fig. 1c-4), which consists of two helical contraction actuators arranged in parallel and covered by a sleeve [104]. (iv) bidirectional twisting actuators proposed in [125] by exploiting the free form surface of the actuator chamber, which allows a free rotation of 116.7° and blocking torque of 0.81 N·m. (v) pure twisting actuators with a PneuNet design, which were also combined with bending and helical actuators in the fabrication of multi-segment soft manipulators which can match complex 3D trajectories on pressurization [105] (Fig. 1c-5). (vi) a multi-modal helically-interlayered actuator composed of two pneumatic chambers coiling together into a tubular implant for tissue repair and regeneration of tubular tissues [126].

D. BIDIRECTIONAL AND OMNIDIRECTIONAL ACTUATORS

Bidirectional actuators [10]–[12], [127] are created using soft actuators with two chambers or by joining two bending

actuators via the bottom layer. Bidirectional actuators with a PneuNet design and sinusoidal bellows are discussed in [128] and [129], respectively.

Omnidirectional actuators were proposed in [130], [131] and further explored in [132]–[134]. The simpler omnidirectional actuator usually has three internal chambers. These actuators have three DoF, which are pitch, yaw, and stretch. When three chambers are actuated with the same pressure, the actuator stretches. In contrast, when only one or two chambers are actuated, the actuator bends in the opposite direction to the pressurized chambers. Actuators with three DoF can also be fabricated using three parallel, externally connected actuators rotated 120° about the longitudinal axis of the actuator in a design inspired by the parallel bellows actuators in pneumatic continuum robots [22], [61]. Parallel bellows actuators have been proposed in soft robotics using fiber-reinforced extending actuators [76], [135], [136], off-the-shelf rubber bellows [83], 3D-printed bellows actuators [49], [137] (Fig. 1d-5) and bellows fabricated with silicone rubber [86], [138]. For omnidirectional actuators, higher bending is achieved with lower wall thickness, greater length, greater chamber diameter, and lower central diameter [132], [139]. In addition, the bending ability of a triangular cross section is superior to that of a circular shape [139]. Chambers with semi-circular cross-sections have the least amount of ballooning, and chambers with a ring-sector cross-section show the highest bending [133].

Novel designs include: (i) omnidirectional actuators with four chambers in a multi-layer cavity series fabricated using a multi-step silicone molding process [140]. (ii) 3D-printed omnidirectional actuators with three or four chambers and a PneuNet-inspired design which can be actuated with both positive and negative pressure [50] (Fig. 1d-1). (iii) a 3D-printed planar SPA capable of a workspace 2.4 times larger than its initial length [141]. (iv) omnidirectional actuators with external cosine shape and four chambers (Fig. 1d-4), which can provide five working patterns with inflation of different chambers [108].

III. MATERIALS AND FABRICATION

A. MATERIALS

Silicone rubbers are the most commonly used materials for soft pneumatic actuators since they are highly flexible and can undergo large deformations during pressurization. Hyperelastic models are used to characterize their behavior in soft robotic applications. In general, silicone rubber is assumed to be isotropic and incompressible, while inelastic phenomena such as viscoelasticity and stress-softening are typically neglected [47]. The foremost hyperelastic models used in soft robotics are summarized in Table 3 and further details on these models are available in [154]–[157]. Each of these models has a corresponding strain energy function W , which is the amount of energy stored elastically in a unit volume of material under the state of stretch specified by the

TABLE 3. Stress-stretch equations for curve fitting with uniaxial tensile testing data.

Model	Deformation range	Strain energy density	Stress-stretch equation
Neo-Hookean	Low	$W = C_1(I_1 - 3) = \frac{\mu}{2}(I_1 - 3)$	$\sigma = 2(\lambda^2 - \lambda^{-1})C_1$
Mooney-Rivlin	Moderate	$W = C_1(I_1 - 3) + C_2(I_2 - 3)$	$\sigma = 2(\lambda^2 - \lambda^{-1})(C_1 + C_2\lambda^{-1})$
Generalized Rivlin	Large	$W = \sum_{i=0}^n \sum_{j=0}^n C_{ij}(I_1 - 3)^i(I_2 - 3)^j$	$\sigma = 2(\lambda^2 - \lambda^{-1})\{C_{10} + C_{01}\lambda^{-1} + C_{20}(\lambda^2 + 2\lambda^{-1} - 3) + 2C_{02}(2\lambda + \lambda^{-2} - 3) + 3C_{11}(\lambda - 1 - \lambda^{-1} + \lambda^{-2})\}$
Yeoh	Large	$W = C_1(I_1 - 3) + C_2(I_1 - 3)^2 + C_3(I_1 - 3)^3$	$\sigma = 2(\lambda^2 - \lambda^{-1})\sum_{i=1}^n iC_i(\lambda^2 + 2\lambda^{-1} - 3)^{i-1}$
Ogden	Large	$W = \sum_{n=1}^N \frac{\mu_n}{\alpha_n}(\lambda_1^{\alpha_n} + \lambda_2^{\alpha_n} + \lambda_3^{\alpha_n} - 3)$	$\sigma = \sum_{p=1}^n \mu_p(\lambda^{\alpha_p-1} - \lambda^{-(\alpha_p/2+1)})$

TABLE 4. Mechanical properties and hyperelastic model parameters for popular soft robotic materials.

Material	Shore Hardness	Elongation at break (%)	Model	Constants	Ref.
Silicone rubber					
Ecoflex 30	00-30	900	Yeoh	$C_1 = 12.7 \text{ kPa}, C_2 = 423 \text{ Pa}, C_3 = -1.46 \text{ Pa}$	[142], [143]
Ecoflex 50	00-50	980	Yeoh	$C_1 = 0.019, C_2 = 0.0009, C_3 = -4.75 \times 10^{-6} \text{ MPa}$	[142], [144], [145]
DragonSkin 10	10A	1000	Neo-Hookean	$C_1 = 0.0425 \text{ MPa}$	[96], [145], [146]
DragonSkin 30	30A	364	Ogden	$\mu_1 = 75.5 \text{ kPa}, \alpha_1 = 5.84$	[147], [148]
Elastosil M4601	28A	700	Yeoh	$C_1 = 0.11, C_2 = 0.02 \text{ MPa}$	[78], [98], [149], [150]
Smooth-Sil 950	50A	320	Neo-Hookean	$C_1 = 0.34 \text{ MPa}$	[96], [146]
3D-Printed					
NinjaFlex	85A	660	Generalized Rivlin	$C_{10} = -0.233, C_{01} = 2.562, C_{20} = 0.116$ $C_{11} = -0.561, C_{02} = 0.900 \text{ MPa}$	[50], [87], [151]
FilaFlex	82A	700	Generalized Rivlin	$C_{10} = 1.5941, C_{01} = 0.4393, C_{11} = -0.0044 \text{ MPa}$	[18]
Agilus30	30-35A	220-270	Generalized Rivlin	$C_{10} = -0.4889, C_{01} = 0.7147, C_{20} = 0.07929$ $C_{11} = -0.2704, C_{02} = 0.4709, D_1 = 0.4574 \text{ MPa}$	[152], [153]

principal stretches λ_1, λ_2 and λ_3 [154], [158], [159]. The stretch ratios λ_i represent the deformation of a differential cubic volume element along the principal axes of a Cartesian coordinate system [160], [161]. Using the principal stretches, the principal invariants are defined as

$$\begin{aligned} I_1 &= \lambda_1^2 + \lambda_2^2 + \lambda_3^2, \\ I_2 &= \lambda_1^2\lambda_2^2 + \lambda_2^2\lambda_3^2 + \lambda_1^2\lambda_3^2, \quad I_3 = \lambda_1^2\lambda_2^2\lambda_3^2 \end{aligned} \quad (1)$$

To account for the multiaxial stress states commonly experienced by soft actuators, uniaxial, biaxial and shear test data are recommended to determine hyperelastic parameters [154], [156]. However, due to the increased complexity of biaxial testing, most published research utilizes only uniaxial testing [162], [163], [163]. The ASTM D142 standard is recommended for uniaxial tensile testing of elastomers [164], [165]. Following tensile testing, the constitutive model parameters can be determined from curve fitting [155], [161], [165] using the stress-stretch equations in Table 3.

The most extensively used silicone rubbers in soft robotics include Ecoflex, DragonSkin, Elastosil M4601 and Smooth-Sil. 3D-printed soft actuators use materials such as NinjaFlex, FilaFlex, Agilus30, and TangoPlus. Ecoflex is softer than the other elastomers and results in high deformation at low pressure but lower blocked force. Mechanical properties and hyperelastic constants for selected silicone rubbers are summarized in Table 4. Comprehensive lists of materials and hyperelastic parameters are presented in [27], [65], [165].

B. MOLDED SOFT ACTUATORS

Soft pneumatic actuators are traditionally fabricated by 3D printing molds into which silicone rubbers are cast and consolidated [52], [53]. 3D printing allows the fabrication of high precision molds with complex features in a low number of manufacturing steps [54], [55]. Soft actuators fabricated with silicone rubber offer durability, biocompatibility, and high deformation at low pressure, especially with low hardness materials such as Ecoflex [80], [133], [135]. However, although low hardness materials provide high deformation, the force output is correspondingly low.

In the literature on soft fluidic actuators [52], [110], [113] and the examples provided in the Soft Robotics Toolkit [45], the following guidelines for fabrication can be deduced: (i) silicone rubber should be degassed to remove air bubbles, (ii) curing should be performed at room temperature. However, curing time can be shortened using an oven at approximately 60°C, (iii) fabricate 3D molds separately to minimize the use of support material and facilitate removal of the soft actuator from the molds, and (iv) employ mold release agent to facilitate removal of the soft actuator body from the mold.

C. 3D-PRINTED SOFT ACTUATORS

The molding process is time-consuming and requires significant manual assembly, which can create issues with weak seams, repeatability, and accuracy [166]. In addition, complex geometries often require multi-stage casts using techniques such as overmolding [167]. The final design

might also require the addition of strain limiting layers or fiber reinforcement, which requires significant operator skill [123]. Alternatively, soft actuators can be fabricated directly using additive manufacturing (AM) [168]. Additive manufacturing reduces manual process steps and is well suited to complex geometries and multi-component designs [166], [169].

Although silicone printing [166], [170]–[176], [176], [177] has been used in the fabrication of soft pneumatic actuators, the foremost 3D-printing techniques for direct fabrication of these actuators are [55], [67], [169]:

1) Material extrusion: heated material is selectively dispensed through a nozzle or orifice onto a surface, which then fuses into a solid object upon cooling. This includes fused deposition modeling (FDM), also known as fused filament fabrication (FFF), and direct ink writing (DIW). Using DIW, bending finger pneumatic actuators were developed in [175] and multi-material soft actuators with programmable contractile, expanding and twisting motions were reported in [173]. FDM is the most commonly used technique due to its accessibility and relatively low price [18]. The range of fabricated actuators include bending actuators [121], [168], [178]–[183], helical actuators [18], [121], [123] and vacuum-powered actuators [87], [184]. The materials include NinjaFlex [87], [121], [123], [178], [180], [184], Filaflex [168], eSUN eFlex [179] and Ultimaker TPU [185]. The printers include Prusa i3 MK3 [180], [182], FelixTec4 [183], Ultimaker 3 [181], Geetech Prusa Pro [178], LulzBot TAZ [121], [123] and Flashforge Inventor [87], [184].

2) Material jetting (Polyjet): droplets of material are selectively deposited then polymerized. Materials include TangoPlus, TangoBlackPlus, VeroClear, VeroWhitePlus and Agilus 30 [49], [84], [137], [186]. Modifications to a Stratasys Objet260 Connex printer were performed in [187] to fabricate actuators with solid and liquid components. A Stratasys Objet 350 Connex 3 was used to fabricate parallel bellow-shaped actuators in [49], [137]. This printer was also used in [186] to incorporate embedded resistive sensors into a fast PneuNet actuator. Polyjet bellows actuators with optimized fatigue life were fabricated in [84]. One-shot 3D printing of entire granular-jamming grippers and multi-material jamming-tendons have also been demonstrated using an Stratasys Objet 500 Connex 3 printer [188], [189].

3) Vat polymerization: liquid photopolymer in a vat is selectively cured by light-activated polymerization. This includes digital light processing (DLP) and stereolithography (SLA). The printing process takes place within a dense liquid bath, which reduces the requirement for support materials to print thin and hollow structures, and offers sub-micrometer resolution [190]. Micro soft pneumatic grippers with fast speed were fabricated in [191], [192] using DLP. In [193], micro-bellows actuators are developed for extension and bending using SLA with the SL5180 photopolymer. In [194], bidirectional actuators with a bellows structure were fabricated using a commercially available elastomeric precursor

and a custom-made SLA printer. Omnidirectional actuators with a PneuNet-inspired design are fabricated in [50] using a Form 3 (Formlabs) SLA printer with a commercial elastic resin.

IV. MODELING

A. STATIC MODELING

Many soft robots can be approximated by a series of mutually tangent constant curvature sections, i.e., piecewise constant curvature (PCC) [195]. This approximation is acceptable as the internal potential energy is uniformly distributed along each section, especially for fluid-driven soft robots [1]. This modeling method was initially applied to beam-like cable-driven continuum robots that undergo a constant moment along the length [2], [196]. The PCC assumption has also been validated using Hamilton's principle in [197]. As discussed in Webster and Jones [195], the kinematics of continuum robots can be separated into robot-specific and robot-independent components. The robot independent mapping can be obtained with arc geometry [2], [198], Denavit-Hartenberg parameters [199]–[201], differential geometry (Serret-Frenet frame) [2], [202], [203], integral representation [202], [204], [205], exponential coordinates [206] or a revolute joint placed at the center of the arc defining the trunk [23]. For the robot-specific transformation, most authors have described the transformation from actuator length to configuration space. This is because the length of cable-driven actuators can be measured using inexpensive and widely-available encoders at the output of motors [23], [207]. For parallel bellows actuators, the robot-specific transformation is described in [1], [195], [200]. For fluid-driven actuators, one must also account for the transformation from input pressure to actuator length or input pressure directly into configuration space. In the latter case, Suzumori *et al.* [130], [131] obtained the robot-specific transformation by linear analysis based on the theory of infinitesimal elastic deformation and the constant curvature assumption. An approach for the parallel bellows design has been described in [22], [137].

The piecewise constant curvature approach is practical when inertia effects are negligible [208]. However, the PCC assumption is affected by the actuator's weight and external loading [209]. Neppalli and Jones [23] have shown that the continuum robot is in good agreement with the PCC assumption when resting on the ground but failed to bend with a uniform curvature considering the effect of gravity. In addition, the classic PCC model does not consider the robot-environment interaction and any additional deformation to the robot geometry is likely to invalidate the kinematics. To solve this problem, Bajo *et al.* [210] proposed a modified PCC model with constrained kinematics for the detection and localization of contacts with the robot. The limitations of the PCC approach have led researchers to investigate real-time dynamics and geometrically exact non-constant curvature models using continuum mechanics. Mahl *et al.* [211] derived a variable curvature

kinematics model for multi-segment pneumatic continuum robots (Festo's Bionic Handling Assistant) with arbitrarily shaped backbone curves assembled from segments with bending and extension motion. The model describes the deformation of a single bendable segment with a finite number of serially connected circular arcs with constant curvature, which yields a section model with variable curvatures.

Aside from constant curvature methods and variations, polynomial curves can be used for the modeling. In [212], a variable curvature kinematic modeling method is presented for a 2D pneumatic soft actuator with the external payload being considered. The variable curvature model utilizes a discrete modeling approach called absolute nodal coordinate formulation [213], where a cubic polynomial is applied to represent the robot geometry being discretized by finite nodes. Singh *et al.* [214] modeled the variable curvature of the Festo's Bionic Handling Assistant using Pythagorean Hodograph curves, where the polynomial parametric curve is defined by five control points and can better fit the actual curve of the specific robot. Likewise, other curve modeling methods can be employed to mathematically represent the soft robot geometry in the robot-independent mapping, such as Bézier [215] and B-spline [216] curves. In [209], the authors propose an Euler spiral-based variable curvature method to kinematically model a long pneumatic-driven continuum robot made of McKibben actuators. The variable curvature model is also shown to outperform the conventional PCC model in [217], [218] in the context of predicting the static geometry of conic shape pneumatic grippers and long curving robots.

Most continuum robots have a slender structure where one dimension is much larger than the other two; hence, they can be modeled using the theory of Cosserat rods [207], [208]. Cosserat rod theory views the continuum arms as an infinite series of infinitesimal rigid bodies that can rotate independently from the rotations of their closest neighbors [219]. The first application of this theory in continuum robotics was presented in [220], where a geometrically exact model was introduced that accounts for the large deformations and loading using the Neo-Hookean model for the nonlinear elasticity and the Cosserat rod theory for the manipulator dynamics. This modeling approach was proven to be ten times more accurate than the constant curvature model when gravitational loading is considered. Jones *et al.* [207] used Cosserat rods to model the continuum robot as a curve in space shaped by shear, extension, and bending. The modeling consists of Hooke's law and force and moment balance equations, which achieved an average error of 0.61% between the measured and predicted tip position, while the PCC approach poorly fits the physical rod. These force and moment balance equations were also considered in [208] but the bending was modeled using the Euler-Bernoulli equation. Cosserat rods have also been applied to PneuNet actuators [221] and more recently to omnidirectional actuators [222], [223].

To account for the mass of the actuator and external loading, models have also been developed from the Euler-Bernoulli equation or Castigliano's method [25], [197], [224]. In Gorissen *et al.* [109], the thick layer of an actuator with an eccentric void is modeled with the Euler-Bernoulli equation, while the bending actuator is modeled as an ideal beam with a load at the tip in [25]. An omnidirectional actuator is modeled using the Euler-Bernoulli principle in [108]. In Drotman *et al.* [137], Castigliano's method is used to develop an analytical expression for the blocked force of a 3D-printed parallel bellows soft actuator.

B. DYNAMIC MODELING

For dynamic modeling of soft robots, Newton-Euler and Lagrange formulations [199], [225] can be used. These formulations were initially employed for tentacle manipulators with a uniformly distributed mass in [28], [203]–[205]. The Euler-Lagrange formalism has also been used to describe the dynamics of soft robotic manipulators in [226]–[228]. A dynamic model for fiber-reinforced bender actuators was derived in [229] using a Lagrangian approach, where the distributed mass effect is accounted for by the constant curvature assumption, and the silicone is described using an incompressible Neo-Hookean model. To reduce computational burden, Taylor series expansions are utilized to simplify the dynamical model by eliminating higher order terms. This approach has been adapted to bending PneuNet actuators [230], [231].

Dynamic models for SPAs can also be developed using an energy-based approach to derive lumped parameter models for fluid circuit components [232], [233]. In particular, pneumatic sources act as current sources, fluidic tubing and channels act as impedances and fluidic chambers act as capacitances [10], [234]. Relying on this electrical circuit equivalence, the dynamic behavior of a bending soft actuator can be approximated as a lumped second-order system [10], [235]. The constant model parameters can be determined by least-squares curve fitting [235], [236] or system identification with a periodic input signal [134], [237]. However, these model parameters vary with bending angle, which can be addressed using robust control techniques [237], [238] or nonlinear model parameters [239].

C. FINITE ELEMENT MODELING

Analytical modeling of soft actuators is challenging due to their complex geometries, strong material nonlinearities, and the compressibility of air [27], [151]. Recent articles involving the application of FEM in soft robotics have drawn the following conclusions [78], [133], [151], [240]: (1) FEM can cope with the large deformations associated with deformation and inflation, (2) FEM can predict the performance of soft actuator designs under various inputs, providing a rapid and efficient design strategy which reduces cost and development time, (3) FEM can improve our understanding of the stress concentration and strain distribution in soft actuators, which can be used to evaluate fatigue performance, and (4) FEM can

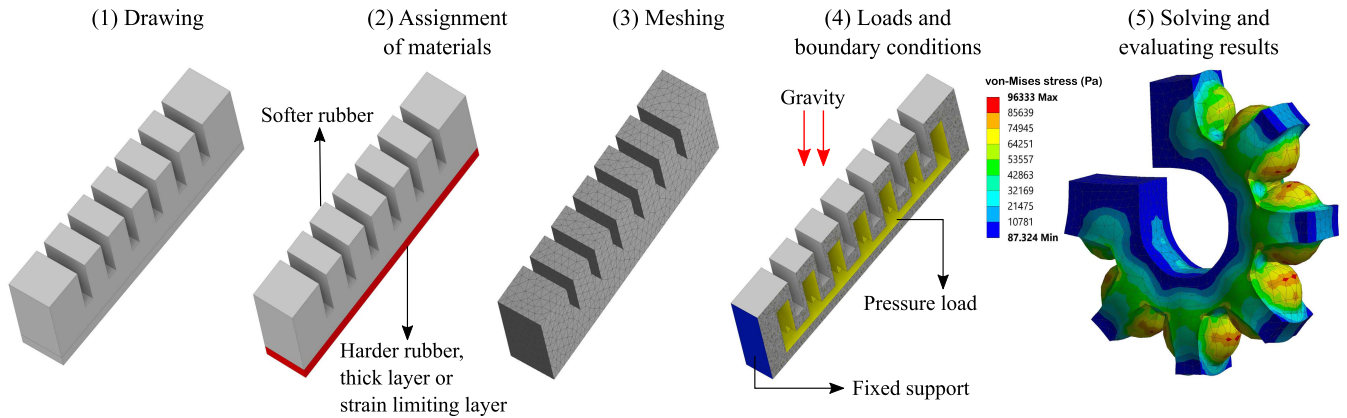


FIGURE 2. Overview of the FEM procedure for soft pneumatic actuators: (1) drawing the soft actuator geometry in CAD software, (2) assignment of material properties, (3) meshing, (4) boundary conditions and loads (internal pressurization, mechanical fixture and gravity), and (5) analysis of results. Adapted with permission from [27].

handle contact nonlinearities associated with environmental interaction.

Commercial FEM software for soft robotics includes Abaqus, ANSYS, COMSOL, and Marc. An overview of the FEM procedure is shown in Fig. 2. FEM has been used to analyze and optimize the various soft actuator designs discussed in Section II, such as pneumatic network [98], [113], [114], fiber-reinforced [76], [78], [122], omnidirectional [86], [108], [140] and 3D-printed actuators [18], [50], [87], [151]. The aforementioned packages also allow for force measurements, modeling of the interaction with other objects, and analysis of multiphysics phenomenon such as fluid-structure interaction [241] and thermostructural analysis [242], [243]. Open-source alternatives for the simulation of soft actuators are MOOSE and VegaFEM. Soft pneumatic fingers with a fiber-reinforced design are modeled with VegaFEM in [244]. However, MOOSE is limited to the Neo-Hookean hyperelastic model [245] and VegaFEM does not implement collision detection or contact handling [246]. The previously described FEM packages have slow computational speed, which inhibits their use for real-time control. SOFA, an open-source toolkit geared towards interactive medical simulation [247], includes a soft robotics plugin [248] and allows for fast, real-time simulation and control [249]–[251].

Many factors influence the accuracy of the FEM results. Firstly, the hyperelastic parameters obtained from uniaxial testing might not be representative of the load conditions and multi-axial stress-strain which occurs during pressurization. Secondly, the properties of hyperelastic materials are also affected by curing temperature, mixing ratio, and degassing. Moreover, compressibility, viscoelasticity, stress softening, and the Mullins effect are usually ignored in FEM but also impact the performance of SPAs [27].

The vast majority of FEM studies employ quasi-static simulations with pressure loads being ramped up at small time steps. However, dynamic effects might need to be included for simulations at high pressures or for fast

actuation, where the quasi-static assumption does not hold and vibrations can be observed [129], [134]. Dynamic finite element analysis was performed in [252] for semi-circular fiber-reinforced actuators. The inflation of the SPA is modeled as a stress in the internal surfaces and triangular actuation is used with time increments set to 1/200-1/100 of the oscillation period. The authors have observed that increased length and lower bottom layer thickness lead to a reduction in the natural frequencies. In addition, while the inflation pressure has a stiffening effect on the first natural frequency, the second and third frequencies are reduced as the pressure is increased. In [253], vibration analysis was conducted on a single-link soft finger from which the first ten fundamental frequencies and mode shapes were computed. Alternatively, a small amount of Rayleigh damping can be added in quasi-static simulations to improve the convergence of the model at high pressures, which keeps kinetic effects to a minimum and ensures quasi-static conditions [122], [240].

D. FLUID-STRUCTURE INTERACTION

Fluid-structure interaction (FSI) is the mutual interaction between a deformable solid body and an internal or surrounding fluid flow where the flow has a strong impact on the structure, and vice versa [241]. The fluid flow exerts hydrodynamic forces which deform the structure and the fluid geometric domain is simultaneously updated since the deformed structure imparts velocity to the fluid domain and changes its shape [254].

While most FEM simulations apply a uniform pressure boundary condition to the internal cavities of the soft actuators in (quasi-) static simulations, physical SPAs are pressurized by applying flow into the actuator from a variety of pneumatic sources, as reviewed in Section V. To achieve more realistic modeling of the pressurization of soft actuators, FSI simulations can be used. FSI allows to investigate the influence of the fluid flow and pressurization rate on the performance of soft actuator, understand the internal fluid mechanics behavior and internal pressure distribution of

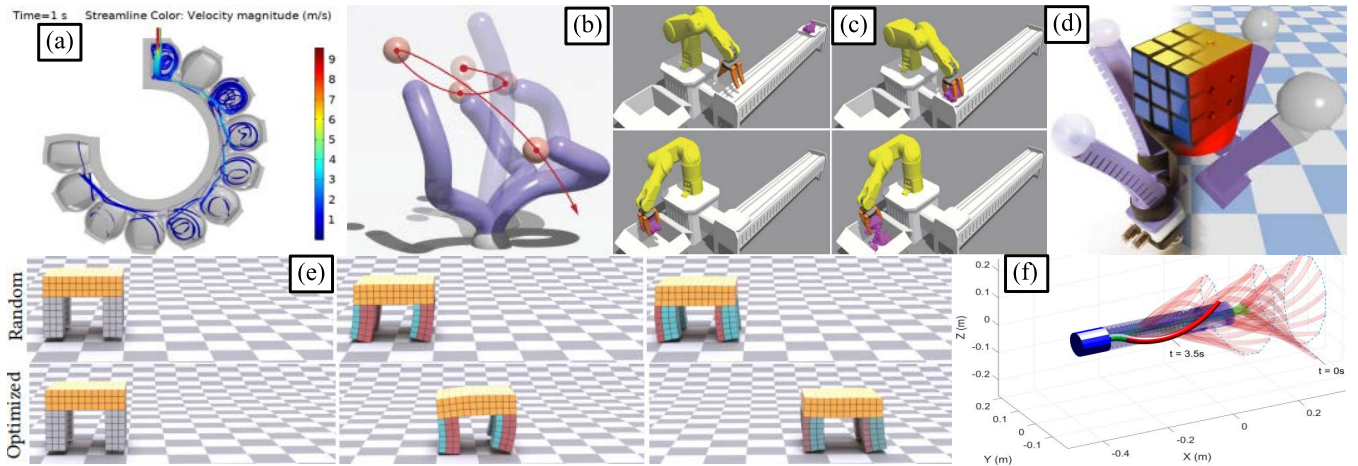


FIGURE 3. Recent advances in the simulation of soft robots. (a) Modeling of internal flow with FSI simulations [256]. (b) Tracking of a moving target in *Elastica* [257]. (c) Manipulation task of a rigid manipulator equipped with a soft pneumatic gripper using Gazebo and ROS [258]. (d) Soft robotic hand manipulating a cube in a hardware experiment (left) and in a simulation using SoMo (right) [259]. (e) Optimization of walking distance of a soft quadruped in DiffPD [260]. (f) Motion of a flagellate soft robot in SoRoSim [261]. All figures are reproduced with permission.

the actuator, and analyze the dynamic characteristics of the actuator.

Modeling of soft fluidic actuators requires two-way FSI simulations since both fluid and solid domains undergo large deformations. The meshless local Petrov–Galerkin method was used to perform two-way FSI analysis of a worm soft robot in [255], where the proposed FSI method was shown to be more accurate than conventional FEM. In [256], COMSOL Multiphysics was used to perform two-way FSI simulations of PneuNet bending actuators using a time-dependent study and the assumption of incompressible and laminar flow (Fig. 3a). The FSI results were compared to static finite element simulations using Abaqus, where FSI simulations better captured the soft actuator motion at high pressurization rates.

E. PHYSICS-BASED AND DIFFERENTIAL SIMULATORS

Among physical simulators, differentiable simulators incorporate gradient-based optimization algorithms. The calculated gradients can be directly input into numerical optimization algorithms, which provides a mathematical framework to: (1) detect and close application specific simulation-reality gaps, (2) optimally control embedded soft actuators for grasping and locomotion tasks, and (3) estimate the mechanical state of the soft system from a set of optimally embedded sensors [262]. Simulation-driven state estimation for soft robots has been demonstrated for an optimal liquid-metal strain sensor network in [263], which combined capacitive and pressure sensing in [264].

Recent efforts have been made to develop simulators that can also train and evaluate controllers, such as those arising from reinforcement learning. ChainQueen is a real-time, differentiable hybrid Lagrangian-Eulerian physical simulator for deformable objects, which also allows for physical inference, control of soft robots, and co-design of robotic arms [265]. DiffPD is a fast differentiable simulator

based on projective dynamics for efficient soft-body learning and control applications [260] (Fig. 3e), which has also been coupled with a differentiable, analytical hydrodynamic model to assist with the modeling and control of an underwater soft robot [266]. Other differential simulators for underwater soft-bodied animals include SoftCon [267] and DiffAqua [268]. SoftGym is a set of open-source simulated benchmarks for manipulating deformable objects with a standard OpenAI Gym application programming interface and a Python interface for creating new environments [269]. *Elastica* couples a Cosserat rods simulator with five state-of-the-art reinforcement learning algorithms (TRPO, PPO, DDPG, TD3, and SAC) for the modeling and control of soft actuators with rod-like structures that can bend, twist, shear, and stretch [257] (Fig. 3b). SoMo is a standardized framework using PyBullet that allows for fast and accurate simulations of soft and soft-rigid hybrid robots in environments with complex contact interactions [259] (Fig. 3d).

Traditional rigid body simulators have also been adapted to soft robotics. Gazebo and ROS have been used in [258] and [270] to simulate robotic manipulation using a rigid robotic arm equipped with a soft pneumatic gripper (Fig. 3c). An open-source ROS-Gazebo toolbox is proposed in [271] for the dynamic simulation of articulated soft robots driven by compliant-actuated joints. SoRoSim is a MATLAB toolbox based on the geometric variable strain approach providing a unified framework for modeling, analysis, and simulation of soft, rigid, and hybrid manipulators [261] (Fig. 3f). Another MATLAB toolkit for soft robotics is SOROTOKI, which includes tools such as FEM with hyperelastic materials, topology optimization, dynamical modeling through differential geometric theory and real-time control of soft robots via Raspi-interface [272]. Evosoro [273] is a soft robot simulator based on Voxelyze, a general-purpose voxel-based soft-matter physics engine for static and dynamic analysis [274]. Other robotic simulators with capabilities for

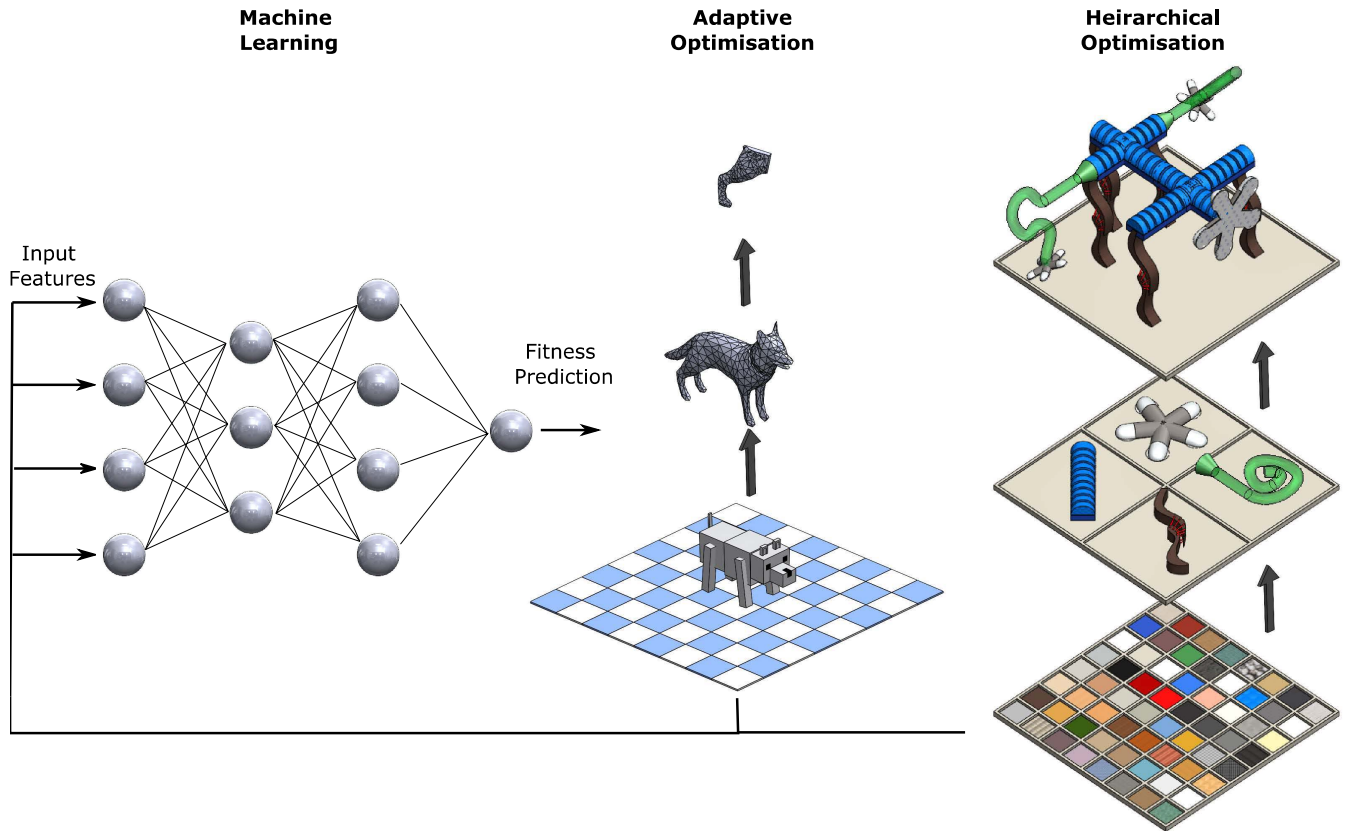


FIGURE 4. A potential future optimization architecture for soft robots. The complex task of designing soft robots is assisted by machine learning surrogates or fitness prediction, and the optimization is divided into a series of smaller problems and optimized by assembling feature libraries into components and robots. We may also adaptively evolve a robot in a physics simulator by progressively increasing resolution and feature density. Learning from both simulated and experimental data increases the efficiency and accuracy of the optimization process. Reproduced with permission from [276].

modeling of soft robotic components include Bullet/PyBullet, MuJoCo, and Chrono [275].

F. COMPUTATIONAL DESIGN

The use of nonlinear materials, large displacements, and distributed actuation make designing and optimizing soft robots vastly more challenging than rigid robots. Rather than modeling a robot as a set of rigid links with exact displacements and rotations, soft robot designers generally employ one of the analytical or numerical methods previously discussed as the basis for design optimization. The methods broadly trade-off accuracy for generality or speed, hence soft robot design optimizations focus on elementary components. In contrast, evolutionary design generates complex morphologies but the simulations translate poorly into real-world performance. Automating the design of soft robots would enable the rapid generation of application-specific soft robots and accelerate the growth of soft robotics. Whilst not yet demonstrated in practice, automated soft robot design through physics-informed, multi-scale modeling is a viable solution in the medium term [276]. It divides the ‘hard’ soft robot design problem into a series of simpler problems and solves them hierarchically by increasing resolution and adding features or building libraries of subcomponents and

assembling them (Fig. 4). Detailed reviews of computational soft robotic design approaches and design optimization of soft robots can be found in [276], [277].

1) PARAMETRIC DESIGN OPTIMIZATION AND TOPOLOGY OPTIMIZATION

The most common soft robotic design optimization method optimizes a small set of design parameters to maximize the performance of a design candidate. In soft components with a defined mechanical objective (force, displacement, bending, etc), a straightforward numerical optimization can meaningfully increase performance with little effort. General guidelines for soft actuator parameter design have been reviewed in Section II. Because of their frequent use in soft robots, the chamber shape and dimensions of PneuNet actuators have been a regular optimization target [112], [278], [279]. Single and multichambered fluidic soft actuators were optimized in FEM to maximize bending angle by evaluating their deformation across a set of geometric parameters [280]–[282].

Even relatively basic soft actuators require dozens of design parameters to fully specify their shape. To optimize across every parameter would require thousands of FEM iterations, and would still be unlikely to find a global

optimum. Rather than extensively searching the design space with a large number of simulations, machine learning can be applied to learn the design space, producing a surrogate model of the design space for use in future designs [180], [283]. Alternately, machine learning [284], [285] can be applied to learn the nonlinear design space and kinematics of SPAs from FEM results, i.e., the finite element simulation is treated as a data generator mechanism that yields the required training data sets for artificial neural networks [286].

Topology optimization is a local computational design method that finds the material distribution which maximizes fitness. Like the parametric methods, it requires the designer to specify the boundary conditions, making it most applicable to fixed manipulators and grippers. However, topology optimization does not require the designer to specify a set of geometric design parameters. Instead, it is parameterized by the elements of a FEM mesh, which are optimized to be either solid material, or empty space. Despite its origins as a structural optimization method for stiff, lightweight components, topology optimization of flexible mechanisms is now well established [30], [287]–[289], including pressure-loaded compliant mechanisms [290], [291]. Several research groups have linearly optimized single-material pneumatic soft actuators. To do so, a pressure load is applied to nodes within a defined hollow section, and the placement of the surrounding material is optimized to maximize bending or output force [292]–[294]. Rather than specifying a fixed input face, the optimizer should ideally permit design-dependent loading, so that the load location forms part of the design space. A binary material optimization was investigated in [153], while capturing the design-dependent loading, it produced disjoint cavities which would not inflate in reality. A 3-material model, which allows solid, high-pressure, and low-pressure regions, overcame this issue by forcing a solid boundary between high and low-pressure [295]. Nonlinear optimizations, which capture the large deformation of soft actuators are desirable to predict the true behavior of SPAs but usually create intractable, non-convergent simulations. A single chamber section was optimized using a nonlinear Solid Isotropic Material with Penalization (SIMP) optimization with design-dependent loading, however, it too produces unworkable discrete chambers [296].

2) EVOLUTIONARY DESIGN

Evolutionary algorithms present an attractive methodology for designing soft robots. Evolution is used as a population-based iterative black-box optimizer where search operators are inspired by genetics and Darwinian selection. The black-box aspect is particularly useful for optimization directly from the quality of observed orchestrated behaviors. Initially, evolutionary algorithms were used to generate a single optimal solution with the population used as a means to an end. Later, the population was used more directly to generate a set of optimal trade-offs between various

desired traits (e.g., [297]). Recent evolutionary algorithms have pushed into a new area called ‘quality diversity’ [298], which generates diverse libraries of high-performance robots, components, or behaviors, and has been used as a basis for future frameworks to realize embodied cognition in soft robots [299], [300]. Examples to date include an impressive array of soft robots (sometimes called ‘animats’), including a range of bioinspired bipeds, quadrupeds, fish-like robots, and plants, as well as grippers and novel uncategorizable designs [301]–[303].

As evolution is population-based and iterative (typically requiring at least hundreds of generations to reach good solutions), experimentation primarily occurs in physics simulation [275], [304], [305], which tends to emphasize computational efficiency over accuracy. Physics simulators that are suitable for evolutionary design typically do not model features essential to physical implementation such as actuators, joints, and materials that capture real-world behavior. As a result, evolved soft robots are primarily used as models of soft robot behavior or as a source of design inspiration, rather than a verbatim design that is directly translatable into experimental settings. Transfer to reality typically requires significant modification [306], [307]. However, purely physical evolution of soft grippers using 3D printing has shown promise [308].

V. ACTUATION

A. OVERVIEW OF PNEUMATIC ENERGY SOURCES

The main components of a pneumatic system is the source for generating pressurized air, the pneumatic line for connection, and the valves for controlling flow direction [309]. Pneumatic energy sources used in autonomous and wearable soft robots are compared in [46]. The role of valves, pneumatic lines, and soft actuator design parameters are discussed in [47], [309]. Generally, pneumatic sources can be approximated as constant flow or constant pressure sources [47], [309]. A popular example of the latter includes pressure-regulated air receivers (gas tanks), which can be added to improve efficiency and minimize the required pump flow rate [234], [309], [310]. Additionally, the presence of the receiver allows for rapid bursts of flow and, therefore, fast actuation with rise times in the milliseconds range.

B. SYRINGE PUMPS AND FLUIDIC DRIVE CYLINDERS

Commercially available syringe pumps are generally expensive and designed for small volumes [49]. Considering these issues, low-cost volumetric control systems using syringe pumps have been investigated in the literature [311]. To convert the rotation of a motor to linear motion, syringe pumps use either a rack and pinion mechanism [312], [313] or lead-screw [49], [314]–[316]. In the latter, the motor rotates a threaded rod that drives a nut attached to a syringe adapter [15]. Alternatively, fluidic drive cylinders have been proposed in [317], [318] to allow precise analog control of airflow to and from actuators in a multi-segment soft robotic arm.

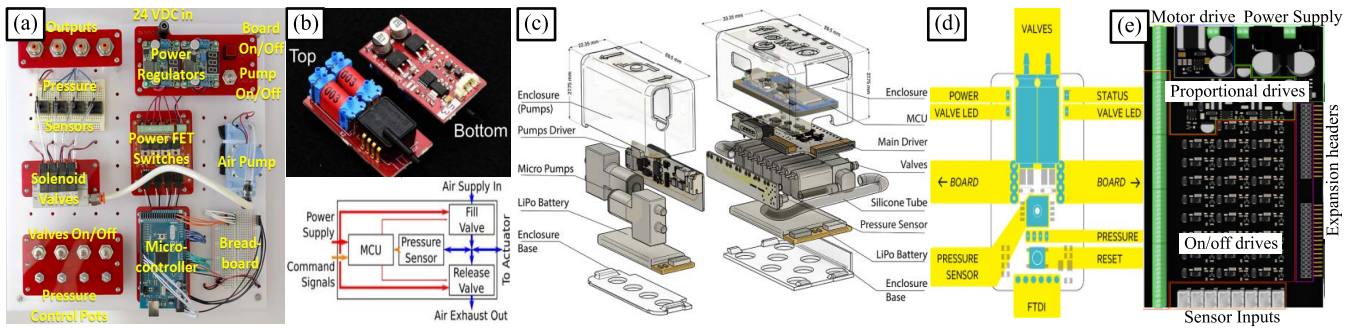


FIGURE 5. Pneumatic control boards for soft robotics: (a) fluidic control board [45], (b) addressable pneumatic regulator [319], (c) FlowIO [320], (d) Pneuduino [321], and (e) PneuSoRD [322]. All figures are reproduced with permission.

C. COMPRESSED-AIR SYSTEMS

Pressure control in the soft actuator is usually achieved with on/off solenoid valves [236], [237], [319] since proportional valves are bulky and expensive. The most popular pneumatic control architecture for soft robotics is the fluidic control board shown in Fig. 5a, an open-source hardware platform available from the Soft Robotics Toolkit [45], which was originally employed in the experimental platforms of [58], [80]. The fluidic control board has since inspired many pneumatic control systems [10], [11], [323]. The board consists mainly of a diaphragm pump and a set of solenoid valves. MOSFETs allow the use of Pulse-Width Modulation (PWM) to control the pressure of a fluid passing through the valves. Pressure sensors provide feedback on the behavior of the system. Pressure can also be controlled using pressure regulators, which are best suited to on/off applications. Basic control options are manually adjusting switches and knobs or control algorithms running on the included Arduino microcontroller [324]. Advanced control options can be implemented using LabVIEW or Simulink [132], [325].

In addition to the fluidic control board, a number of pneumatic boards have also been proposed in the literature. FlowIO (Fig. 5c) is a miniature, modular, fully integrated development platform with 5 pneumatic input/output (I/O) ports for driving soft robots with pressure ranges from -26 psi to 30 psi and flow rates up to 3.2 LPM (liters per minute) [320]. Pneuduino (Fig. 5d) comprises two pneumatic valves (S070C), an air pressure sensor (MPXHZ6400), and an ATmega328P microprocessor for pneumatic control of one soft actuator [326]. Programmable Air provides similar capabilities to Pneuduino while using more affordable parts and integrating two 3.2 LPM pumps into the device itself [321]. The Pneumatic Soft Robotics Driver (PneuSoRD) proposed in [322] (Fig. 5e) can be used to drive both proportional and on/off valves, acquire data from up to 12 sensors and control up to 31 pneumatic actuators simultaneously. User-friendly interfaces for pressure control with Proportional-Integral-Derivative (PID) and on-off controllers and various valve configurations are provided in [322] with LabVIEW or Simulink options. A miniature, multi-mode pressure regulator is proposed in [319] (Fig. 5b) for integration directly into a centimeter-scale soft robot using the I2C protocol.

Practical soft robotic systems usually require a large number of actuators, possibly in closed-loop, with multiple input lines and valves, which results in multiple control inputs and, consequently, complex control strategies and hardware setups. To address this issue, passive band-pass valves are proposed in [327] to control serially connected soft robotic actuators from a single pressure source. The effects of viscous flow in narrow tubes can be exploited to achieve a range of functionalities in interconnected soft actuators using a single input line [328]. A single on/off valve and 3D-printed flow resistor tubes are used in [329] for passive control and sequential activation through the principle of pressure drop in multi-capillary orifices. Alternatively, fully integrated fluidic circuitry can be embedded into the soft actuator during fabrication [330], [331], which provides a powerful alternative to enhance soft robot autonomy and eliminate tethering requirements [332].

D. PARAMETER ANALYSIS AND SELECTION

Several advanced control techniques for soft pneumatic actuators are reviewed in Section VII. However, these are only effective if the response time is not limited by the dynamics of the pneumatic system. While the actuation mode, force, and displacement are governed by the SPA design and loading conditions, the actuation speed is largely determined by the pressure and flow dynamics of the SPA [333]. Therefore, regardless of the soft actuator design, the pneumatic system critically affects the pressure dynamics of soft actuators [234], [309] and plays a major role in the overall performance of soft robots [236], [334].

To ensure the open-loop response time is sufficient for a given application, appropriate parameters must be selected to satisfy requirements on the actuator response. A step towards resolving this issue is the work of [309] in which the authors introduce a mathematical model of the pneumatic system for the selection of source, valve, and pneumatic lines. In [47], the authors present a practical process for pneumatic component selection and controller design based on Simscape Fluids simulations. The effect of various pneumatic parameters in the rise time of the soft actuator response and air consumption during actuation are summarized in Table 5. Generally, faster actuation can

TABLE 5. General guidelines for pneumatic parameter selection. The upward arrows indicate larger rise time or energy consumption for increased parameter values, the opposite is valid for downward arrows.

Parameter	Rise time	Air consumption
Pump/compressor flow rate	↓	—
Valve conductance/flow coefficient	↓	—
Valve critical pressure ratio	↓	—
Receiver pressure	↓	—
Receiver volume	—	—
Actuator volume	↑	↑
Tubing length	↑	↑
Tubing diameter	↓	↑

be achieved with greater valve sonic conductance, greater receiver pressures, and lower actuator volumes. The receiver volume has little impact on the response as long as it is above 10 times the volume of the actuator [47], [309]. The selection of tube diameter requires careful consideration since a large diameter has minimum flow resistance but large capacitance, while small diameters increase flow resistance [335].

Valve configuration is another important characteristic to consider when designing a pneumatic system for soft robotic applications. 3/2 (3-way, 2-position) valve systems are economical and straightforward to implement at the expense of low accuracy and high energy consumption. Dual 2/2 (2-way, 2-position) valve systems improve energy-efficiency and valve lifetime by reducing the number of switching events. Alternatively, more complex 3/3 or 5/3 valves can be used to obtain the same behavior as dual 2/2 valve systems [134]. Proportional valves can further increase the accuracy of controllers but these are significantly more expensive [322], [336]. For further details on the selection of pneumatic system configurations and components, the reader is referred to [47], [309], [322], [333].

E. UNTETHERED ACTUATION

Pneumatic sources for SPAs are traditionally outside the body of the robot. Untethered actuation was reviewed in [3], including actuation methods based on light, combustion, electrothermal force, and electrostatic force. On-board pneumatic sources are described in [337], [338]. Embedded microfluidic or pressure activated valves and self-contained fluidic engines can control systems with many degrees of freedom, which reduces the number of external connections [339]. These methods are highly scalable and can perform complex logical behaviors.

F. STIFFENING AND HYBRID ACTUATION

In applications that require high force and low deformation due to externally applied forces, pneumatic actuation may not be suitable. Variable-stiffness SPAs offer adaptive stiffness (from very compliant to rigid), allowing the SPA to achieve both high compliance/deformability and high force transference. Stiffness can also be seen as a tuneable property that can be exploited to elicit specific continuums

of performance from the actuator. Stiffening SPAs can be realized in numerous ways, including [340]:

- Jamming structures, which can be granular, fibres, or layered in nature [189], [341], [342] and typically use negative pressure to vary stiffness,
- Electro Active Polymers (EAPs), which deform under electric field [33], [343], [344],
- Electro- and magneto-rheological materials (ERM/ MRM), which use embedded magnetic/electric particles that cause stiffening under a magnetic/electric field,
- Low Melting Point Alloys/Polymers (LMPA/LMPP) [345], [346] which display rapid stiffness change with varying temperature,
- Fluidic actuators [347] (e.g., PneuNets), and
- Shape memory materials (SMMs) which can be alloys or polymers [348]–[352] and deform due to temperature.

Comparatively, jamming provides higher maximum stiffness than fluidic actuation, SMM, EAP, ERM, and MRM mechanisms, but typically requires attachment to a vacuum pump which may be infeasible depending on the application. Similarly, EAPs and ERMs require electric fields to be generated, MRMs require magnetic fields, SMMs, LMPAs and LMPPs can be difficult to modulate with temperature. Additionally, SMMs, LMPAs and LMPPs have comparatively slow stiffness transitions due to cooling requirements, whereas jamming, fluidic actuation, EAPs, ERMs, and MRMs are often faster. Each also has unique footprint requirements, with some infeasible geometries. Jamming actuation is particularly popular in the field, due to a combination of low cost, rapid stiffness variation, and dramatic differences between attainable minimum and maximum stiffness [353].

Granular jamming is the most popular jamming mechanism, being popularized in 2010 [354]. Granular jamming is the natural phenomenon of transitioning a compliant, low density packing of granular matter into a rigid, high-density packing via externally applied stress. Loose, unjammed grains function as fluids, while rigid, jammed grains behave as solids [355]. Both naturally-occurring (coffee, corn, gravel, rice, pepper, salt, sugar), and man-made (plastic, glass, and rubber) granular materials have been studied in the literature [353]. Rubber cubes are frequently used in robotic ‘paws’ as they are more controllable and have favorable force dissipation properties. Recent work makes grain choice a part of the design problem, either 3D printing promising grains from modeling [356], or using machine learning to decide on grain shape with 3D printed grains [297], [357]. Optimal membrane morphology for granular jamming grippers can also be decided through machine learning [308]. Several studies have shown the benefits of auxiliary mechanisms in increasing performance, including positive pressure [358] and vibration [359].

Jamming is not restricted to granular materials; for example, layers of sheets [360]–[366] (layer jamming) and bundles of threads [189], [367]–[369] (fiber jamming) can also transition from compliant to rigid structures. However,

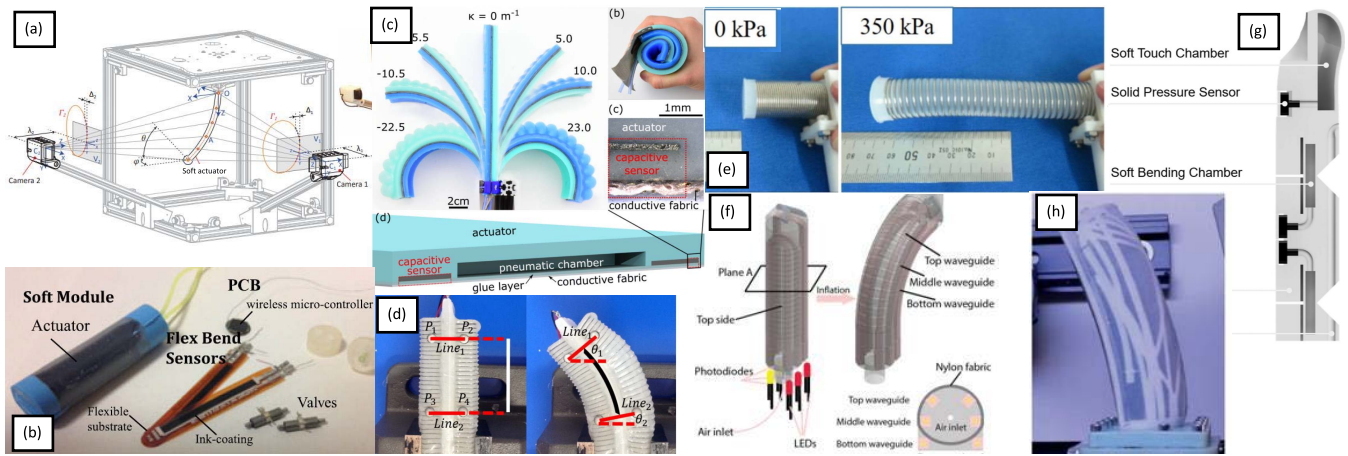


FIGURE 6. Sensing methods for soft robotics: (a) vision-based sensor [392], (b) resistive sensor [393], (c) capacitive sensor [394], (d) magnetic sensor [395], (e) inductive sensor [396], (f) optical waveguide [397], (g) embedded pneumatic sensing [387], and (h) optimized strain sensor [263]. All figures are reproduced with permission.

neither function as fluids when unjammed so stiffness variation is less than in the granular case. Hybrid SPAs utilizing more than one jamming mechanism are a recent trend [370], [371]. Negative pressure is most commonly used to force a phase transition [354], [358], [372]–[374]; however, the following methods have also been reported: interstitial liquid [375], [376], inflation of a neighboring cavity [362], [371], cable-driven volume reduction [377], [378], external membrane compression [364], injection of grains [379], and linking via a thread [380]. Jamming structures are relatively unrestricted in their possible morphologies, and as such have been deployed in a variety of use cases including minimally invasive surgical tools [381], supportive exoskeletons [382], [383], robotic paws [384], [385] and tendons [189], and damping end effectors for UAVs [386]. Modern additive manufacturing techniques serve to facilitate more thorough design exploration [188] and are poised to further increase the range of useful application domains whilst reducing required labor.

Cable-driven and pneumatic actuation have also been combined in several practical applications for improved speed and external force, including soft robotic fingers, [387], hands [388], manipulators [23], [389] and grippers [390]. A novel dual-actuation mechanism is proposed in [391] to switch between two stable states, which utilizes pneumatic pressure for closing and tendons for opening. This process provides large force exertion, fast closing and opening speeds, and robust damping effects.

VI. SENSING

A. OVERVIEW OF SENSING TECHNOLOGIES

Closed-loop control of soft robots requires sensors to measure the pose of the actuator [393]. Embedded sensing strategies have been proposed using commercial flex bend sensors [237], [393], inclinometers [238], optical waveguide sensors [129], liquid conductors [399] and magnetic sensors [127]. Generally, soft sensors should be more compliant

than the soft actuator to minimize any mechanical resistance to actuation, ensure sensing stability, and prolong the sensors lifetime [400].

For a soft actuator to be bodily aware, it must be integrated with proprioceptive and exteroceptive sensors [401]. Proprioceptive sensors are used to measure the state of the soft robots and are usually embedded in their structure, while exteroceptive sensors are used to measure the state of the environment that soft robots are interacting with. In this section, the main sensing technologies for SPAs are reviewed, as shown in Fig. 6. For further details on sensing for soft robotics, the reader is referred to [398], [402].

B. RESISTIVE AND PIEZORESISTIVE SENSORS

The most commonly used strain sensors in soft robotics are resistive-based sensors. Resistive sensors measure the variation in resistance of a liquid, embedded elastomer, conductive polymer, or hydrogels due to the deformation of a soft actuator [398] (Fig. 7a). They are first calibrated using an electromagnetic positioning system [393] or, more commonly, camera tracking systems [230], [403]. Commercially available resistive flex bend sensors (Fig. 6a) have been embedded within the strain limiting layer and used for modeling and closed-loop control of bending actuators [237], [393], [404], [405]. Three conductive rubber cord stretch sensors (Adafruit) were used for sensing three dimensional deformation of fiber-reinforced actuators in [406]. A stretchable strain sensor composed of a thin layer of screen-printed silver nanoparticles on an elastomeric substrate is fabricated using conventional screen printing technology in [407] and employed to detect bending with strains over 20% with a gauge factor above 50000.

Strain sensors were also 3D-printed by integration of single-walled carbon nanotubes (SWCNT) and TPU [408]. These piezoresistive sensors improved the repeatability of strain measurements [409]. The optimum sensor performance

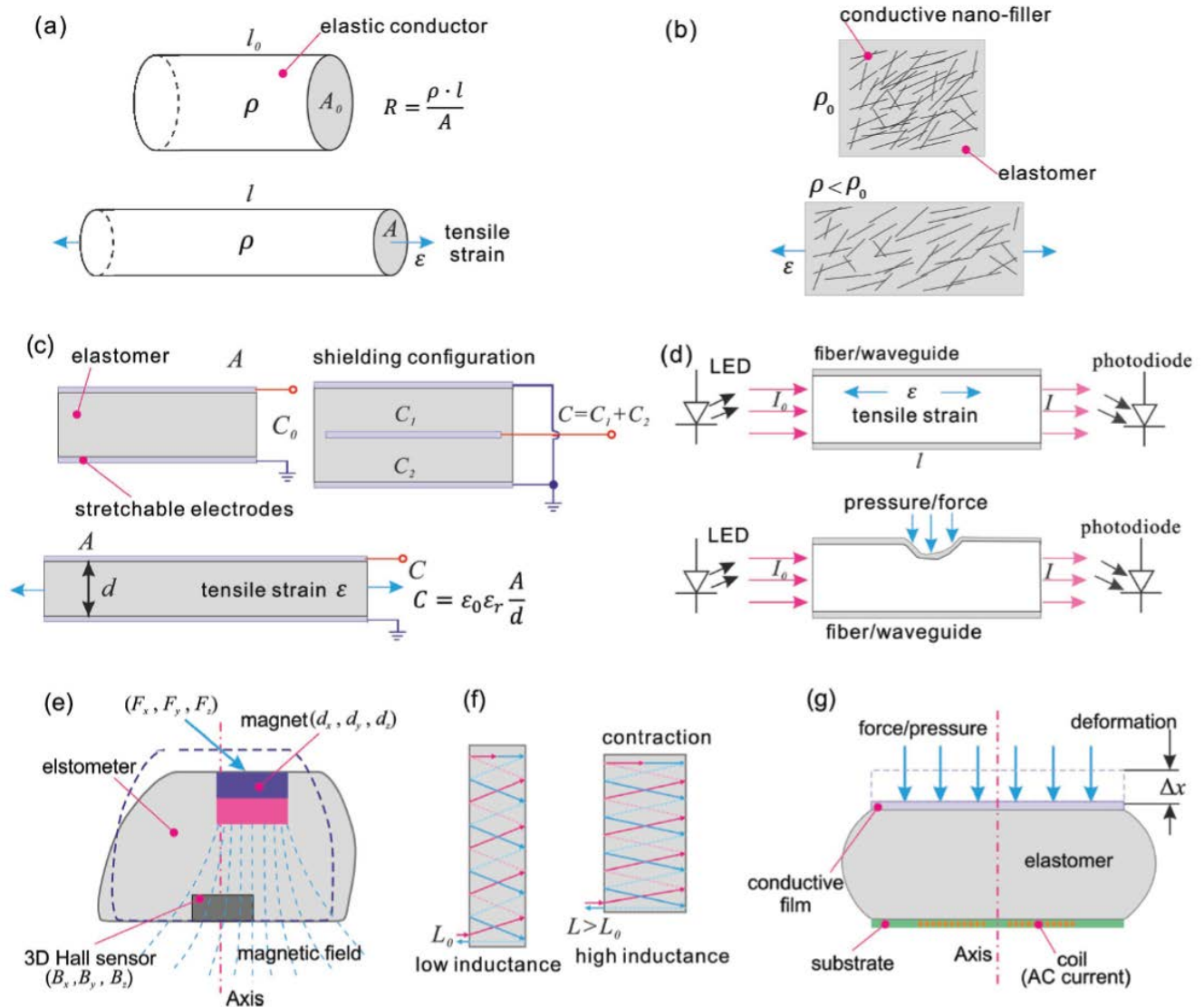


FIGURE 7. Soft robotics sensing methods mechanics overview [398]: (a) resistive sensor, (b) piezoresistive sensor, (c) capacitive sensor, (d) optical fiber/waveguide-based pressure and strain sensor, (e) magnetic tactile or deformation sensor, (f) smart braid, and (g) inductive tactile sensor. Reproduced with permission from [398].

was observed with 0.2% by weight SWCNTs in the composite matrix. TPU-based filament and carbon black (CB) were used to create a 3D-printed tactile piezo-resistive sensor as the conductive filler [410]. In comparison to standard CNT-Ecoflex, the printed CNT-Ecoflex shows encouraging outcomes. TPU and PLA-G filaments are combined to create a piezoelectric tactile sensor that can be 3D-printed with promising lifetime in [411]. A gel piezoelectric sensor is 3D-printed and embedded into a jellyfish-like soft robot that utilizes certain composite gel materials, including ion gel, ionic liquid, and shape-memory gel. The study demonstrates that an ion gel could be used for pressure sensing due to its variable impedance properties [412]. Piezo-based gel sensors are 3D-printed among other composite materials with potential applications in SPAs [412], [413].

C. CAPACITIVE SENSORS

Capacitive sensors measure the change in distance between conductive plates, or the change in area of an elastic conductive plate [398] (Fig. 7c). The soft continuum proprioceptive arm proposed in [428] includes a 2-axis capacitive flex sensors (Bend Labs Inc.), which allows shape measurement and external contact force estimation. The silicone-based capacitive strain sensors proposed in [429] were used to control bidirectional PneuNet bending actuators in [394] (Fig. 6c). The sensors are constructed as a parallel-plate capacitor using an expanded graphite silicone composite for the active conductive layer and unmodified silicone elastomer for the dielectric layer [394]. Two paper-based resistive and capacitive sensors are integrated into a soft gripper in [430] as strain limiting layers.

TABLE 6. Integrated 3D printing of sensors and SPAs.

Sensor types	3D Printer	Materials	Pros (+) and Cons (-)	Ref.
Resistive	FDM	TPU	+ Non-degradable – Agglomeration	[408]
	FDM	TPU	+ Force and contact point – Hysteresis	[410]
	SLA	Cilia	+ High resolution – Nonlinearity	[411]
	Inkjet	Tango Black	+ Pressure and shear – High-stress deviation	[412]
	FDM	Bioagents/PLA/ABS	+ High precision – Post-treatment	[413]
	FDM	PLA/carbon fiber	+ Negative Poisson's ratio – Strain shift	[414]
	Extrusion	TPU/silver	+ Low cost – Adhesion	[409]
Capacitive	FDM	TPU	+ High sensitivity – Simple geometries	[415]
	Extrusion	Ionic gel	+ High sensitivity – Environmental effects	[416]
	DLW	Nanocrystals	+ High Spatial resolution – Coupling loss	[417]
	FDM	TPU/PI-ETPU	+ Negative Poisson's ratio – Low stretch	[418]
Magnetic	FDM	Copper/ABS	+ Non-contact + High temperature range	[419]
	FDM	Magnetite/ABS	– Low sensitivity – Environmental effect	[420]
Inductive	Inkjet	VisiJet/silver	+ Wireless – Dissolving sacrificial	[421]
	FDM	Magnetite/PCL	+ Linear response – Delamination	[422]
Optical	FDM	ABS	+ Linear response – High Deviation	[423]
	Inkjet	InkOrmo/InkEpo	+ Mass production – Coupling loss	[424]
	FDM	FBG/PLA	+ High sensitivity – Post assembling	[425]
Pneumatic	FDM	TPU	+ Multi-sensing – Noisy	[387], [426]
Ultrasound	Polyjet	Phononic crystals	+ Non-contact – Post assembling	[427]

3D-printed capacitive strain gauge sensors [431]–[433] have also been utilized to manage strain with a defined sensitivity that can be adjusted by the printing parameters. A metamaterial capacitive uniaxial stretch sensor array has been 3D-printed for the measurement of normal forces during a stretching process. The electrodes are fabricated from electrically conductive carbon black thermoplastic polyurethane (PI-ETPU). The negative Poisson ratio designed via auxetic patterns enhanced the compliance and deformation in common SPAs [418]. Micro-sized force sensors have also been 3D-printed on complicated geometries for tactile applications including touch location and intensity detection [415]. Direct laser writing (DLW) has been widely utilized to create 3D-printed capacitive sensors using conductive inks for temperature and humidity measurements [416], [417].

D. MAGNETIC SENSORS

Magnetic sensors are comprised of a permanent magnetic source and a magnetic field sensor. As the soft actuator deforms the position and orientation of the permanent magnet relative to the magnetic sensor varies, which is used to determine the actuator deformation [398] (Fig. 7e). Custom magnetic sensors have been used to measure the curvature of bending actuators in [127], [395] (Fig. 6d). These sensors utilize a magnet and a one-dimensional Hall effect sensor on a flexible circuit board [434]. This approach is simple to manufacture and instrument. In [395], magnetic sensors returned noisy but accurate data, while the

commercial resistive flex sensor had an offset at steady-state conditions.

The deformation of SPAs can also be detected using 3D-printed magnetic displacement sensors, which have been created for non-contact operation with a broad temperature range. These sensors are advantageous for harsh environments due to their non-contact nature [419], [420], [435], [436].

E. INDUCTIVE SENSORS

The inductance of a coil is determined by the coil diameter and the spacing between the coil windings. As the actuator elongates, the space between turns increases while the coil diameter decreases, which reduces inductance, and vice versa [398] (Fig. 7e). Compared to 3D-printed resistive and capacitive sensors, inductive sensors provide more design freedom and are compatible with a wide range of materials [421], [437]. In [396], a metal spring covering a cylindrical soft actuator is used to limit the radial expansion of an extending actuator and estimate length as the inductance of the spring changes during pressurization (Fig. 6e).

F. OPTICAL SENSORS

Optical sensors measure variations in light intensity and phase. As the length of an optical guide changes, the measured phase is related to deformation. Deformation can also be inferred from the intensity of received light if the optical guide is partially or fully obstructed along its

length [398] (Fig. 7d). A customized optical waveguide made from flexible polymethyl methacrylate material is used to measure bidirectional bending in [129]. This sensor is free of radial deformation and can provide steady linear output under pressure. Hybrid rigid and soft optical fibers have been demonstrated for measuring the bending and grasping force PneuNet actuators [438]. In [439], a soft optical waveguide with an embedded LED, a photodiode, and a reflective metal coating are integrated into bending actuators. In [397], stretchable optical waveguides were used as curvature, elongation, and force sensors in a fiber-reinforced soft prosthetic hand. Fiber optic sensors such as Fibre Bragg grating (FBG) sensors are significantly more linear than resistive and capacitive sensors. They are inexpensive, transparent, highly sensitive, and can be directly 3D-printed with SPAs [423]–[425], [440].

G. PNEUMATIC SENSING

Soft pneumatic deformable sensing chambers rely on volume change in their internal structures when they are mechanically deformed [43]. Such sensors can be used in soft wearable gloves for virtual reality applications, human motion tracking, soft grippers telecontrol [441], real-time position and force control of soft robotic fingers [387], [426] (Fig. 6g), soft robotic interactive skins [442], [443], force and curvature measurement [444], three-axis force measurement [445], and tactile sensing for cooperative robots and manipulation [446], [447]. Also, haptic feedback devices [441], game controllers [448], throttle controllers [441] and robotic controllers [449] are developed based on soft pneumatic sensing chambers.

H. ACOUSTIC SENSING

Tactile sensors based on polymeric acoustic waveguides have been developed for strain, deformation, localization, and twist measurement [450]. Contact sensors for soft robotic hands have also been developed using active acoustic sensing [451], [452]. Acoustic sensors for extending SPAs were used to measure the length by generating a broadband acoustic signal in the tube and measuring the resonance characteristics [453]. 3D-printed waveguides can also be integrated into the SPA to reduce air leakage [427].

I. ESTIMATION

Integrating sensors into soft robots remains a challenge due to their flexible nature. Angular velocity, for example, is generally required by control laws for precise closed-loop bending control. While this is often achieved using solid-state sensors such as tachometers, speedometers or gyroscopes with rigid robots, these sensors cannot be used with soft actuators since they would affect their flexibility [230], [231].

State estimation is an attractive alternative for indirect sensing where the robot dynamics and available sensor measurements are used to estimate variables that cannot be measured directly [454]. For nonlinear systems such as soft robots, nonlinear variants of the Kalman filter [455] such

as the Extended Kalman Filter (EKF), Unscented Kalman Filter (UKF) and Particle Filter (PF) can be used. Extended Kalman filters have been used in [456], [457] to estimate the curvature of soft bending actuators using empirical state-space models with measurements from an embedded flex sensor. An adaptive unscented Kalman filter based on a neural network was proposed in [458] using pressure and flex sensor readings to estimate the proprioceptive state and exteroceptive inputs of a pneumatic soft finger.

The aforementioned filters, however, disregard the motion dynamics of soft robots and have not been employed for control purposes. A high-order sliding mode observer using a dynamic model based on the Euler–Lagrange method is proposed in [231] to estimate velocity and track desired trajectories. In [459], simulation results are presented where a state observer is used with a nonlinear feedback controller to regulate the position of a pneumatic soft bionic fin. Observer-based controllers are implemented for pneumatic soft robotic arms using an EKF in [460] and an adaptive Kalman filter in [461]. Observer-based nonlinear controllers are also proposed in [462] for bending angle control, where a feedback linearization controller is used with estimated variables from the UKF based on measurements from a pressure sensor and an embedded resistive flex sensor.

VII. CONTROL

Soft robots are difficult to control with conventional model-based methods due to their significant degrees of freedom and highly nonlinear dynamics [285], [334]. The nonlinearities arising from hyperelasticity are compounded by nonlinearities associated with pneumatic actuation including the compressibility of air, the nonlinearity of flow through valves, and actuation time delays [235], [238], [463]. Although numerous soft sensing technologies were described in Section VI, the use of such technologies in closed-loop control is still in its infancy [464]. In addition, soft sensors are usually limited by multiple factors including a slow and nonlinear response, hysteresis, and drift [43]. In the following, we review control methods used in pneumatic-driven soft robotics.

A. EXPERIMENTALLY-TUNED CONTROLLERS

Most fluid-powered soft robots use experimentally-tuned controllers. For example, in the control of robots including snake-like [10], [11], worm-like [14], [15], [465], soft-bodied fish [16], and manta rays [20], [466]. Experimentally-tuned PID controllers are commonly used [116], [137], [237], [393], [467]. In [467], a PID controller was shown to outperform a sliding mode controller for trajectory tracking at the expense of higher overshoot and lower robustness to external forces. Conversely, the sliding mode controller with a PID sliding surface in [134] damps vibrations compared to a model-free PID controller. In [468], the authors argue that existing work on model-free control uses manually tuned parameters, which is a laborious task. Consequently, automatic tuning of ordinary, piecewise, and

fuzzy PID controllers using a heuristic-based coordinate descent algorithm is proposed in addition to manual tuning using the Ziegler-Nichols method [469], [470] as a starting point.

In [10], bang-bang control was used regulate the pressure of a pneumatic receiver. In [14], [465], [471], the same approach is used to actuate valves for peristaltic locomotion. A dead zone can also be introduced to reduce frequent switching of the valves [78], [472].

B. MODEL-BASED CONTROLLERS

Model-based static or kinematic controllers are most commonly based on the piecewise constant curvature assumption. A theoretical model based on the incompressible Neo-Hookean model was used to control the bending angle of a fiber-reinforced actuator in [26]. A model predictive neural controller was designed to control the grasping force of a soft robotic manipulator under slippery conditions in [473]. Cascade control structures have also been proposed where the faster inner layer performs pressure control and the outer layer is responsible for open-loop angle control [474], [475] with the angle mapping obtained from experimentally extracted mapping functions [474].

Currently, model-based dynamic controllers for soft fluidic actuators are still in their nascent stage [237], as summarized in Table 7. By using the energy-based second-order models described in Section IV-B, sliding mode controllers are developed in [127], [134], [235] to control the bending of soft actuators governed by high-speed on/off solenoid valves. A sliding mode controller with a static feedforward input [235] improved the tracking performance with dynamic trajectories. A model reference adaptive controller augmented by inverse feedforward control was also demonstrated in [236].

Adaptive fuzzy-sliding mode [476] and energy-based [477] nonlinear controllers have been proposed for pneumatic artificial muscles using dynamic models derived using Lagrange's method. Energy-based controllers for soft pneumatic actuators using the interconnection and damping assignment passivity based control (IDA-PBC) methodology have been used in [478], [479], where the system dynamics is represented in port-Hamiltonian form. The port-Hamiltonian approach focuses on the energy interactions associated with the system and offers an alternative for the modeling of multi-domain physical systems based on the concept of power conjugate variables [480], [481].

Many articles have described high-level controllers for bending angle or extension [334]. However, few works have considered the impact of the pneumatic system, which requires low-level pressure control. In [237], a pneumatic model was used to control the bending angle of a pneumatic network actuator using a robust backstepping controller with 2-way, 2-position on/off valves. Sliding mode controllers are proposed in [467], [482] to control the pressure of a soft actuator using proportional valves. State-Dependent Riccati Equation (SDRE), sliding mode and feedback linearization controllers are compared in [483] for low-level control of

soft actuators driven by a pressure-regulated receiver and single on/off solenoid valve. In [238], a pneumatic model is included to control the bending angle of a fiber-reinforced actuator using two 3-way, 2-position on/off valves with a backstepping adaptive controller and sliding mode controller. These controllers have also been employed in [239] using a second-order model with nonlinear parameters, where the experimental results demonstrated high performance of the adaptive robust controller. In [484], feedback linearization is proposed to control the motion of a bellow-shaped continuum manipulator with proportional valves.

C. VISION-BASED SENSING AND CONTROL

A vision equipped robotic system can measure the robot shape and gather information from the surrounding environment. Hence, visual sensing can be used to determine the position and orientation of the soft robot for modeling and feedback control [392], [485], [486]. 2D or 3D vision system can be installed at a fixed location near the robot (eye-to-hand) or attached to the robot (eye-in-hand).

Model-less feedback controllers with vision-based sensing for continuum robots have been described in [487], [488]. This method avoids the accurate model formulation and calibration between camera and robot required in model-based approaches [487], which is particularly relevant considering the complicated kinematic and dynamic models required for soft robots and interaction with the external environment. Shape-based [487] and color-based tracking [488], [489] have been studied for concentric tube robots. Visual servoing has also been proposed for various cable-driven soft robots. In [490], an adaptive controller using eye-in-hand visual servoing is presented for a soft manipulator in a constrained environment. In [491], the visual servoing method was used to attain the inverse kinematics in robot-specific spaces and collision detection. The work in [492] presented an underwater dynamic eye-to-hand visual servoing method for a cable-driven soft robot arm with online distortion correction. Lai *et al.* [493] presented an eye-to-hand closed-loop controller to manipulate a two-segment soft robot with payload in 2D using an online estimate of the Jacobian matrix.

Although the aforementioned methods can be generalized to soft robots with different actuation technologies, few works describe the application of visual servoing to fluid-driven soft robots. In [494], a motion capture system is used to implement a model-less proportional controller on a honeycomb pneumatic network manipulator [495], which resulted in compensation of gravity and external loads. In [496], an eye-in-hand visual servoing method was applied to a single segment pneumatic soft robot to regulate the tip position. Color-based camera tracking using colored markers embedded around a worm-like soft robot is described in [15]. These markers allow a single camera to determine the 2D position of an actuator within the field of view of the camera. The employment of 3D vision enabled by RGB-D cameras [497] and stereo cameras have also been reported for soft robotic arms [498], [499].

TABLE 7. Summary of model-based controllers for soft pneumatic actuators. ESOLD: empirical second-order lumped dynamics, VVC: variable volume chamber, CVC: constant volume chamber, NVM: nonlinear valve model, NTM: nonlinear tube model, EL: Euler-Lagrange, ESOD: empirical second-order dynamics.

Task	Model Pneumatic	Motion	Valve	Sensing	Estimation	Controller	Ref.
Bending	ESOLD		Proportional	Pressure, Optical		Sliding mode	[129]
Bending	ESOLD		3/2 On/off	Pressure, Magnetic		Iterative liding mode	[127]
Bending	ESOLD		3/2 On/off	Pressure, Magnetic		Model reference adaptive control	[236]
						Dynamic feedforward control	
Bending	ESOLD		3/2 On/off	Pressure, Optical		Sliding mode with feedforward	[235]
Bending	VVC, NVM, NTM		Proportional	Pressure, Flow		Sliding mode, PID	[467]
Bending	ESOLD		3/3 On/off	Pressure, IMU		Sliding mode with PID surface	[134]
Bending	VVC, NVM	ESOLD	Dual 2/2 on/off	Pressure, Resistive		Robust backstepping	[237]
Bending	CVC, NVM	ESOLD	Dual 3/2 on/off	Pressure, Inclinometer		Backstepping, Sliding mode, PID	[238]
Bending	CVC, NVM	ESOLD	Dual Proportional	Pressure, Inclinometer		Backstepping, Sliding mode	[239]
						PID with feedforward	
Bending		EL		Pressure, Resistive		Robust PD-type controller	[230]
Bending		EL		Pressure, Resistive	Sliding mode observer	Adaptive sliding mode	[231]
Bending	VVC, NVM, NTM		5/3 Proportional	Pressure, IMU	Static inverse measurement	Sliding mode, PID	[482]
Bending		ESOD	Proportional		Extended state observer	Nonlinear error feedback control	[459]
Extension		ESOD	Proportional	Pressure, Inductive		PID	[396]

Motion capture allows high accuracy sensing and control; however, there are several difficulties. First, an unobstructed line of sight from the actuator to the camera system is required for stable visual feedback. Second, visual servoing requires the development and use of robust image processing algorithms, such as image segmentation, auto-focusing, contour detection, image distortion, object recognition, and 3D reconstruction. Third, camera calibration plays an essential role in vision-based robotic systems. The calibration includes the estimation of intrinsic and extrinsic parameters, which require time and effort in the preparation stage. Computational speed may also restrict the use of this method. Fourth, many stationary cameras surrounding the markers are required to resolve the 3D orientation and translation of the tracked object.

D. MODEL-FREE AND DATA-DRIVEN MODELING AND CONTROL

As previously discussed, soft robots are difficult to control with conventional model-based controllers. Also, analytical models for SPAs are usually established based on assumptions that are only applicable to certain simplified designs and in structured environments. This has created fertile ground for the application of machine and deep learning approaches in soft robotics [257].

Effective bending control of SPAs is challenging due to nonlinearities arising from the pneumatic system and material properties. The nonlinearity due to solenoid valves has been modeled using a data-driven machine learning technique [405]. A purely data-driven approach can be used to control the bending angle of soft actuators using a static model with combined measurements from commercially available pressure and flex sensors [404], [405]. This approach avoids the need for precise physical and material models, and the experimental data generated implicitly accounts for variations in operating conditions that are otherwise difficult to model mathematically. However, this approach requires sufficient experimental data describing the

behavior of the SPA under various operating conditions so that the derived models can be generalized to new untrained scenarios [404]. To better understand the dynamics of SPAs in unconstrained dynamic settings, data-driven modeling might be used to learn nonlinearity and hysteresis in SPA dynamics models. The visco-hyperelasticity of SPAs was modeled using a modified Kelvin–Voigt model in [500]–[503]. Model-based feedback control could be achieved using the suggested model, which was confirmed using experimental data to properly capture the SPA’s nonlinear and hysteresis behavior.

Hyperelastic material characteristics and design geometry make the kinematics of SPAs extremely nonlinear in an unstructured environment [404]. Linear regression and artificial neural network (ANN) models were shown to predict the bending angle of SPAs with more accuracy than the linear regression model in [504]–[506]. ANN models were used to approximate the Jacobian function of SPAs and find the PID gains of the controller to attenuate external disturbances [334]. Due to the nonlinearity of SPAs, conventional PID controller design methods may not be appropriate. As an alternative, position tracking accuracy was improved using cascade controllers with machine learning to optimize PID gains [507], [508]. Extended Kalman Filters and nonlinear observers based on wavelet and sigmoid networks were created to accurately forecast SPA behavior [456]. Nonlinear regression was employed to simulate SPA behavior in an unstructured environment using a flexible sensor.

Reinforcement learning (RL) can be implemented as model-based learning in SPAs. In model-based RL, optimal feedback commands are calculated based on supervised learning algorithms to minimize a cost function [267], [509], [510]. The data required for training is acquired from sensors during the interaction of soft robots with their surroundings. A model-free approach, on the other hand, eliminates the need to learn a model to predict optimal actions [511]. Control rules can also be optimized through model-free approaches known as Q-learning [284], [512]–[515]. A direct

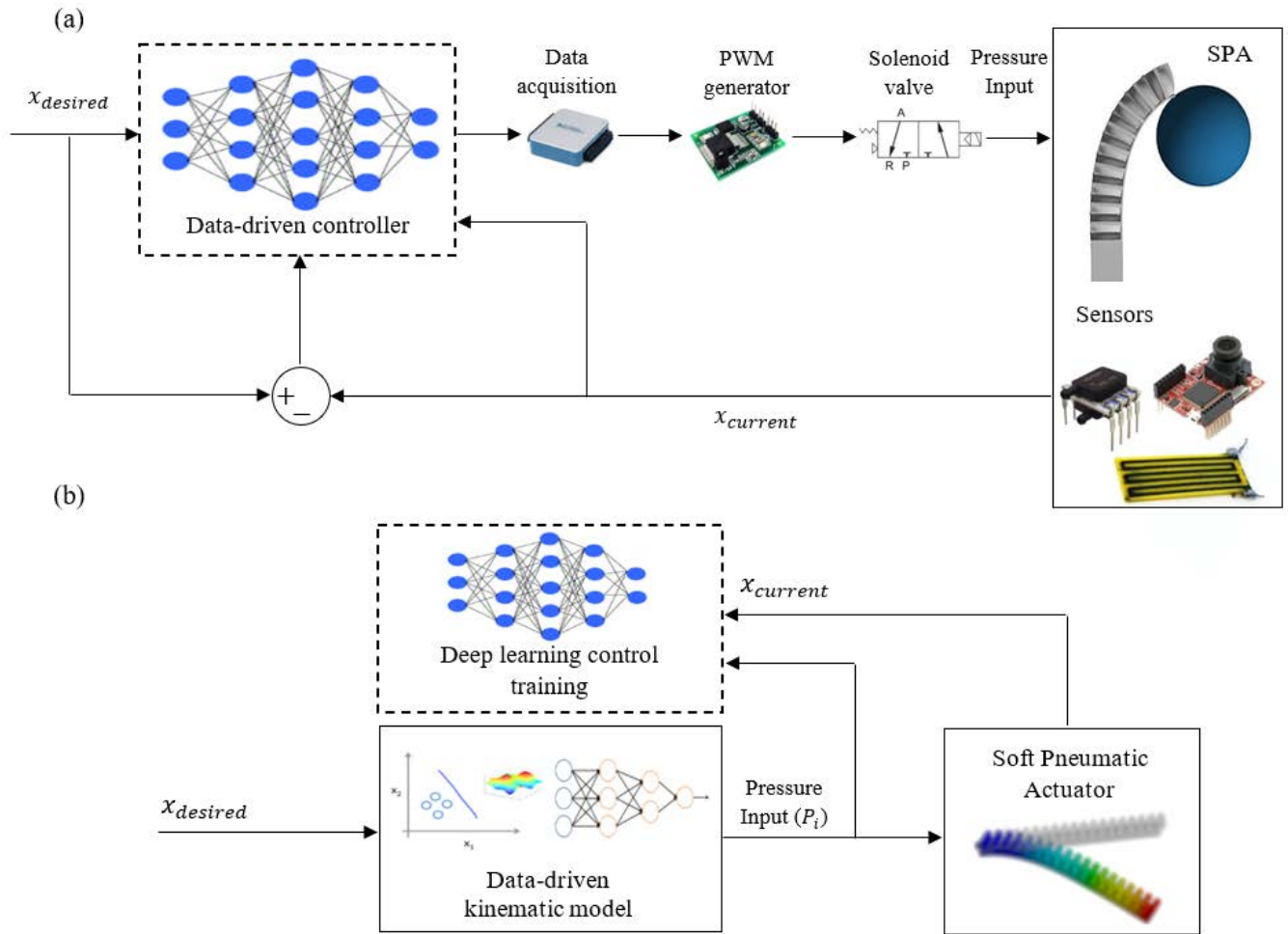


FIGURE 8. Schematic procedure of: (b) data-driven deep learning control policies training and (a) closed-loop data-driven control of SPAs.

policy model-free method for closed-loop dynamic control of SPAs can be implemented in three steps. First, the forward dynamics can be formulated using training data and a deep learning ANN algorithm to generate the possible trajectories of the SPA [516]. Trajectory optimization algorithms generate samples to learn open-loop control policies in real environments [517]. Next, the trajectories provide samples for the appropriate control action to drive each region of the manipulator to the desired states. To develop a closed-loop optimal control policy, the control actions for each reachable state of the manipulator are required. Finally, accessing all the new trajectories, a supervised learning model can be employed to directly learn the appropriate closed-loop control policies for each system state via the dynamic adaptability of deep and RL algorithms [516].

Deep learning is an autonomous training algorithm based on existing data to identify trends. Additionally, the algorithm is capable of producing predictions for new future data by altering previous patterns using several ANN layers [518]. As a result of recent advances in deep learning, prediction

models can now be built for SPAs that analyze unexpected data sets in an unstructured environment based on the model earlier developed using training data [519]. The combination of deep learning and RL has shown encouraging results in the control of autonomous SPAs [520], [521]. Reinforcement learning is used to extract needed information from embedded printed sensors, and to optimize the control algorithm in response to environmental conditions [522], [523]. Using FEM as part of a machine learning loop may also help reduce risk factors by exploring additional movements and situations. Fig. 8 illustrates a procedure for the data-driven control of SPAs.

Soft pneumatic actuators have seen a radical development in manufacturing and design with the aid of 3D printing and functional materials [524]–[526]. Therefore, a concurrent advancement in deep learning algorithms is required to provide increased autonomy when dealing with complex manipulation tasks, which may include stable operation with uncertain and perhaps fragile environments [29], [527]–[534].

TABLE 8. Summary of bioinspired pneumatic soft robots. Adapted with permission from [276].

Animal/Feature	Bioinspiration	Applications	Actuation/Movement Principle	References
Octopus/Cephalopod Tentacles	Muscular Hydrostats Kinematics	Soft Grasping	Pneumatic Artificial Muscles	[540]–[542]
Elephant Trunk	Muscular Hydrostat Kinematics	Soft Grasping	Pneumatic Artificial Muscles	[543]
			Tendon Guided Pneumatic Actuation	[23], [389]
	Stiffness Adjustable Compliant Gripping	Soft Grasping	Pneumatic	[544]
Worm	Muscular Hydrostatic Locomotion through Propagating Waves	Complex Terrain Navigation	Pneumatic Artificial Muscles with Jamming	[545]
	Peristaltic Locomotion	Pipe-crawling	Fiber-Reinforced Pneumatic Actuator	[14], [79], [122]
	Inchworm Locomotion	Locomotion in Confined Spaces	Pneumatic Bending	[546]
Caterpillar	Propagating Wave Motion	Locomotion in Confined Spaces	Pneumatic	[547]
	Propagating Wave Motion and Passive Adhesion Feet	Climbing	Pneumatic Actuation with Compliant Gripping	[548]
	Propagating Wave Motion and Passive Adhesion Feet	Confined Space Locomotion	Pneumatic Actuation with Friction Gripping	[549]
Snake	Serpentine and Sidewinding Motion	Ground-based Locomotion	Pneumatic Bending Actuator	[135]
	Climbing Locomotion through Coiled Grasping	Tree Climbing	Pneumatic	[550]
	Serpentine Motion	Ground-based Locomotion	Pneumatic Bending Actuator	[10], [323]
			Fibre Reinforced Pneumatic Actuator	[12]
Gecko	Climbing through adhesion and gait	Climbing Mobile Robots	Pneumatic Kinematics/Active Suction	[551]
Quadruped	Walking Gait	Human Assistance	Tendon Guided Pneumatic Actuation	[552]
	Dynamic Galloping Gait	High-Speed Locomotion	Bistable Pneumatic Actuator	[553]
Fish	Underwater navigation through tail and fin movement	Aquatic Mobile Robots	Pneumatic Bending via Synthetic Vascular System	[554]
	High-speed maneuverability of flexible tail	Aquatic Mobile Robots	Pneumatic Bending	[16]
Rays/Batoid	Swimming through Undulatory Flapping Motion	Aquatic Locomotion	Pneumatic Bending	[20]
			Tendon Guided Pneumatic Actuation	[555]
Squid	Soft Morphing Fins	Aquatic/Aerial Hybrid Locomotion	Pneumatic Bending Actuator	[17]
Frog	Paddling Gait	Aquatic Locomotion	Pneumatic	[556]
Starfish	Multigait Locomotion	Rough Terrain Exploration	Pneumatic Artificial Muscles	[557]
			Pneumatic Bending Actuator	[558]
Octopus	Soft Body	Soft Mobile Robots	Fluidic via a Chemical Reaction	[4]
Octopus Tentacle	Positive Pressure Adhesion	Climbing Inclined Surfaces	Pneumatic	[559]

VIII. APPLICATIONS

A. BIOINSPIRED SOFT ROBOTS

Biological creatures have designs that evolution has spent millennia perfecting. Animals exploit soft structures to move effectively in complex natural environments. They can achieve locomotion such as morphing, squeezing, climbing, growing, and crawling that would not be possible with an approach based only on rigid links. Consequently, bioinspired design has proven to be extremely beneficial toward the advancement of soft robotics [9]. Soft roboticists have often drawn inspiration from the rich and diverse set of designs found in nature, including natural materials, actuators, and locomotion strategies. We also note that, although complete understanding and duplication of the complex actuation mechanisms of biological materials and structures are unlikely in the foreseeable future, bioinspired designs will continue to be an important source of inspiration for the design of soft robots [535].

The following section discusses some common bioinspired designs. A summary of bioinspired soft robotic designs are presented in Table 8. For further details on bioinspired materials, structures and locomotion modes, the reader is referred to [536]–[539].

1) ELEPHANT TRUNKS AND OCTOPUS TENTACLES

Soft continuum manipulators inspired by muscular hydrostats (such as octopus tentacles and elephant trunks) have been investigated for more than two decades. The parallel bellows

continuum actuator described in [22] and included in AMADEUS [560] consists of three oil-filled bellows and is controlled by hydraulic pressure. Two other popular pneumatic designs are the Air-Octor [389] and OctArm [543]. The Air-Octor consists of a single central chamber (dryer hose) with 3 cables separated by 120°, it is less complex to build and control but has high cable friction and low flexibility and strength. The OctArm consists of multiple pressurized chambers (McKibben actuators), it is flexible and has good strength and performance, but is complex to build and control. A new design proposed in [23] combines the advantages of both of these designs in a single central rubber tube covered with an expandable nylon sleeve and three cables.

2) WORM AND SNAKE-LIKE SOFT ROBOTS

A popular alternative for locomotion in soft robotics is peristaltic crawling, whereby longitudinal muscles are contracted in the anchoring segments, while circumferential muscles are contracted in the advancing segments [561]. Pneumatic-driven soft peristaltic robots composed of three artificial muscles were discussed in [14], [15], [122]. They consist of a back radial actuator, a central axial actuator, and a frontal radial actuator. The posterior and anterior actuators are used to anchor the robot, while the central actuator is used to extend and contract the robot. This mechanism can be used to develop catheters and endoscopes to navigate inside the human digestive and circulatory systems with

little human intervention [14]. The inchworm-inspired soft robot developed by [546] is composed of three modules with two bending PneuNet actuators and can reach a speed of 7.89 mm/s and pass obstacles with a height 42.8 mm. The addition of adhesive feet enables inchworm soft robots to climb smooth vertical surfaces. In [559], two adhesive feet deform in response to pressure, and a central pneumatic bending actuator produces forward movement through cycles of expansion and contraction.

Soft snake robots, which utilize serpentine locomotion, have also been developed to navigate unstructured terrain and confined spaces [10], [12], [135], [317], [323]. Serpentine motion relies on anisotropic friction to generate a forward thrust that exceeds the drag produced by its body [537]. In Onal *et al.* [10], the robot consists of four bidirectional fluidic actuators in series with valves and passive wheels attached between segments and on-board electronics at the tail. A detailed model of this robot is reported in [323] using a similar approach to [562]. In [11], a new thin and long fluidic elastomer actuator with semi-circular shape and fiber reinforcements is proposed for snake robots, resulting in high deflection and short response time. Fiber-reinforced actuators were also used in [12]. Qin *et al.* [135] presented a soft robotic snake, where each tube is made of silicone rubber wrapped in thread and the three tubes are fused together with silicone.

3) FISH AND RAY-INSPIRED SOFT ROBOTS

Despite the diversity of aquatic locomotion methods, swimming soft robots are primarily inspired by the flapping motion of fishtails [16], [563] or the undulatory waves produced by rays' pectoral fins [20]. Soft ray robots generate waves through one or more multichamber pneumatic bending actuators on each side of the ray. While a single actuator produces an up-down flap of each fin, multiple actuators enable more complex traveling waves. In [20], fiber-reinforced actuators with bidirectional motion are analyzed using FEM and employed to drive a manta robot composed of silicone rubber. Drawing inspiration from PneuNets actuators, multichambered fins have been developed in [17], [466]. In contrast, 10 tendon-guided pneumatic actuators enable smooth continuous motion in [555].

B. BIOMEDICAL APPLICATIONS

Soft robots can elastically deform and adapt their shape to external constraints and obstacles, which makes them ideal for biomedical devices. Compared to conventional robots, soft robots do not compromise tissue integrity, freedom of movement, conformability, and overall human bio-compatibility [564], [565]. In the following, the main biomedical applications of fluid-driven soft robotics are reviewed.

1) MINIMALLY INVASIVE SURGERY

Soft robotic devices have been developed for improved maneuverability and safety during surgical procedures.

Robotic steerable catheters and endoscopes can reduce trauma, pain, blood loss, and recovery time [41], [56], [565]. The most popular designs for steerable catheters using fluidic actuation resemble the flexible microactuator of Suzumori *et al.* [130], [131]. Garbin *et al.* [83] has proposed a disposable pneumatic endoscope composed of off-the-shelf rubber bellows. An endoscope for colonoscopy was developed in [573] with three active pneumatic chambers and three additional chambers to reduce the radial expansion of the active chambers. A 6-mm diameter two-DoF soft pneumatic actuator, able to bend more than 180 deg in every direction and incorporating a 1 mm working channel, is presented in [574] for endoscopy. An 18 mm diameter inchworm-inspired soft robot for colonoscopy is reported in [575] and consists of two balloons connected by a three-DoF soft pneumatic actuator. A low-cost, soft robotic endoscope for gastrointestinal tract procedures was presented in [576]. Ikuta *et al.* [312], [577], [578] has designed a single-input, multi-output control mechanism for soft catheters in which a single input system drives bellows-type actuators. Forceps manipulator with four chambers and metal spring reinforcements are proposed in [579] for surgical robots, which achieved bending motion in two DoF and maximum angle of 53 deg. Pneumatically actuated, origami-inspired soft robots have also been explored for gastrointestinal endoscopic applications [580] and neurosurgical brain retraction [581].

A multi-module variable stiffness manipulator was developed in [24], [381] for surgical applications (Fig. 9a). The so-called STIFF-FLOP (STIFFness controllable Flexible and Learnable Manipulator for surgical OPERations) offers omnidirectional bending and includes variable stiffness through granular jamming and an external braided sheath to limit radial expansion and maximize longitudinal deformation. A 2-module robot also offering omnidirectional motion is proposed in [106] for laparoscopic procedures which includes an internal free lumen along the central axis to guide flexible endoscopic tools or house endoscopic sensors. A stiffening system based on fiber jamming transition (Fig. 9b) is discussed in [368] to widen the applicability of the STIFF-FLOP by increasing its stability and producing higher forces. A soft polymer tip with 50 μm diameter microfluidic channels distally attached to a 1.6 m catheter with a contiguous lumen is presented in [582], where the authors have demonstrated the ability of their device to navigate through vessels and to deliver embolization coils to the cerebral vessels in a live porcine model.

2) WEARABLE ROBOTICS, REHABILITATION, AND ASSISTANCE

Over the last decade, the number of publications on soft wearable robotics has increased 10 fold [583]. Due to advantages such as high power density, high output force, compliance, durability, and affordability, pneumatically actuated soft structures are used in wearable robotics applications such as ankle-foot orthosis, exosuits for gait and upper



FIGURE 9. Biomedical application of pneumatic soft robotics: (a) STIFF-FLOP [566], (b) novel STIFF-FLOP with fiber jamming [368], (c) soft robotic gastric simulator [567], (d) soft robotic heart sleeve [568], (e) soft robotic glove [569], (f) soft elbow exosuit [570], (g) soft robotic ankle-foot orthosis exosuit [571], (h) pneumatic force jacket [572], and (i) I-support soft arm for bathing assistance [564]. All figures are reproduced with permission.

body rehabilitation, robotic gloves for hand and thumb rehabilitation, assistive robots for elderly care and haptic feedback systems [584]–[587].

Wearables with pneumatic actuation can be based on chambered actuators or fabric-based inflatables and textiles [583], [588]. Such actuators have been used for joint rehabilitation of the finger, hand, wrist, elbow (Fig. 9f), ankle (Fig. 9g), and shoulder [58], [324], [589]–[591]. Other applications include massage [592] and functional assistance [123], [593], [594]. Pneumatic actuators are also used in assistive devices such as soft wearable upper and lower exoskeletons for human performance augmentation [595]–[598]. In [189], a pneumatic jamming ankle used variable stiffness tendons to damp impacts and improve the ability to traverse variable terrains. An elastic ligament was used to reduce the peak load experienced by an elbow in [599].

Haptic feedback systems based on soft pneumatic actuators assist stroke patients by improving the biofeedback provided during their rehabilitation process [600]–[602]. Other haptic applications include actuator skins for contact sensing and vibrotactile feedback [603], soft inflatable rings for rich haptic feedback [604], soft inflatable balloon actuators for robotic surgery [605], worn haptic interfaces (e.g., armbands) [606], and for tactile sensing on fingertips [607], [608]. Soft pneumatic hands may soon recover some of the function from lost upper limbs [609] with integrated tactile feedback and simultaneous myoelectric control [610]. Soft wearable pneumatic gloves [569] (Fig. 9e) are potential candidates for virtual reality applications [611].

3) IMPLANTABLE DEVICES, ARTIFICIAL ORGANS, AND BODY SIMULATORS

Soft robotic devices for the heart, including ventricular assist and direct cardiac compression devices, have received significant attention due to their relatively simple function

(similar to a pump) and can assist cardiac function, which may be required before transplant. A soft robotic sleeve with embedded McKibben-based actuators is proposed in [242], [568] (Fig. 9d), which is implanted around the heart and actively compresses and twists to act as a cardiac ventricular assist device. Alternatively, individual McKibben actuators are wrapped around the heart ventricles in [612] to contract and relax in synchrony with the beating heart. Soft actuators with a McKibben pneumatic artificial muscle design are also used in [613] to provide external compression to the outer ventricle wall and, therefore, dynamically augment left ventricular contraction. Entire soft artificial hearts have also been explored using soft silicone [614], fluid-powered low-density foam actuators [615], and 3D-printed lost-wax casting techniques [616].

Soft body simulators can be used to simulate the physiological motions of the human body for training applications and to reduce animal or human testing. A soft robotic gastric simulator is discussed in [567], [617] that emulates peristaltic contractions using an array of circular air chambers (Fig. 9c). A soft robotic respiratory simulator is addressed in [618] which recreates the motion and function of the diaphragm using pneumatic artificial muscles. A soft robotic esophagus with layers of pneumatic hollow chambers is developed in [619] for stent testing.

C. GRIPPERS AND PARALLEL MANIPULATORS

Soft manipulators are continuum arms that are used for manipulation tasks [40], [42] or gripping. A soft manipulator can also be equipped with a soft gripper [63] for improved maneuverability [39], [620]. Soft robotic grippers can employ two [621], [622], three [623]–[625] or four fingers, and may use vacuum jamming mechanisms, or employ suction. Soft grippers come in many varieties to suit the wide range of applications [39]. Soft grippers based on SPAs can be

fabricated using commercially available soft materials, and can handle a wide variety of payload stiffnesses without the need for closed-loop control. Due to their inherent softness, pneumatic grippers are safe to operate alongside humans and in unstructured environments. Soft grippers based on SPAs are widely used for pick and place applications [626]–[628], including fruit and vegetable harvesting [629], food packing [630], and warehouse automation. Soft grippers based on SPAs can be designed with self-healing properties [631], conformability [632], dexterity [633], versatility [625], [634], high payload [120], [635], stiffness variation [347], [636], enhanced grasping [637] and micro-gripping capabilities [191].

The development of universal grippers that can handle a wide variety of objects remains a challenge. To overcome this in both static and dynamic conditions, a large contact area between the object being handled and the gripper is required [632]. Layer-jamming suction grippers with a kirigami pattern for stiffness tuning were developed by [363], which only requires a single vacuum pump, and is able to lift 154 times its own weight for curved surfaces. In [473], a soft manipulator was equipped with a bionic polydimethylsiloxane nanofiber film to increase friction and achieve grasping performance under wet or slippery conditions. In [632], [638], a 3D-printed modular soft gripper with highly conformal fingers was developed with positive pressure bending soft pneumatic actuators. The passive component consists of a soft auxetic structure and compliant ribs which enhances the conformability of the soft gripper and reduces out-of-plane deformation.

IX. DISCUSSION

A. CAPABILITIES

SPAs possess several capabilities and functionalities which make them the most used actuators in soft robotic systems including self-healing properties, fail-safe features, resilience, scalability, customizability, modularity, multimodal programmable actuation, fast actuation, and most importantly their amenability to different 3D printing technologies. A review of these capabilities is included below.

1) SELF-HEALING

The ability of biological muscles to self-heal after being damaged or mechanically stressed is a desirable property because any damage or crack in their structure would lead to air leaks and consequently their failure [639]–[641]. Developing SPAs with self-healing properties lead to the realization of more mechanically robust soft systems that can handle extreme mechanical loading without catastrophic failure [641]. Sunlight can be focused on the structure of soft bidirectional bending actuators to rapidly self-heal punctures and restore functionality [642]. SPAs with self-healing capabilities were used to develop soft grippers, hands, and artificial muscles [631], [643]. Another example is the ability

of SPAs to self-heal and re-operate after being cut into different pieces and then brought into contact [644].

2) SAFETY

SPAs can remain functional after a rupture or crack in their structure. For instance, vacuum-based SPAs remain operational under a continuous supply of negative pressure [87], [137]. Positive pressure SPAs based on a composite of elastomer and fibers resist puncture from sharp objects and continue to operate even after being punctured [645]. SPAs are highly resilient [646], [647] due to their tolerance to extreme mechanical deformation and harsh environments [648]–[650].

3) SCALABILITY AND MODULARITY

SPAs can be scaled in their overall size and internal volume from micro-scale to macro-scale and extremely large robots [651]. Miniature soft robotic systems and devices include grippers, artificial muscles, locomotion robots, and camouflage robots [191], [193]. SPAs can be ultrathin for applications requiring lightweight robots that can fit in small spaces [652].

Similarly, macro-sized SPAs can be scaled either in terms of their internal volume or in terms of the number of actuators assembled in one single unit [87]. Modular SPAs allow soft robots to self-reconfigure so that they can form new morphologies and consequently adapt to different environments and tasks [184], [653]. In addition, the modularity of SPAs allows the distribution of actuation and sensing, and consequently improves the functionality and reliability of the actuators and leads to reduced overall costs [654], [655]. Distributed actuation and sensing allow for different configurations of the same soft robot to target specific requirements [13], [601], [656], [657].

4) MULTIMODAL ACTUATION

SPAs that can bend, twist, contract, and extend simultaneously are essential for various robotic applications that require multiple modes of deformation to accomplish the desired task. For example, the gripping performance of a soft gripper can be enhanced by using soft helical actuators that wrap around grasped objects to realize a firm grip by generating bending and twisting motions simultaneously [18], [658], [659]. The function of soft actuators can be programmed by 3D printing [173], [660], or by fiber orientation [96], [122] and structures such as soft pads [661]. Vacuum-based SPAs generate simultaneous linear and twisting motion [662]. Bellow-inspired actuators generate linear and bending motion [50], [87] and additional twisting in some designs [124]. Bubble SPAs are monolithic actuators where shape can be tailored to applications ranging from artificial muscles to grippers. [663].

5) FAST ACTUATION

SPAs can be designed to actuate very rapidly, e.g., fast PneuNets. The components of a pneumatic system can be

selected to reduce the rise time of the actuator response, as discussed in Section V-D. Alternatively, elastic instabilities can be harnessed to realize fast SPA-based locomotion robots [553] and actuators [664]. Similarly, the stored elastic energy in SPAs is exploited to achieve very fast actuation speeds [665]. Ultra-fast miniature SPAs were constructed using melt electrowriting [666]. SPAs can also be actuated rapidly through the use of valves with snapping shells [667].

B. CHALLENGES AND FUTURE OUTLOOK

A number of challenges limit the performance of soft robotic actuators, as discussed below. Despite these challenges, the future of soft robotics is promising in terms of growth and adaptation to a wide range of applications [668], [669]. For each of these limitations, we also present recent efforts and directions for future research.

1) PORTABILITY

SPAs require a pneumatic source that is typically larger than the actuator itself and may include a pump, power supplies, driving circuits, and pneumatic valves. This equipment limits the adoption of SPAs in portable applications such as robotic hands [670]. Peripheral components can be significantly downsized when only small forces or deformations are required [603]. Many research projects are currently underway to develop lightweight and portable pneumatic pumps [671], hydraulic and self-healing soft portable pumps [672], and electronics-free pneumatic circuits for soft robots control [673].

2) NOISE AND VIBRATION

SPAs do not emit significant acoustic noise but their actuation requires potentially noisy air compressors or vacuum pumps, which are undesirable in many applications [674]. This challenge is being addressed by silent pumps based on electrostatically actuated pressure vessels [675] and bidirectional pumps based on charge-injection electrohydrodynamics [676]. Vibration in soft actuator responses are usually a result of the small natural damping of soft materials, but can also arise from the pneumatic system, e.g., on/off valves. Note, however, in some applications, such as granular jamming [359], vibration can be desirable. In addition, note that noise and vibration also limit the portability of SPAs since they reduce patient comfort and satisfaction, especially when additional volume or weight is required for their suppression.

3) ADDITIVE MANUFACTURING AND FABRICATION TIME

One of the foremost challenges in 3D printing is the development of materials with low elastic moduli, for example, when attempting to mimic tissue with a modulus ranging of 3 kPa to 900 kPa [55], [642]. To address such a challenge, novel additive manufacturing technologies along with polymer chemistries must be developed [55]. Recently developed 3D-printable materials such as silicones [177] and hydrogels [677] can be used. Moreover, multi-material 3D

printing is essential to fabricate soft actuators and robots in a single manufacturing step [332].

3D printing technologies such as FDM require multiple hours to produce a single airtight SPA [87]. However, the printing speed can be increased using novel 3D printing technologies to produce silicone-based soft pneumatic actuators [678]. The capability of FDM to produce complex geometries and features such as thin walls also requires improvement.

4) 3D-PRINTED INTEGRATED SENSING

Composite materials are the focus of current studies to enhance the durability and performance of 3D printed sensors. Advances in fabrication include new materials and machine learning algorithms [679]–[681]. The quality of 3D printed sensors tends to be sensitive to common artefacts of 3D printing such as delamination between layers and discontinuity. Continuous operation reduces the longevity of 3D-printed SPAs with integrated sensors due to the lifetime of conductive circuits. Further advances in soft sensing will require soft structures with individual layers with specific optical, electrical, and magnetic characteristics. This is expected to require multi-material 3D printing, external fields during printing, or core-shell printing to introduce heterogeneities or anisotropies.

5) MASS PRODUCTION, REPEATABILITY AND REPRODUCIBILITY

The majority of SPAs in the literature are produced using slow prototyping methods that are not suitable for mass production. At present, mass production tends to be in-house, which requires significant repeat development of processes. We also recall that the molding fabrication process using silicone rubbers is time-consuming and requires significant manual assembly, which can create issues with repeatability and reproducibility.

On the other hand, 3D-printed soft robots can be easily mass-produced and address the aforementioned issues with molding. Advances in 3D-printing equipment, automation methods and the inclusion of learning-based techniques towards integrated fabrication workflows are expected to facilitate mass production. For example, an advanced computerized machine knitting method is proposed in [682] to manufacture pneumatic knitted actuators towards viable mass production. Alternatively, topology optimization can be used to simplify the mechanical structure of SPAs, which increases reproducibility and the potential for mass production [683].

6) NONLINEAR MATERIAL PROPERTIES AND DURABILITY

The nonlinearities arising from material properties affect the performance of SPAs and hinder the development of modeling and control techniques. Visco-hyperelasticity, stress-softening, hysteresis and polymer aging, for example, affect the dynamic response of soft actuators and result in nonlinear time and rate dependent behavior [240], [684]. Data-driven modeling might be used to learn these nonlinearities in dynamic models for SPAs [685]. Material-based models for

viscoelastic behavior have been developed in [500] using a modified Kelvin-Voigt model, and in [240] by measuring stress relaxation. A Bouc-Wen hysteresis model is presented and experimentally validated in [686] for a pneumatic muscle. In [684], hysteresis is modeled and compensated using the Prandtl-Ishlinskii method.

These characteristics also affect the durability and lifetime of SPAs, i.e., the maximum number of cycles that the actuators can sustain before failure. We note that the lifetime of soft actuators can be improved using materials with self-healing capabilities and by exploiting the fail-safe feature of vacuum-based SPAs, as discussed in Section IX-A.

7) IMPACT AND ACCESSIBILITY

The rapid growth in soft robotics has highlighted the need to consider the impact and contribution of soft robotics to the wider fields of robotics and engineering [687]. For example, are soft robotic devices addressing practical industrial challenges? And are the proposed design and fabrication methods cost-effective compared to conventional technologies? To address the somewhat limited scope of industrial applications of pneumatic-driven soft robots, a synergy between fundamental research in academia and applied research in industry is required. In addition, based on this review, it is clear that the advancements in the soft robotics field require multidisciplinary teams of scientists and engineers.

Accessibility to soft robotics can be improved by its inclusion in early formal academic programs. This will require the development of suitable soft robotics textbooks, and the availability of development kits that can be integrated into a curriculum. The field would also benefit from the availability of non-technical short courses that convey capabilities and limitations to end users such as biomedical device developers and health professionals.

8) COMPUTATIONAL MODELING

Although FEM studies have been widely employed for soft robotic modeling, the field has been primarily driven by experimental research and prototype-based development. Further work is required to improve the modeling of environmental interactions, and to reduce the reality gap between simulations and experiments. Future development in soft robotic applications will require fast simulation and optimization tools to support the design process and development of controllers [262]. Custom physics-based and differential simulators developed for soft robotic applications, such as ChainQueen and Elastica, are expected to grow in popularity and facilitate time-effective co-design of robot geometry, materials, and optimization-based closed-loop control [265]. Topology optimization techniques assisted by high-level calibration, machine learning and evolutionary design algorithms can also facilitate fast and automated soft robot design. A key challenge for future evolutionary soft robotics is the provision of techniques that

combine simulation with data-driven modeling and physical experimentation to combine scalability with practicality.

Alternatively, mesh-free methods such as Smoothed Particle Hydrodynamics (SPH) [688], [689] show strong potential to bridge the reality gap and have many advantages over mesh-based methods such as the FEM. SPH uses spatially distributed nodes, known as particles, to represent matter (whether solid or fluid) but, unlike FEM, these nodes are not constrained by element connectivity. Instead, the particles can flow and rearrange [690], which has many potential benefits in soft robotics. First, fluid interactions with deforming and moving solids can be handled naturally and without re-meshing [691]. Second, the mesh creation component of model development is not needed and therefore complex geometries can be considered with little additional pre-processing. Third, material history flows with deforming or moving matter which avoids the numerical diffusion in mesh-based methods and enables high levels of coupling between mechanical and chemical processes [692]. SPH has been used for human movement simulation in sports such as swimming, diving, and kayaking in which robotics algorithms are used to represent skeletal motions [693]–[695]. SPH has also been used to model swimming and crawling elastic worms in fluid [696], and coupled FEM-SPH methods have modeled thin elastic objects in a liquid [697]. It is expected that the benefits of SPH to soft robotics will increase as the technique advances and more software tools become available.

9) ROBUST STATE ESTIMATION AND INTELLIGENT CONTROL

The complex geometries and high compliance of soft actuators impose significant challenges to the development of sensing and control strategies, especially in real-world applications that involve interactions with the environment. Future work is expected to require the integration of multiple sensing techniques with robust sensor fusion for state estimation. Intelligent controllers will also be required that can provide high-level functionality without major design effort, for example self-learning methods.

X. CONCLUSION

This article provides an overview of soft pneumatic actuators including the design, fabrication, modeling, actuation, characterization, sensing, control, and applications. The capabilities of these actuators and associated challenges are also identified and discussed. We anticipate this article will inspire, guide, and assist current and prospective researchers to explore the soft robotics field and its advancements, as well as spark new ideas and multidisciplinary collaborations that can address current challenges.

REFERENCES

- [1] I. D. Walker, "Continuous backbone 'continuum' robot manipulators," *ISRN Robot.*, vol. 2013, pp. 1–19, Jul. 2013.
- [2] M. W. Hannan and I. D. Walker, "Kinematics and the implementation of an elephant's trunk manipulator and other continuum style robots," *J. Robot. Syst.*, vol. 20, no. 2, pp. 45–63, 2003.

- [3] S. I. Rich, R. J. Wood, and C. Majidi, "Untethered soft robotics," *Nature Electron.*, vol. 1, no. 2, pp. 102–112, Feb. 2018.
- [4] M. Wehner, R. L. Truby, D. J. Fitzgerald, B. Mosadegh, G. M. Whitesides, J. A. Lewis, and R. J. Wood, "An integrated design and fabrication strategy for entirely soft, autonomous robots," *Nature*, vol. 536, no. 7617, pp. 451–455, Aug. 2016.
- [5] P. Rothemund, Y. Kim, R. H. Heisser, X. Zhao, R. F. Shepherd, and C. Keplinger, "Shaping the future of robotics through materials innovation," *Nature Mater.*, vol. 20, no. 12, pp. 1582–1587, Dec. 2021.
- [6] C. Majidi, "Soft-matter engineering for soft robotics," *Adv. Mater. Technol.*, vol. 4, no. 2, Dec. 2018, Art. no. 1800477.
- [7] G. Robinson and J. B. C. Davies, "Continuum robots—A state of the art," in *Proc. IEEE Int. Conf. Robot. Autom.*, vol. 4, May 1999, pp. 2849–2854.
- [8] D. Trivedi, C. D. Rahn, W. M. Kier, and I. D. Walker, "Soft robotics: Biological inspiration, state of the art, and future research," *Appl. Bionics Biomech.*, vol. 5, no. 3, pp. 99–117, 2008.
- [9] S. Kim, C. Laschi, and B. Trimmer, "Soft robotics: A bioinspired evolution in robotics," *Trends Biotechnol.*, vol. 31, no. 5, pp. 287–294, May 2013.
- [10] C. D. Onal and D. Rus, "Autonomous undulatory serpentine locomotion utilizing body dynamics of a fluidic soft robot," *Bioinspiration Biomimetics*, vol. 8, no. 2, Mar. 2013, Art. no. 026003.
- [11] M. Luo, W. Tao, F. Chen, T. K. Khoo, S. Ozel, and C. D. Onal, "Design improvements and dynamic characterization on fluidic elastomer actuators for a soft robotic snake," in *Proc. IEEE Int. Conf. Technol. Practical Robot. Appl. (TePRA)*, Apr. 2014, pp. 1–6.
- [12] C. Branyan, C. Fleming, J. Remaley, A. Kothari, K. Tumer, R. L. Hatton, and Y. Menguc, "Soft snake robots: Mechanical design and geometric gait implementation," in *Proc. IEEE Int. Conf. Robot. Biomimetics (ROBIO)*, Dec. 2017, pp. 282–289.
- [13] X. Qi, H. Shi, T. Pinto, and X. Tan, "A novel pneumatic soft snake robot using traveling-wave locomotion in constrained environments," *IEEE Robot. Autom. Lett.*, vol. 5, no. 2, pp. 1610–1617, Apr. 2020.
- [14] A. A. Calderón, J. C. Ugalde, J. C. Zagal, and N. O. Pérez-Arancibia, "Design, fabrication and control of a multi-material-multi-actuator soft robot inspired by burrowing worms," in *Proc. IEEE Int. Conf. Robot. Biomimetics (ROBIO)*, Dec. 2016, pp. 31–38.
- [15] M. S. Xavier, A. J. Fleming, and Y. K. Yong, "Image-guided locomotion of a pneumatic-driven peristaltic soft robot," in *Proc. IEEE Int. Conf. Robot. Biomimetics (ROBIO)*, Dec. 2019, pp. 2269–2274.
- [16] A. D. Marchese, C. D. Onal, and D. Rus, "Autonomous soft robotic fish capable of escape maneuvers using fluidic elastomer actuators," *Soft Robot.*, vol. 1, no. 1, pp. 75–87, 2014.
- [17] T. Hou, X. Yang, H. Su, L. Chen, T. Wang, J. Liang, and S. Zhang, "Design, fabrication and morphing mechanism of soft fins and arms of a squid-like aquatic-aerial vehicle with morphology tradeoff," in *Proc. IEEE Int. Conf. Robot. Biomimetics (ROBIO)*, Dec. 2019, pp. 1020–1026.
- [18] W. Hu and G. Alici, "Bioinspired three-dimensional-printed helical soft pneumatic actuators and their characterization," *Soft Robot.*, vol. 7, no. 3, pp. 267–282, Jun. 2020.
- [19] J. Zhang, J. Tang, J. Hong, T. Lu, and H. Wang, "The design and analysis of pneumatic rubber actuator of soft robotic fish," in *Proc. Int. Conf. Intell. Robot. Appl.*, 2014, pp. 320–327.
- [20] K. Suzumori, S. Endo, T. Kanda, N. Kato, and H. Suzuki, "A bending pneumatic rubber actuator realizing soft-bodied manta swimming robot," in *Proc. IEEE Int. Conf. Robot. Autom.*, Apr. 2007, pp. 4975–4980.
- [21] Y. Cai, S. Bi, L. Zhang, and J. Gao, "Design of a robotic fish propelled by oscillating flexible pectoral foils," in *Proc. IEEE/RSJ Int. Conf. Intell. Robots Syst.*, Oct. 2009, pp. 2138–2142.
- [22] D. O'Brien and D. M. Lane, "3D force control system design for a hydraulic parallel bellows continuum actuator," in *Proc. IEEE Int. Conf. Robot. Autom.*, vol. 3, May 2001, pp. 2375–2380.
- [23] S. Neppalli and B. A. Jones, "Design, construction, and analysis of a continuum robot," in *Proc. IEEE/RSJ Int. Conf. Intell. Robots Syst.*, Oct. 2007, pp. 1503–1507.
- [24] M. Cianchetti, T. Ranzani, G. Gerboni, T. Nanayakkara, K. Althofer, P. Dasgupta, and A. Menciassi, "Soft robotics technologies to address shortcomings in today's minimally invasive surgery: The STIFF-FLOP approach," *Soft Robot.*, vol. 1, no. 2, pp. 122–131, 2014.
- [25] B. Gorissen, D. Reynaerts, S. Konishi, K. Yoshida, J.-W. Kim, and M. De Volder, "Elastic inflatable actuators for soft robotic applications," *Adv. Mater.*, vol. 29, no. 43, Nov. 2017, Art. no. 1604977.
- [26] P. Polygerinos, N. Correll, S. A. Morin, B. Mosadegh, C. D. Onal, K. Petersen, M. Cianchetti, M. T. Tolley, and R. F. Shepherd, "Soft robotics: Review of fluid-driven intrinsically soft devices; manufacturing, sensing, control, and applications in human-robot interaction," *Adv. Eng. Mater.*, vol. 19, no. 12, Dec. 2017, Art. no. 1700016.
- [27] M. S. Xavier, A. J. Fleming, and Y. K. Yong, "Finite element modeling of soft fluidic actuators: Overview and recent developments," *Adv. Intell. Syst.*, vol. 3, no. 2, Feb. 2021, Art. no. 2000187.
- [28] H. Mochiyama and T. Suzuki, "Kinematics and dynamics of a cable-like hyper-flexible manipulator," in *Proc. Int. Conf. Robot. Autom. (ICRA)*, vol. 3, Sep. 2003, pp. 3672–3677.
- [29] M. Calisti, M. Giorelli, G. Levy, B. Mazzolai, B. Hochner, C. Laschi, and P. Dario, "An octopus-bioinspired solution to movement and manipulation for soft robots," *Bioinspiration Biomimetics*, vol. 6, no. 3, Sep. 2011, Art. no. 036002.
- [30] F. Chen, W. Xu, H. Zhang, Y. Wang, J. Cao, M. Y. Wang, H. Ren, J. Zhu, and Y. F. Zhang, "Topology optimized design, fabrication, and characterization of a soft cable-driven gripper," *IEEE Robot. Autom. Lett.*, vol. 3, no. 3, pp. 2463–2470, Jul. 2018.
- [31] H. Jin, E. Dong, M. Xu, C. Liu, G. Alici, and Y. Jie, "Soft and smart modular structures actuated by shape memory alloy (SMA) wires as tentacles of soft robots," *Smart Mater. Struct.*, vol. 25, no. 8, Aug. 2016, Art. no. 085026.
- [32] W. Wang and S.-H. Ahn, "Shape memory alloy-based soft gripper with variable stiffness for compliant and effective grasping," *Soft Robot.*, vol. 4, no. 4, pp. 379–389, Dec. 2017.
- [33] S. Pourazadi, H. Bui, and C. Menon, "Investigation on a soft grasping gripper based on dielectric elastomer actuators," *Smart Mater. Struct.*, vol. 28, no. 3, Mar. 2019, Art. no. 035009.
- [34] G.-Y. Gu, J. Zhu, L.-M. Zhu, and X. Zhu, "A survey on dielectric elastomer actuators for soft robots," *Bioinspiration Biomimetics*, vol. 12, no. 1, Jan. 2017, Art. no. 011003.
- [35] X. Tang, K. Li, Y. Liu, D. Zhou, and J. Zhao, "A general soft robot module driven by twisted and coiled actuators," *Smart Mater. Struct.*, vol. 28, no. 3, Mar. 2019, Art. no. 035019.
- [36] X. Tang, Y. Liu, K. Li, W. Chen, and J. Zhao, "Finite element and analytical models for twisted and coiled actuator," *Mater. Res. Exp.*, vol. 5, no. 1, Jan. 2018, Art. no. 015701.
- [37] B. Pawlowski, J. Sun, J. Xu, Y. Liu, and J. Zhao, "Modeling of soft robots actuated by twisted-and-coiled actuators," *IEEE/ASME Trans. Mechatronics*, vol. 24, no. 1, pp. 5–15, Feb. 2018.
- [38] W. Dou, G. Zhong, J. Cao, Z. Shi, B. Peng, and L. Jiang, "Soft robotic manipulators: Designs, actuation, stiffness tuning, and sensing," *Adv. Mater. Technol.*, vol. 6, no. 9, Sep. 2021, Art. no. 2100018.
- [39] S. Zaidi, M. Maselli, C. Laschi, and M. Cianchetti, "Actuation technologies for soft robot grippers and manipulators: A review," *Curr. Robot. Rep.*, vol. 2, no. 3, pp. 1–15, 2021.
- [40] X. Chen, X. Zhang, Y. Huang, L. Cao, and J. Liu, "A review of soft manipulator research, applications, and opportunities," *J. Field Robot.*, vol. 39, no. 3, pp. 281–311, May 2022.
- [41] J. Zhu, L. Lyu, Y. Xu, H. Liang, X. Zhang, H. Ding, and Z. Wu, "Intelligent soft surgical robots for next-generation minimally invasive surgery," *Adv. Intell. Syst.*, vol. 3, no. 5, May 2021, Art. no. 2170046.
- [42] L. Zongxing, L. Wanxin, and Z. Liping, "Research development of soft manipulator: A review," *Adv. Mech. Eng.*, vol. 12, no. 8, Aug. 2020, Art. no. 168781402095009.
- [43] C. Tawk and G. Alici, "A review of 3D-printable soft pneumatic actuators and sensors: Research challenges and opportunities," *Adv. Intell. Syst.*, vol. 3, no. 6, Jun. 2021, Art. no. 2000223.
- [44] G. M. Whitesides, "Soft robotics," *Angew. Chem. Int. Edition.*, vol. 57, no. 16, pp. 4258–4273, Mar. 2018.
- [45] (2019). *Soft Robotics Toolkit*. Accessed: Mar. 27, 2019. [Online]. Available: <https://softroboticstoolkit.com/components>
- [46] M. Wehner, M. T. Tolley, Y. Mengüç, Y.-L. Park, A. Mozeika, Y. Ding, C. Onal, R. F. Shepherd, G. M. Whitesides, and R. J. Wood, "Pneumatic energy sources for autonomous and wearable soft robotics," *Soft Robot.*, vol. 1, no. 4, pp. 263–274, Dec. 2014.
- [47] M. S. Xavier, A. J. Fleming, and Y. K. Yong, "Design and control of pneumatic systems for soft robotics: A simulation approach," *IEEE Robot. Autom. Lett.*, vol. 6, no. 3, pp. 5800–5807, Jul. 2021.
- [48] N. El-Atab, R. B. Mishra, F. Al-Modaf, L. Joharji, A. A. Alsharif, H. Alamoudi, M. Diaz, N. Qaiser, and M. M. Hussain, "Soft actuators for soft robotic applications: A review," *Adv. Intell. Syst.*, vol. 2, no. 10, Oct. 2020, Art. no. 2000128.

- [49] T. Kalisky, Y. Wang, B. Shih, D. Drotman, S. Jadhav, E. Aronoff-Spencer, and M. T. Tolley, "Differential pressure control of 3D printed soft fluidic actuators," in *Proc. IEEE/RSJ Int. Conf. Intell. Robots Syst. (IROS)*, Sep. 2017, pp. 6207–6213.
- [50] M. S. Xavier, C. D. Tawk, Y. K. Yong, and A. J. Fleming, "3D-printed omnidirectional soft pneumatic actuators: Design, modeling and characterization," *Sens. Actuators A, Phys.*, vol. 332, Dec. 2021, Art. no. 113199.
- [51] L. Hines, K. Petersen, G. Z. Lum, and M. Sitti, "Soft actuators for small-scale robotics," *Adv. Mater.*, vol. 29, no. 13, Apr. 2017, Art. no. 1603483.
- [52] A. D. Marchese, R. K. Katschmann, and R. Daniela, "A recipe for soft fluidic elastomer robots," *Soft Robot.*, vol. 2, no. 1, pp. 7–25, 2015.
- [53] F. Schmitt, O. Piccin, L. Barbé, and B. Bayle, "Soft robots manufacturing: A review," *Frontiers Robot. AI*, vol. 5, p. 84, Jul. 2018.
- [54] J. Gul, M. Sajid, M. Rehman, G. Siddiqui, I. Shah, K.-H. Kim, J.-W. Lee, and K. Choi, "3D printing for soft robotics—A review," *Sci. Technol. Adv. Mat.*, vol. 19, no. 1, pp. 243–262, 2018.
- [55] T. J. Wallin, J. Pikul, and R. F. Shepherd, "3D printing of soft robotic systems," *Nature Rev. Mater.*, vol. 3, no. 6, pp. 84–100, Jun. 2018.
- [56] M. Runciman, A. Darzi, and G. P. Mylonas, "Soft robotics in minimally invasive surgery," *Soft Robot.*, vol. 6, no. 4, pp. 423–443, Aug. 2019.
- [57] X. Hu, A. Chen, Y. Luo, C. Zhang, and E. Zhang, "Steerable catheters for minimally invasive surgery: A review and future directions," *Comput. Assist. Surgery*, vol. 23, no. 1, pp. 21–41, Jan. 2018.
- [58] P. Polygerinos, S. Lyne, Z. Wang, L. F. Nicolini, B. Mosadegh, G. M. Whitesides, and C. J. Walsh, "Towards a soft pneumatic glove for hand rehabilitation," in *Proc. IEEE/RSJ Int. Conf. Intell. Robots Syst.*, Nov. 2013, pp. 1512–1517.
- [59] M. Wehner, B. Quinlivan, P. M. Aubin, E. Martínez-Villalpando, M. Baumann, L. Stirling, K. Holt, R. Wood, and C. Walsh, "A lightweight soft exosuit for gait assistance," in *Proc. IEEE Int. Conf. Robot. Autom.*, May 2013, pp. 3362–3369.
- [60] Y. Ansari, M. Manti, E. Falotico, Y. Mollard, M. Cianchetti, and C. Laschi, "Towards the development of a soft manipulator as an assistive robot for personal care of elderly people," *Int. J. Adv. Robotic Syst.*, vol. 14, no. 2, Mar. 2017, Art. no. 172988141668713.
- [61] A. D. Greef, P. Delchambre, and A. Delchambre, "Towards flexible medical instruments: Review of flexible fluidic actuators," *Precis. Eng.*, vol. 33, no. 4, pp. 311–321, Oct. 2009.
- [62] T. Noritsugu, "Pneumatic soft actuator for human assist technology," in *Proc. 6th Int. Symp. Fluid Power (JFPS)*, 2005, pp. 11–20.
- [63] J. Shintake, V. Cacucciolo, D. Floreano, and H. Shea, "Soft robotic grippers," *Adv. Mater.*, vol. 30, no. 29, Jul. 2018, Art. no. 1707035.
- [64] R. Deimel and O. Brock, "A compliant hand based on a novel pneumatic actuator," in *Proc. IEEE Int. Conf. Robot. Autom.*, May 2013, pp. 2047–2053.
- [65] A. Pagoli, F. Chapelle, J.-A. Corrales-Ramon, Y. Mezouar, and Y. Lapusta, "Review of soft fluidic actuators: Classification and materials modeling analysis," *Smart Mater. Struct.*, vol. 31, no. 1, Jan. 2022, Art. no. 013001.
- [66] C. Zhang, P. Zhu, Y. Lin, W. Tang, Z. Jiao, H. Yang, and J. Zou, "Fluid-driven artificial muscles: Bio-design, manufacturing, sensing, control, and applications," *Bio-Des. Manuf.*, vol. 4, no. 1, pp. 123–145, Mar. 2021.
- [67] A. Zolfagharian, M. A. P. Mahmud, S. Gharaie, M. Bodaghi, A. Z. Kouzani, and A. Kaynak, "3D/4D-printed bending-type soft pneumatic actuators: Fabrication, modelling, and control," *Virtual Phys. Prototyping*, vol. 15, no. 4, pp. 373–402, Oct. 2020.
- [68] J. Walker, T. Zidek, C. Harbel, S. Yoon, F. S. Strickland, S. Kumar, and M. Shin, "Soft robotics: A review of recent developments of pneumatic soft actuators," *Actuators*, vol. 9, no. 1, p. 3, Jan. 2020.
- [69] J. Zhang, J. Sheng, C. T. O'Neill, C. J. Walsh, R. J. Wood, J.-H. Ryu, J. P. Desai, and M. C. Yip, "Robotic artificial muscles: Current progress and future perspectives," *IEEE Trans. Robot.*, vol. 35, no. 3, pp. 761–781, Jun. 2019.
- [70] B. Tondou, "Modelling of the McKibben artificial muscle: A review," *J. Intell. Mater. Syst. Struct.*, vol. 23, no. 3, pp. 225–253, Feb. 2012.
- [71] B. Tondou and P. Lopez, "Modeling and control of McKibben artificial muscle robot actuators," *IEEE Control Syst. Mag.*, vol. 20, no. 2, pp. 15–38, Apr. 2000.
- [72] F. Daerden and D. Lefeber, "Pneumatic artificial muscles: Actuators for robotics and automation," *Eur. J. Mech. Environ. Eng.*, vol. 47, no. 1, pp. 11–21, 2002.
- [73] A. J. Veale, S. Q. Xie, and I. A. Anderson, "Modeling the peano fluidic muscle and the effects of its material properties on its static and dynamic behavior," *Smart Mater. Struct.*, vol. 25, no. 6, Jun. 2016, Art. no. 065014.
- [74] A. J. Veale, S. Q. Xie, and I. A. Anderson, "Characterizing the Peano fluidic muscle and the effects of its geometry properties on its behavior," *Smart Mater. Struct.*, vol. 25, no. 6, 2016, Art. no. 065013.
- [75] S. Konishi, F. Kawai, and P. Cusin, "Thin flexible end-effector using pneumatic balloon actuator," *Sens. Actuators A, Phys.*, vol. 89, nos. 1–2, pp. 28–35, Mar. 2001.
- [76] Z. Zhang, X. Wang, S. Wang, D. Meng, and B. Liang, "Design and modeling of a parallel-pipe-crawling pneumatic soft robot," *IEEE Access*, vol. 7, pp. 134301–134317, 2019.
- [77] X. Xue, Z. Zhan, Y. Cai, L. Yao, and Z. Lu, "Design and finite element analysis of fiber-reinforced soft pneumatic actuator," in *Proc. Int. Conf. Intell. Robot. Appl.*, 2019, pp. 641–651.
- [78] P. Polygerinos, Z. Wang, J. Overvelde, K. Galloway, R. Wood, K. Bertoldi, and C. Walsh, "Modeling of soft fiber-reinforced bending actuators," *IEEE Trans. Robot.*, vol. 31, no. 3, pp. 778–789, Jun. 2015.
- [79] M. S. Xavier, A. J. Fleming, and Y. K. Yong, "Experimental characterisation of hydraulic fiber-reinforced soft actuators for worm-like robots," in *Proc. 7th Int. Conf. Control, Mechatronics Autom. (ICCA)*, Nov. 2019, pp. 204–209.
- [80] K. C. Galloway, P. Polygerinos, C. J. Walsh, and R. J. Wood, "Mechanically programmable bend radius for fiber-reinforced soft actuators," in *Proc. 16th Int. Conf. Adv. Robot. (ICAR)*, Nov. 2013, pp. 1–6.
- [81] J. Fras and K. Althoefer, "Soft fiber-reinforced pneumatic actuator design and fabrication: Towards robust, soft robotic systems," in *Proc. Towards Auton. Robot. Syst. Conf.*, 2019, pp. 103–114.
- [82] Y. Miao and F. Chen, "Shape optimization of soft pneumatic bellows for high energy density," in *Proc. 27th Int. Conf. Mechatronics Mach. Vis. Pract. (M VIP)*, Nov. 2021, pp. 480–485.
- [83] N. Garbin, L. Wang, J. H. Chandler, K. L. Obstein, N. Simaan, and P. Valdastri, "A disposable continuum endoscope using piston-driven parallel bellow actuator," in *Proc. Int. Symp. Med. Robot. (ISMR)*, Mar. 2018, pp. 1–6.
- [84] G. Dämmer, S. Gablenz, A. Hildebrandt, and Z. Major, "PolyJet-printed bellows actuators: Design, structural optimization, and experimental investigation," *Frontiers Robot. AI*, vol. 6, p. 34, May 2019.
- [85] D. Drotman, S. Jadhav, M. Karimi, P. de Zonia, and M. T. Tolley, "3D printed soft actuators for a legged robot capable of navigating unstructured terrain," in *Proc. IEEE Int. Conf. Robot. Autom. (ICRA)*, May 2017, pp. 5532–5538.
- [86] J. Zhang, H. Wei, Y. Shan, P. Li, Y. Zhao, L. Qi, and H. Yu, "Modeling and experimental study of a novel multi-DOF parallel soft robot," *IEEE Access*, vol. 8, pp. 62932–62942, 2020.
- [87] C. Tawk, G. M. Spinks, M. Panhuis, and G. Alici, "3D printable linear soft vacuum actuators: Their modeling, performance quantification and application in soft robotic systems," *IEEE/ASME Trans. Mechatronics*, vol. 24, no. 5, pp. 2118–2129, Oct. 2019.
- [88] W. Felt, M. A. Robertson, and J. Paik, "Modeling vacuum bellows soft pneumatic actuators with optimal mechanical performance," in *Proc. IEEE Int. Conf. Soft Robot. (RoboSoft)*, Apr. 2018, pp. 534–540.
- [89] D. Yang, M. S. Verma, J.-H. So, B. Mosadegh, C. Keplinger, B. Lee, F. Khashai, E. Lossner, Z. Suo, and G. M. Whitesides, "Buckling pneumatic linear actuators inspired by muscle," *Adv. Mater. Technol.*, vol. 1, no. 3, Jun. 2016, Art. no. 1600055.
- [90] S. Li, D. M. Vogt, D. Rus, and R. J. Wood, "Fluid-driven origami-inspired artificial muscles," *Proc. Nat. Acad. Sci. USA*, vol. 114, no. 50, pp. 13132–13137, Dec. 2017.
- [91] J.-G. Lee and H. Rodrigue, "Origami-based vacuum pneumatic artificial muscles with large contraction ratios," *Soft Robot.*, vol. 6, no. 1, pp. 109–117, Feb. 2019.
- [92] B. Yu, J. Yang, R. Du, and Y. Zhong, "A versatile pneumatic actuator based on scissor mechanisms: Design, modeling, and experiments," *IEEE Robot. Autom. Lett.*, vol. 6, no. 2, pp. 1288–1295, Apr. 2021.
- [93] Z. Zhang, W. Fan, G. Chen, J. Luo, Q. Lu, and H. Wang, "A 3D printable origami vacuum pneumatic artificial muscle with fast and powerful motion," in *Proc. IEEE 4th Int. Conf. Soft Robot. (RoboSoft)*, Apr. 2021, pp. 551–554.
- [94] C.-Y. Chen, K. P. May, and C.-H. Yeow, "3D printed soft extension actuator," in *Proc. IEEE 4th Int. Conf. Soft Robot. (RoboSoft)*, Apr. 2021, pp. 435–441.

- [95] Y. Wang, C. Liu, L. Ren, and L. Ren, "Bioinspired soft actuators with highly ordered skeletal muscle structures," *Bio-Des. Manuf.*, vol. 5, no. 1, pp. 174–188, Jan. 2022.
- [96] F. Connolly, C. J. Walsh, and K. Bertoldi, "Automatic design of fiber-reinforced soft actuators for trajectory matching," *Proc. Nat. Acad. Sci. USA*, vol. 114, no. 1, pp. 51–56, Jan. 2017.
- [97] R. V. Martinez, C. R. Fish, X. Chen, and G. M. Whitesides, "Elastomeric origami: Programmable paper-elastomer composites as pneumatic actuators," *Adv. Funct. Mater.*, vol. 22, no. 7, pp. 1376–1384, Apr. 2012.
- [98] B. Mosadegh, P. Polygerinos, C. Keplinger, S. Wennstedt, R. F. Shepherd, U. Gupta, J. Shim, K. Bertoldi, C. J. Walsh, and G. M. Whitesides, "Pneumatic networks for soft robotics that actuate rapidly," *Adv. Funct. Mater.*, vol. 24, no. 15, pp. 2163–2170, Apr. 2014.
- [99] X. Zhang and A. E. Oseyemi, "A herringbone soft pneu-net actuator for enhanced conformal gripping," *Robotica*, vol. 40, no. 5, pp. 1–16, 2021.
- [100] D. Gonzalez, J. Garcia, R. M. Voyles, R. A. Nawrocki, and B. Newell, "Characterization of 3D printed pneumatic soft actuator," *Sens. Actuators A, Phys.*, vol. 334, Feb. 2022, Art. no. 113337.
- [101] M. Fatahillah, N. Oh, and H. Rodrigue, "A novel soft bending actuator using combined positive and negative pressures," *Frontiers Bioeng. Biotechnol.*, vol. 8, p. 472, May 2020.
- [102] T. Wang, L. Ge, and G. Gu, "Programmable design of soft pneu-net actuators with oblique chambers can generate coupled bending and twisting motions," *Sens. Actuators A, Phys.*, vol. 271, pp. 131–138, Mar. 2018.
- [103] W. Xiao, D. Hu, W. Chen, G. Yang, and X. Han, "A new type of soft pneumatic torsional actuator with helical chambers for flexible machines," *J. Mech. Robot.*, vol. 13, no. 1, Feb. 2021, Art. no. 011003.
- [104] P. Yuan and H. Tsukagoshi, "Double helical soft pneumatic actuator capable of generating complex 3D torsional motions," *IEEE Robot. Autom. Lett.*, vol. 6, no. 4, pp. 8142–8149, Oct. 2021.
- [105] C. Jiang, D. Wang, B. Zhao, Z. Liao, and G. Gu, "Modeling and inverse design of bio-inspired multi-segment pneu-net soft manipulators for 3D trajectory motion," *Appl. Phys. Rev.*, vol. 8, no. 4, Dec. 2021, Art. no. 041416.
- [106] H. Abidi, G. Gerboni, M. Brancadoro, J. Frasc, A. Diodato, M. Cianchetti, H. Wurdemann, K. Althofer, and A. Menciassi, "Highly dexterous 2-module soft robot for intra-organ navigation in minimally invasive surgery," *Int. J. Med. Robot. Comput. Assist. Surgery*, vol. 14, no. 1, p. e1875, Feb. 2018.
- [107] E. H. Skorina, M. Luo, W. Y. Oo, W. Tao, F. Chen, S. Youssefian, N. Rahbar, and C. D. Onal, "Reverse pneumatic artificial muscles (rPAMs): Modeling, integration, and control," *PLoS ONE*, vol. 13, no. 10, Oct. 2018, Art. no. e0204637.
- [108] W. Xiao, D. Hu, W. Chen, G. Yang, and X. Han, "Modeling and analysis of bending pneumatic artificial muscle with multi-degree of freedom," *Smart Mater. Struct.*, vol. 30, no. 9, Sep. 2021, Art. no. 095018.
- [109] B. Gorissen, M. De Volder, A. De Greef, and D. Reynaerts, "Theoretical and experimental analysis of pneumatic balloon microactuators," *Sens. Actuators A, Phys.*, vol. 168, no. 1, pp. 58–65, Jul. 2011.
- [110] Y. Sun, Y. Seong Song, and J. Paik, "Characterization of silicone rubber based soft pneumatic actuators," in *Proc. IEEE/RSJ Int. Conf. Intell. Robots Syst.*, Nov. 2013, pp. 4446–4453.
- [111] R. Shepherd, F. Ilievski, W. Choi, S. Morin, A. Stokes, A. Mazzeo, X. Chen, M. Wang, and G. Whitesides, "Multigait soft robot," *Proc. Nat. Acad. Sci. USA*, vol. 108, no. 51, pp. 20400–20403, 2011.
- [112] W. Hu, R. Mutlu, W. Li, and G. Alici, "A structural optimisation method for a soft pneumatic actuator," *Robotics*, vol. 7, no. 2, p. 24, Jun. 2018.
- [113] Y. Hwang, O. H. Paydar, and R. N. Candler, "Pneumatic microfinger with balloon fins for linear motion using 3D printed molds," *Sens. Actuators A, Phys.*, vol. 234, pp. 65–71, Oct. 2015.
- [114] F. Yang, Q. Ruan, Y. Man, Z. Xie, H. Yue, B. Li, and R. Liu, "Design and optimize of a novel segmented soft pneumatic actuator," *IEEE Access*, vol. 8, pp. 122304–122313, 2020.
- [115] Z. Wang, P. Polygerinos, J. T. Overvelde, K. C. Galloway, K. Bertoldi, and C. J. Walsh, "Interaction forces of soft fiber reinforced bending actuators," *IEEE/ASME Trans. Mechatronics*, vol. 22, no. 2, pp. 717–727, Apr. 2016.
- [116] M. Memarian, R. Gorbet, and D. Kulić, "Control of soft pneumatic finger-like actuators for affective motion generation," in *Proc. IEEE/RSJ Int. Conf. Intell. Robots Syst. (IROS)*, Sep. 2015, pp. 1691–1697.
- [117] R. R. Deimel and O. Brock, "A novel type of compliant and underactuated robotic hand for dexterous grasping," *Int. J. Robot. Res.*, vol. 35, pp. 161–185, Jan. 2016.
- [118] B. Wang, K. C. Aw, M. Biglari-Abhari, and A. McDaid, "Design and fabrication of a fiber-reinforced pneumatic bending actuator," in *Proc. IEEE Int. Conf. Adv. Intell. Mechatronics (AIM)*, Jul. 2016, pp. 83–88.
- [119] I. N. A. M. Nordin, M. R. M. Razif, A. M. Faudzi, E. Natarajan, K. Iwata, and K. Suzumori, "3-D finite-element analysis of fiber-reinforced soft bending actuator for finger flexion," in *Proc. IEEE/ASME Int. Conf. Adv. Intell. Mechatron.*, Jul. 2013, pp. 128–133.
- [120] H. Li, J. Yao, P. Zhou, X. Chen, Y. Xu, and Y. Zhao, "High-force soft pneumatic actuators based on novel casting method for robotic applications," *Sens. Actuators A, Phys.*, vol. 306, May 2020, Art. no. 111957.
- [121] B. A. W. Keong and R. Y. C. Hua, "A novel fold-based design approach toward printable soft robotics using flexible 3D printing materials," *Adv. Mater. Technol.*, vol. 3, no. 2, Feb. 2018, Art. no. 1700172.
- [122] F. Connolly, P. Polygerinos, C. J. Walsh, and K. Bertoldi, "Mechanical programming of soft actuators by varying fiber angle," *Soft Robot.*, vol. 2, no. 1, pp. 26–32, Mar. 2015.
- [123] L. Rosalia, B. W.-K. Ang, and R. C.-H. Yeow, "Geometry-based customization of bending modalities for 3D-printed soft pneumatic actuators," *IEEE Robot. Autom. Lett.*, vol. 3, no. 4, pp. 3489–3496, Oct. 2018.
- [124] R. Balak and Y. C. Mazumdar, "Multi-modal pneumatic actuator for twisting, extension, and bending," in *Proc. IEEE/RSJ Int. Conf. Intell. Robots Syst. (IROS)*, Oct. 2020, pp. 8673–8679.
- [125] F. Chen, Y. Miao, G. Gu, and X. Zhu, "Soft twisting pneumatic actuators enabled by freeform surface design," *IEEE Robot. Autom. Lett.*, vol. 6, no. 3, pp. 5253–5260, Jul. 2021.
- [126] E. Perez-Guagnelli, J. Jones, A. H. Tokel, N. Herzig, B. Jones, S. Miyashita, and D. D. Damian, "Characterization, simulation and control of a soft helical pneumatic implantable robot for tissue regeneration," *IEEE Trans. Med. Robot. Bionics*, vol. 2, no. 1, pp. 94–103, Feb. 2020.
- [127] M. Luo, E. H. Skorina, W. Tao, F. Chen, S. Ozel, Y. Sun, and C. D. Onal, "Toward modular soft robotics: Proprioceptive curvature sensing and sliding-mode control of soft bidirectional bending modules," *Soft Robot.*, vol. 4, no. 2, pp. 117–125, 2017.
- [128] Y. Liu, W. Chen, and C. Xiong, "Simulation and fabrication of a pneumatic network actuator with capability of bending in multi-planes," in *Proc. IEEE/ASME Int. Conf. Adv. Intell. Mechatronics (AIM)*, Jul. 2019, pp. 313–317.
- [129] W. Chen, C. Xiong, C. Liu, P. Li, and Y. Chen, "Fabrication and dynamic modeling of bidirectional bending soft actuator integrated with optical waveguide curvature sensor," *Soft Robot.*, vol. 6, no. 4, pp. 495–506, Aug. 2019.
- [130] K. Suzumori, S. Iikura, and H. Tanaka, "Flexible microactuator for miniature robots," in *Proc. IEEE Micro Electro Mech. Syst.*, Jan. 1991, pp. 204–209.
- [131] K. Suzumori, S. Iikura, and H. Tanaka, "Development of flexible microactuator and its applications to robotic mechanisms," in *Proc. IEEE Int. Conf. Robot. Automat.*, vol. 2, Apr. 1991, pp. 1622–1627.
- [132] J. Yan, H. Dong, X. Zhang, and J. Zhao, "A three-chambered soft actuator module with omnidirectional bending motion," in *Proc. IEEE Int. Conf. Real-Time Comput. Robot. (RCAR)*, Jun. 2016, pp. 505–510.
- [133] Y. Elsayed, A. Vincenzi, C. Lekakou, T. Geng, C. M. Saaj, T. Ranzani, M. Cianchetti, and A. Menciassi, "Finite element analysis and design optimization of a pneumatically actuating silicone module for robotic surgery applications," *Soft Robot.*, vol. 1, no. 4, pp. 255–262, Dec. 2014.
- [134] A. H. Khan and S. Li, "Sliding mode control with PID sliding surface for active vibration damping of pneumatically actuated soft robots," *IEEE Access*, vol. 8, pp. 88793–88800, 2020.
- [135] Y. Qin, Z. Wan, Y. Sun, E. H. Skorina, M. Luo, and C. D. Onal, "Design, fabrication and experimental analysis of a 3-D soft robotic snake," in *Proc. IEEE Int. Conf. Soft Robot. (RoboSoft)*, Apr. 2018, pp. 77–82.
- [136] J. Zhang, J. Zhou, Z. K. Cheng, and S. Yuan, "Fabrication, mechanical modeling, and experiments of a 3D-motion soft actuator for flexible sensing," *IEEE Access*, vol. 8, pp. 159100–159109, 2020.
- [137] D. Drotman, M. Ishida, S. Jadhav, and M. T. Tolley, "Application-driven design of soft, 3-D printed, pneumatic actuators with bellows," *IEEE/ASME Trans. Mechatronics*, vol. 24, no. 1, pp. 78–87, Feb. 2019.
- [138] Z. Xue, Q. Wu, and F. Gao, "Design and modeling of omni-directional bending pneumatic flexible arm," in *Proc. 3rd Int. Conf. Adv. Robot. Mechatronics (ICARM)*, Jul. 2018, pp. 835–839.
- [139] R. Xie, M. Su, Y. Zhang, and Y. Guan, "3D-PSA: A 3D pneumatic soft actuator with extending and omnidirectional bending motion," in *Proc. IEEE Int. Conf. Robot. Biomimetics (ROBIO)*, Dec. 2018, pp. 618–623.

- [140] W. Huang, Z. Xu, J. Xiao, W. Hu, H. Huang, and F. Zhou, "Multimodal soft robot for complex environments using bionic omnidirectional bending actuator," *IEEE Access*, vol. 8, pp. 193827–193844, 2020.
- [141] S. M. Zeyb Sayyadan and M. M. Moniri, "A bio-inspired soft planar actuator capable of broadening its working area," *Eng. Res. Exp.*, vol. 3, no. 2, Jun. 2021, Art. no. 025029.
- [142] P. Kulkarni, "Centrifugal forming and mechanical properties of silicone-based elastomers for soft robotic actuators," M.S. thesis, School-New Brunswick, Rutgers Univ.-Graduate, Newark, NJ, USA, 2015.
- [143] G. Decroly, B. Mertens, P. Lambert, and A. Delchambre, "Design, characterization and optimization of a soft fluidic actuator for minimally invasive surgery," *Int. J. Comput. Assist. Radiol. Surg.*, vol. 15, no. 2, pp. 333–340, 2019.
- [144] G. Runge, M. Wiese, L. Gunther, and A. Raatz, "A framework for the kinematic modeling of soft material robots combining finite element analysis and piecewise constant curvature kinematics," in *Proc. 3rd Int. Conf. Control, Autom. Robot. (ICCAR)*, Apr. 2017, pp. 7–14.
- [145] D. Sarkar, S. Dasgupta, A. Arora, and S. Sen, "A soft bending-type actuator using hyper-elastic materials: Development, analysis and characterization," in *Proc. Adv. Robot.*, Jul. 2019, pp. 1–7.
- [146] P. Polygerinos, K. Galloway, Z. Wang, F. Connolly, and H. Young. (2020). *Fiber Reinforced Actuators: Finite Element Modelling*. Accessed: Feb. 10, 2019. [Online]. Available: <https://softroboticstoolkit.com/book/fr-modeling>
- [147] E. Milana, M. Bellotti, B. Gorissen, M. De Volder, and D. Reynaerts, "Precise bonding-free micromoulding of miniaturized elastic inflatable actuators," in *Proc. 2nd IEEE Int. Conf. Soft Robot. (RoboSoft)*, Apr. 2019, pp. 768–773.
- [148] E. Milana, B. V. Raemdonck, K. Cornelis, E. Dehaerne, J. D. Clerck, Y. D. Groof, T. D. Vil, B. Gorissen, and D. Reynaerts, "EELWORM: A bioinspired multimodal amphibious soft robot," in *Proc. 3rd IEEE Int. Conf. Soft Robot. (RoboSoft)*, May 2020, pp. 766–771.
- [149] J. Zhang, H. Wang, J. Tang, H. Guo, and J. Hong, "Modeling and design of a soft pneumatic finger for hand rehabilitation," in *Proc. IEEE Int. Conf. Inf. Autom.*, Aug. 2015, pp. 2460–2465.
- [150] X. Peng, N. Zhang, L. Ge, and G. Gu, "Dimension optimization of pneumatically actuated soft continuum manipulators," in *Proc. 2nd IEEE Int. Conf. Soft Robot. (RoboSoft)*, Apr. 2019, pp. 13–18.
- [151] C. Tawk and G. Alici, "Finite element modeling in the design process of 3D printed pneumatic soft actuators and sensors," *Robotics*, vol. 9, no. 3, p. 52, Jul. 2020.
- [152] C. Pasquier, T. Chen, S. Tibbits, and K. Shea, "Design and computational modeling of a 3D printed pneumatic toolkit for soft robotics," *Soft Robot.*, vol. 6, no. 5, pp. 657–663, Oct. 2019.
- [153] Y. Chen, Z. Xia, and Q. Zhao, "Optimal design of soft pneumatic bending actuators subjected to design-dependent pressure loads," *IEEE/ASME Trans. Mechatronics*, vol. 24, no. 6, pp. 2873–2884, Dec. 2019.
- [154] G. Marckmann and E. Veron, "Comparison of hyperelastic models for rubber-like materials," *Rubber Chem. Technol.*, vol. 79, no. 5, pp. 835–858, Nov. 2006.
- [155] P. A. L. S. Martins, R. M. N. Jorge, and A. J. M. Ferreira, "A comparative study of several material models for prediction of hyperelastic properties: Application to silicone-rubber and soft tissues," *Strain*, vol. 42, pp. 135–147, Jul. 2006.
- [156] A. Ali, M. Hosseini, and B. B. Sahari, "A review of constitutive models for rubber-like materials," *Amer. J. Eng. Appl. Sci.*, vol. 3, no. 1, pp. 232–239, Jan. 2010.
- [157] L. Mihai and A. Goriely, "How to characterize a nonlinear elastic material? A review on nonlinear constitutive parameters in isotropic finite elasticity," *Proc. R. Soc. A, Math. Phys. Eng. Sci.*, vol. 473, no. 2207, 2017, Art. no. 20170607.
- [158] A. G. Holzapfel, *Nonlinear Solid Mechanics: A Continuum Approach for Engineering*. Hoboken, NJ, USA: Wiley, 2000.
- [159] R. W. Ogden, *Non-Linear Elastic Deformations*. Chelmsford, MA, USA: Courier Corporation, 1997.
- [160] W. M. Lai, D. H. Rubin, E. Krempl, and D. Rubin, *Introduction to Continuum Mechanics*. Oxford, U.K.: Butterworth-Heinemann, 2009.
- [161] M. Rackl, "Curve fitting for Ogden, Yeoh and polynomial models," in *Proc. ScilabTEC Conf. (Regensburg)*, 2015, pp. 1–11.
- [162] M. Shahzad, A. Kamran, M. Z. Siddiqui, and M. Farhan, "Mechanical characterization and FE modelling of a hyperelastic material," *Mater. Res.*, vol. 18, no. 5, pp. 918–924, Oct. 2015.
- [163] K. Miller, "Testing elastomers for finite element analysis," Axel Products, Ann Arbor, MI, USA, Tech. Rep., 2004.
- [164] *Standard Test Methods for Vulcanized Rubber and Thermoplastic Elastomers—Tension*, Standard ASTM-D412-16, ASTM International, 2016.
- [165] L. Marechal, P. Ballard, L. Lindenroth, F. Petrou, C. Kontovounisios, and F. Bello, "Toward a common framework and database of materials for soft robotics," *Soft Robot.*, vol. 8, no. 3, pp. 284–297, Jun. 2021.
- [166] S. Walker, O. Yirmibeşoğlu, U. Daalkhajav, and Y. Mengüç, "Additive manufacturing of soft robots," in *Robotic Systems and Autonomous Platforms*. Amsterdam, The Netherlands: Elsevier, 2019, pp. 335–359.
- [167] T. Hainsworth, L. Smith, S. Alexander, and R. MacCurdy, "A fabrication free, 3D printed, multi-material, self-sensing soft actuator," *IEEE Robot. Autom. Lett.*, vol. 5, no. 3, pp. 4118–4125, Jul. 2020.
- [168] H. M. C. M. Anver, R. Mutlu, and G. Alici, "3D printing of a thin-wall soft and monolithic gripper using fused filament fabrication," in *Proc. IEEE Int. Conf. Adv. Intell. Mechatronics (AIM)*, Jul. 2017, pp. 442–447.
- [169] G. Stano and G. Percoco, "Additive manufacturing aimed to soft robots fabrication: A review," *Extreme Mech. Lett.*, vol. 42, Jan. 2021, Art. no. 101079.
- [170] J. Morrow, S. Hemleben, and Y. Menguc, "Directly fabricating soft robotic actuators with an open-source 3-D printer," *IEEE Robot. Autom. Lett.*, vol. 2, no. 1, pp. 277–281, Jan. 2016.
- [171] O. D. Yirmibesoglu, J. Morrow, S. Walker, W. Gosrich, R. Canizares, H. Kim, U. Daalkhajav, C. Fleming, C. Branyan, and Y. Menguc, "Direct 3D printing of silicone elastomer soft robots and their performance comparison with molded counterparts," in *Proc. IEEE Int. Conf. Soft Robot. (RoboSoft)*, Apr. 2018, pp. 295–302.
- [172] A. Miriyev, K. Stack, and H. Lipson, "Soft material for soft actuators," *Nature Commun.*, vol. 8, no. 1, p. 596, 2017.
- [173] M. Schaffner, J. A. Faber, L. Pianegonda, P. A. Rühs, F. Coulter, and A. R. Studart, "3D printing of robotic soft actuators with programmable bioinspired architectures," *Nature Commun.*, vol. 9, no. 1, pp. 1–9, Dec. 2018.
- [174] A. Hamidi and Y. Tadesse, "3D printing of very soft elastomer and sacrificial carbohydrate glass/elastomer structures for robotic applications," *Mater. Des.*, vol. 187, Feb. 2020, Art. no. 108324.
- [175] J. Plott and A. Shih, "The extrusion-based additive manufacturing of moisture-cured silicone elastomer with minimal void for pneumatic actuators," *Additive Manuf.*, vol. 17, pp. 1–14, Oct. 2017.
- [176] S. Walker, U. Daalkhajav, D. Thrush, C. Branyan, O. D. Yirmibesoglu, G. Olson, and Y. Menguc, "Zero-support 3D printing of thermoset silicone via simultaneous control of both reaction kinetics and transient rheology," *3D Printing Additive Manuf.*, vol. 6, no. 3, pp. 139–147, Jun. 2019.
- [177] T. J. Wallin, L.-E. Simonsen, W. Pan, K. Wang, E. Giannelis, R. F. Shepherd, and Y. Mengüç, "3D printable tough silicone double networks," *Nature Commun.*, vol. 11, no. 1, p. 4000, Dec. 2020.
- [178] H. K. Yap, H. Y. Ng, and C.-H. Yeow, "High-force soft printable pneumatics for soft robotic applications," *Soft Robot.*, vol. 3, no. 3, pp. 144–158, Sep. 2016.
- [179] W. Irawan, A. S. Ritonga, and A. Prastowo, "Design and fabrication in the loop of soft pneumatic actuators using fused deposition modelling," *Sens. Actuators A, Phys.*, vol. 298, Oct. 2019, Art. no. 111556.
- [180] K. G. Demir, Z. Zhang, J. Yang, and G. X. Gu, "Computational and experimental design exploration of 3D-printed soft pneumatic actuators," *Adv. Intell. Syst.*, vol. 2, no. 7, Jul. 2020, Art. no. 2070072.
- [181] G. Stano, L. Arleo, and G. Percoco, "Additive manufacturing for soft robotics: Design and fabrication of airtight, monolithic bending PneuNets with embedded air connectors," *Micromachines*, vol. 11, no. 5, p. 485, May 2020.
- [182] Q. Ji, X. Zhang, M. Chen, X. V. Wang, L. Wang, and L. Feng, "Design and closed loop control of a 3D printed soft actuator," in *Proc. IEEE 16th Int. Conf. Autom. Sci. Eng. (CASE)*, Aug. 2020, pp. 842–848.
- [183] M. A. Saleh, M. Soliman, M. A. Mousa, M. Elsamanty, and A. G. Radwan, "Design and implementation of variable inclined air pillow soft pneumatic actuator suitable for bioimpedance applications," *Sens. Actuators A, Phys.*, vol. 314, Oct. 2020, Art. no. 112272.
- [184] C. Tawk, M. Panhuis, G. M. Spinks, and G. Alici, "Bioinspired 3D printable soft vacuum actuators for locomotion robots, grippers and artificial muscles," *Soft Robot.*, vol. 5, no. 6, pp. 685–694, Dec. 2018.
- [185] R. B. N. Scharff, J. Wu, J. M. P. Geraedts, and C. C. L. Wang, "Reducing out-of-plane deformation of soft robotic actuators for stable grasping," in *Proc. 2nd IEEE Int. Conf. Soft Robot. (RoboSoft)*, Apr. 2019, pp. 265–270.

- [186] B. Shih, C. Christianson, K. Gillespie, S. Lee, J. Mayeda, Z. Huo, and M. T. Tolley, "Design considerations for 3D printed, soft, multimaterial resistive sensors for soft robotics," *Frontiers Robot. AI*, vol. 6, p. 30, Apr. 2019.
- [187] R. MacCurdy, R. Katzschmann, Y. Kim, and D. Rus, "Printable hydraulics: A method for fabricating robots by 3D co-printing solids and liquids," in *Proc. IEEE Int. Conf. Robot. Autom. (ICRA)*, May 2016, pp. 3878–3885.
- [188] G. D. Howard, J. Brett, J. O'Connor, J. Letchford, and G. W. Delaney, "One-shot 3D-printed multimaterial soft robotic jamming grippers," *Soft Robot.*, Jun. 2021.
- [189] J. Brett, K. Lo Surdo, L. Hanson, J. Pinski, and D. Howard, "Jammkle: Fibre jamming 3D printed multi-material tendons and their application in a robotic ankle," 2021, *arXiv:2109.04681*.
- [190] D. K. Patel, A. H. Sakhaei, M. Layani, B. Zhang, Q. Ge, and S. Magdassi, "Highly stretchable and UV curable elastomers for digital light processing based 3D printing," *Adv. Mater.*, vol. 29, no. 15, Apr. 2017, Art. no. 1606000.
- [191] Y. Zhang, C. J. Ng, Z. Chen, W. Zhang, S. Panjwani, K. Kowsari, H. Y. Yang, and Q. Ge, "Miniature pneumatic actuators for soft robots by high-resolution multimaterial 3D printing," *Adv. Mater. Technol.*, vol. 4, no. 10, Oct. 2019, Art. no. 1900427.
- [192] L. Ge, L. Dong, D. Wang, Q. Ge, and G. Gu, "A digital light processing 3D printer for fast and high-precision fabrication of soft pneumatic actuators," *Sens. Actuators A, Phys.*, vol. 273, pp. 285–292, Apr. 2018.
- [193] H.-W. Kang, I. H. Lee, and D.-W. Cho, "Development of a micro-bellows actuator using micro-stereolithography technology," *Microelectronic Eng.*, vol. 83, no. 4, pp. 1201–1204, 2006.
- [194] B. N. Peele, T. J. Wallin, H. Zhao, and R. F. Shepherd, "3D printing antagonistic systems of artificial muscle using projection stereolithography," *Bioinspiration Biomimetics*, vol. 10, no. 5, Sep. 2015, Art. no. 055003.
- [195] R. J. Webster and B. A. Jones, "Design and kinematic modeling of constant curvature continuum robots: A review," *Int. J. Robot. Res.*, vol. 29, no. 13, pp. 1661–1683, Jun. 2010.
- [196] N. Simaan, R. Taylor, and P. Flint, "A dexterous system for laryngeal surgery," in *Proc. IEEE Int. Conf. Robot. Autom.*, vol. 1, Apr. 2004, pp. 351–357.
- [197] I. A. Gravagne, C. D. Rahn, and I. D. Walker, "Large deflection dynamics and control for planar continuum robots," *IEEE/ASME Trans. Mechatronics*, vol. 8, no. 2, pp. 299–307, Jun. 2003.
- [198] Y. Bailly and Y. Amirat, "Modeling and control of a hybrid continuum active catheter for aortic aneurysm treatment," in *Proc. IEEE Int. Conf. Robot. Autom.*, Apr. 2005, pp. 924–929.
- [199] M. Spong, S. Hutchinson, and M. Vidyasagar, *Robot Modeling and Control*. Hoboken, NJ, USA: Wiley, 2005.
- [200] B. A. Jones and I. D. Walker, "Kinematics for multisection continuum robots," *IEEE Trans. Robot.*, vol. 22, no. 1, pp. 43–55, Feb. 2006.
- [201] Y. Ganji and F. Janabi-Sharifi, "Catheter kinematics for intracardiac navigation," *IEEE Trans. Biomed. Eng.*, vol. 56, no. 3, pp. 621–632, Jan. 2009.
- [202] G. Chirikjian and J. Burdick, "The kinematics of hyper-redundant robot locomotion," *IEEE Trans. Robot. Autom.*, vol. 11, no. 6, pp. 781–793, Dec. 1995.
- [203] H. Mochiyama and T. Suzuki, "Dynamical modelling of a hyper-flexible manipulator," in *Proc. 41st Annu. Conf. (SICE)*, vol. 3, Aug. 2002, pp. 1505–1510.
- [204] M. Ivanescu, "Position dynamic control for a tentacle manipulator," in *Proc. IEEE Int. Conf. Robot. Autom.*, vol. 2, May 2002, pp. 1531–1538.
- [205] M. Ivanescu, N. Popescu, and D. Popescu, "A variable length tentacle manipulator control system," in *Proc. IEEE Int. Conf. Robot. Autom.*, Apr. 2005, pp. 3274–3279.
- [206] R. Murray, Z. Li, and S. S. Sastry, *A Mathematical Introduction to Robotic Manipulation*. Boca Raton, FL, USA: CRC Press, 1994.
- [207] B. A. Jones, R. L. Gray, and K. Turlapati, "Three dimensional statics for continuum robotics," in *Proc. IEEE/RSJ Int. Conf. Intell. Robots Syst.*, Oct. 2009, pp. 2659–2664.
- [208] M. Dehghani and S. A. A. Moosavian, "Modeling and control of a planar continuum robot," in *Proc. IEEE/ASME Int. Conf. Adv. Intell. Mechatronics (AIM)*, Jul. 2011, pp. 966–971.
- [209] P. S. Gonthina, A. D. Kapadia, I. S. Godage, and I. D. Walker, "Modeling variable curvature parallel continuum robots using Euler curves," in *Proc. Int. Conf. Robot. Autom. (ICRA)*, May 2019, pp. 1679–1685.
- [210] A. Bajo and N. Simaan, "Kinematics-based detection and localization of contacts along multisection continuum robots," *IEEE Trans. Robot.*, vol. 28, no. 2, pp. 291–302, Apr. 2011.
- [211] T. Mahl, A. Hildebrandt, and O. Sawodny, "A variable curvature continuum kinematics for kinematic control of the bionic handling assistant," *IEEE Trans. Robot.*, vol. 30, no. 4, pp. 935–949, Aug. 2014.
- [212] X. Huang, J. Zou, and G. Gu, "Kinematic modeling and control of variable curvature soft continuum robots," *IEEE/ASME Trans. Mechatronics*, vol. 26, no. 6, pp. 3175–3185, Dec. 2021.
- [213] A. A. Shabana and R. Y. Yakoub, "Three dimensional absolute nodal coordinate formulation for beam elements: Theory," *J. Mech. Des.*, vol. 123, no. 4, pp. 606–613, 2001.
- [214] I. Singh, Y. Amara, A. Melingui, P. Mani Pathak, and R. Merzouki, "Modeling of continuum manipulators using Pythagorean hodograph curves," *Soft Robot.*, vol. 5, no. 4, pp. 425–442, Aug. 2018.
- [215] S. Song, Z. Li, M. Q.-H. Meng, H. Yu, and H. Ren, "Real-time shape estimation for wire-driven flexible robots with multiple bending sections based on quadratic Bézier curves," *IEEE Sensors J.*, vol. 15, no. 11, pp. 6326–6334, Nov. 2015.
- [216] S. Luo, M. Edmonds, J. Yi, X. Zhou, and Y. Shen, "Spline-based modeling and control of soft robots," in *Proc. IEEE/ASME Int. Conf. Adv. Intell. Mechatronics (AIM)*, Jul. 2020, pp. 482–487.
- [217] A.-F. Hassanin, D. Steve, and N.-M. Samia, "A novel, soft, bending actuator for use in power assist and rehabilitation exoskeletons," in *Proc. IEEE/RSJ Int. Conf. Intell. Robots Syst. (IROS)*, Sep. 2017, pp. 533–538.
- [218] C. Laschi, M. Cianchetti, B. Mazzolai, L. Margheri, M. Follador, and P. Dario, "Soft robot arm inspired by the octopus," *Adv. Robot.*, vol. 26, no. 7, pp. 709–727, 2012.
- [219] M. Giorelli, F. Renda, M. Calisti, A. Arienti, G. Ferri, and C. Laschi, "Neural network and Jacobian method for solving the inverse statics of a cable-driven soft arm with nonconstant curvature," *IEEE Trans. Robot.*, vol. 31, no. 4, pp. 823–834, Apr. 2015.
- [220] D. Trivedi, A. Lotfi, and C. D. Rahn, "Geometrically exact models for soft robotic manipulators," *IEEE Trans. Robot.*, vol. 24, no. 4, pp. 773–780, Aug. 2008.
- [221] K. M. de Payrebrune and O. M. O'Reilly, "On constitutive relations for a rod-based model of a pneu-net bending actuator," *Extreme Mech. Lett.*, vol. 8, pp. 38–46, Sep. 2016.
- [222] M. Bartholdt, M. Wiese, M. Schappler, S. Spindeldreier, and A. Raatz, "A parameter identification method for static cosserat rod models: Application to soft material actuators with exteroceptive sensors," in *Proc. IEEE/RSJ Int. Conf. Intell. Robots Syst. (IROS)*, Sep. 2021, pp. 624–631.
- [223] R. Berthold, M. N. Bartholdt, M. Wiese, S. Kahms, S. Spindeldreier, and A. Raatz, "A preliminary study of soft material robotic modelling: Finite element method and cosserat rod model," in *Proc. 9th Int. Conf. Control, Mechatronics Autom. (ICCA)*, Nov. 2021, pp. 7–13.
- [224] Y. Shapiro, A. Wolf, and K. Gabor, "Bi-bellows: Pneumatic bending actuator," *Sens. Actuators A, Phys.*, vol. 167, no. 2, pp. 484–494, Jun. 2011.
- [225] J. Craig, *Introduction to Robotics: Mechanics and Control*. London, U.K.: Pearson, 2005.
- [226] V. Falkenhahn, T. Mahl, A. Hildebrandt, R. Neumann, and O. Sawodny, "Dynamic modeling of bellows-actuated continuum robots using the Euler–Lagrange formalism," *IEEE Trans. Robot.*, vol. 31, no. 6, pp. 1483–1496, Dec. 2015.
- [227] M. Azizkhani, I. S. Godage, and Y. Chen, "Dynamic control of soft robotic arm: A simulation study," *IEEE Robot. Autom. Lett.*, vol. 7, no. 2, pp. 3584–3591, Apr. 2022.
- [228] M. Mazare, S. Tolu, and M. Taghizadeh, "Adaptive variable impedance control for a modular soft robot manipulator in configuration space," *Meccanica*, vol. 57, no. 1, pp. 1–15, Jan. 2022.
- [229] T. Wang, Y. Zhang, Y. Zhu, and S. Zhu, "A computationally efficient dynamical model of fluidic soft actuators and its experimental verification," *Mechatronics*, vol. 58, pp. 1–8, Apr. 2019.
- [230] G. Cao, B. Huo, L. Yang, F. Zhang, Y. Liu, and G. Bian, "Model-based robust tracking control without observers for soft bending actuators," *IEEE Robot. Autom. Lett.*, vol. 6, no. 3, pp. 5175–5182, Jul. 2021.
- [231] G. Cao, Y. Liu, Y. Jiang, F. Zhang, G. Bian, and D. H. Owens, "Observer-based continuous adaptive sliding mode control for soft actuators," *Nonlinear Dyn.*, vol. 105, no. 1, pp. 1–16, 2021.
- [232] C. W. De Silva, *Mechatronics: An Integrated Approach*. Boca Raton, FL, USA: CRC Press, 2004.

- [233] J. Watton, *Fluid Power Systems: Modeling, Simulation, Analog and Microcomputer Control*. Upper Saddle River, NJ, USA: Prentice-Hall, 1989.
- [234] M. S. Xavier, A. J. Fleming, and Y. K. Yong, "Modelling and simulation of pneumatic sources for soft robotic applications," in *Proc. IEEE/ASME Int. Conf. Adv. Intell. Mechatronics (AIM)*, Jul. 2020, pp. 916–921.
- [235] E. H. Skorina, M. Luo, S. Ozel, F. Chen, W. Tao, and C. D. Onal, "Feedforward augmented sliding mode motion control of antagonistic soft pneumatic actuators," in *Proc. IEEE Int. Conf. Robot. Autom. (ICRA)*, May 2015, pp. 2544–2549.
- [236] E. H. Skorina, M. Luo, W. Tao, F. Chen, J. Fu, and C. D. Onal, "Adapting to flexibility: Model reference adaptive control of soft bending actuators," *IEEE Robot. Autom. Lett.*, vol. 2, no. 2, pp. 964–970, Apr. 2017.
- [237] T. Wang, Y. Zhang, Z. Chen, and S. Zhu, "Parameter identification and model-based nonlinear robust control of fluidic soft bending actuators," *IEEE/ASME Trans. Mechatronics*, vol. 24, no. 3, pp. 1346–1355, Jun. 2019.
- [238] C. Chen, W. Tang, Y. Hu, Y. Lin, and J. Zou, "Fiber-reinforced soft bending actuator control utilizing on/off valves," *IEEE Robot. Autom. Lett.*, vol. 5, no. 4, pp. 6732–6739, Oct. 2020.
- [239] C. Chen and J. Zou, "Adaptive robust control of soft bending actuators: An empirical nonlinear model-based approach," *J. Zhejiang Univ.-Science A*, vol. 22, no. 9, pp. 681–694, Sep. 2021.
- [240] P. Moseley, J. M. Florez, H. A. Sonar, G. Agarwal, W. Curtin, and J. Paik, "Modeling, design, and development of soft pneumatic actuators with finite element method," *Adv. Eng. Mater.*, vol. 18, no. 6, pp. 978–988, Jun. 2016.
- [241] A. El Hami and B. Radi, *Fluid-Structure Interactions and Uncertainties: Ansys and Fluent Tools*, vol. 6. Hoboken, NJ, USA: Wiley, 2017.
- [242] E. T. Roche, R. Wohlfarth, J. T. B. Overvelde, N. V. Vasilyev, F. A. Pigula, D. J. Mooney, K. Bertoldi, and C. J. Walsh, "A bioinspired soft actuated material," *Adv. Mater.*, vol. 26, no. 8, pp. 1200–1206, Feb. 2014.
- [243] S. K. Chimakurthi, S. Reuss, M. Tooley, and S. Scamporrì, "ANSYS workbench system coupling: A state-of-the-art computational framework for analyzing multiphysics problems," *Eng. with Comput.*, vol. 34, no. 2, pp. 385–411, Apr. 2018.
- [244] M. Pozzi, E. Miguel, R. Deimel, M. Malvezzi, B. Bickel, O. Brock, and D. Prattichizzo, "Efficient FEM-based simulation of soft robots modeled as kinematic chains," in *Proc. IEEE Int. Conf. Robot. Autom. (ICRA)*, May 2018, pp. 4206–4213.
- [245] K. Wandke, "MOOSE-based finite element hyperelastic modeling for soft robot simulations," *IEEE Access*, vol. 9, pp. 139627–139635, 2021.
- [246] H. Wang, F. J. Abu-Dakka, T. N. Le, V. Kyrki, and H. Xu, "A novel soft robotic hand design with human-inspired soft palm: Achieving a great diversity of grasps," *IEEE Robot. Autom. Mag.*, vol. 28, no. 2, pp. 37–49, Jun. 2021.
- [247] F. Faure, C. Duriez, H. Delingette, J. Allard, B. Gilles, S. Marchesseau, H. Talbot, H. Courtecuisse, G. Bousquet, and I. Peterlik, "SOFA: A multi-model framework for interactive physical simulation," in *Soft Tissue Biomechanical Modeling for Computer Assisted Surgery*. Cham, Switzerland: Springer, 2012, pp. 283–321.
- [248] E. Coevoet, T. Morales-Bieze, F. Largilliere, Z. Zhang, M. Thieffry, M. Sanz-Lopez, B. Carez, D. Marchal, O. Goury, and J. Dequidt, "Software toolkit for modeling, simulation, and control of soft robots," *Adv. Robot.*, vol. 31, no. 22, pp. 1208–1224, 2017.
- [249] C. Duriez, "Control of elastic soft robots based on real-time finite element method," in *Proc. IEEE Int. Conf. Robot. Autom.*, May 2013, pp. 3982–3987.
- [250] F. Largilliere, V. Verona, E. Coevoet, M. Sanz-Lopez, J. Dequidt, and C. Duriez, "Real-time control of soft-robots using asynchronous finite element modeling," in *Proc. IEEE Int. Conf. Robot. Autom. (ICRA)*, May 2015, pp. 2550–2555.
- [251] M. Thieffry, A. Kruszewski, C. Duriez, and T.-M. Guerra, "Control design for soft robots based on reduced-order model," *IEEE Robot. Autom. Lett.*, vol. 4, no. 1, pp. 25–32, Jan. 2019.
- [252] L. Gharavi, M. Zareinejad, and A. Ohadi, "Dynamic finite-element analysis of a soft bending actuator," *Mechatronics*, vol. 81, Feb. 2022, Art. no. 102690.
- [253] E. Natarajan, A. A. M. Faudzi, V. M. Jeevanantham, M. R. M. Razif, and I. N. A. M. Nordin, "Numerical dynamic analysis of a single link soft robot finger," *Appl. Mech. Mater.*, vol. 459, pp. 449–454, Oct. 2013.
- [254] F.-K. Benra, H. J. Dohmen, J. Pei, S. Schuster, and B. Wan, "A comparison of one-way and two-way coupling methods for numerical analysis of fluid-structure interactions," *J. Appl. Math.*, vol. 2011, pp. 1–16, Aug. 2011.
- [255] D.-H. Moon, S.-H. Shin, J.-B. Na, and S.-Y. Han, "Fluid–structure interaction based on meshless local Petrov–Galerkin method for worm soft robot analysis," *Int. J. Precis. Eng. Manuf.-Green Technol.*, vol. 7, no. 3, pp. 727–742, May 2020.
- [256] D. Maruthavanan, A. Seibel, and J. Schlattmann, "Fluid-structure interaction modelling of a soft pneumatic actuator," *Actuators*, vol. 10, no. 7, p. 163, Jul. 2021.
- [257] N. Naughton, J. Sun, A. Tekinalp, T. Parthasarathy, G. Chowdhary, and M. Gazzola, "Elastica: A compliant mechanics environment for soft robotic control," *IEEE Robot. Autom. Lett.*, vol. 6, no. 2, pp. 3389–3396, Apr. 2021.
- [258] J. Chen, H. Deng, W. Chai, X. Xiong, and Z. Xia, "Manipulation task simulation of a soft pneumatic gripper using ROS and gazebo," in *Proc. IEEE Int. Conf. Real-Time Comput. Robot. (RCAR)*, Aug. 2018, pp. 378–383.
- [259] M. A. Graule, C. B. Teeple, T. P. McCarthy, G. R. Kim, R. C. St. Louis, and R. J. Wood, "SoMo: Fast and accurate simulations of continuum robots in complex environments," in *Proc. IEEE/RSJ Int. Conf. Intell. Robots Syst. (IROS)*, Sep. 2021, pp. 3934–3941.
- [260] T. Du, K. Wu, P. Ma, S. Wah, A. Spielberg, D. Rus, and W. Matusik, "DiffPD: Differentiable projective dynamics," *ACM Trans. Graph.*, vol. 41, no. 2, pp. 1–21, Apr. 2022.
- [261] A. Teejo Mathew, I. Ben Hmida, C. Armanini, F. Boyer, and F. Renda, "SoRoSim: A MATLAB toolbox for soft robotics based on the geometric variable-strain approach," 2021, *arXiv:2107.05494*.
- [262] M. Bächer, E. Knoop, and C. Schumacher, "Design and control of soft robots using differentiable simulation," *Current Robotics Reports*, vol. 2, no. 2, pp. 211–221, 2021.
- [263] J. Tapia, E. Knoop, M. Mutný, M. A. Otaduy, and M. Bächer, "MakeSense: Automated sensor design for proprioceptive soft robots," *Soft Robot.*, vol. 7, no. 3, pp. 332–345, Jun. 2020.
- [264] S. E. Navarro, S. Nagels, H. Alagi, L.-M. Faller, O. Goury, T. Morales-Bieze, H. Zangl, B. Hein, R. Ramakers, W. Deferme, G. Zheng, and C. Duriez, "A model-based sensor fusion approach for force and shape estimation in soft robotics," *IEEE Robot. Autom. Lett.*, vol. 5, no. 4, pp. 5621–5628, Oct. 2020.
- [265] Y. Hu, J. Liu, A. Spielberg, J. B. Tenenbaum, W. T. Freeman, J. Wu, D. Rus, and W. Matusik, "ChainQueen: A real-time differentiable physical simulator for soft robotics," in *Proc. Int. Conf. Robot. Autom. (ICRA)*, May 2019, pp. 6265–6271.
- [266] T. Du, J. Hughes, S. Wah, W. Matusik, and D. Rus, "Underwater soft robot modeling and control with differentiable simulation," *IEEE Robot. Autom. Lett.*, vol. 6, no. 3, pp. 4994–5001, Jul. 2021.
- [267] S. Min, J. Won, S. Lee, J. Park, and J. Lee, "SoftCon: Simulation and control of soft-bodied animals with biomimetic actuators," *ACM Trans. Graph.*, vol. 38, no. 6, pp. 1–12, Dec. 2019.
- [268] P. Ma, T. Du, J. Z. Zhang, K. Wu, A. Spielberg, R. K. Katzschmann, and W. Matusik, "DiffAqua: A differentiable computational design pipeline for soft underwater swimmers with shape interpolation," *ACM Trans. Graph.*, vol. 40, no. 4, pp. 1–14, Aug. 2021.
- [269] X. Lin, Y. Wang, J. Olkin, and D. Held, "SoftGym: Benchmarking deep reinforcement learning for deformable object manipulation," in *Proc. Conf. Robot Learn.*, 2020, pp. 432–448.
- [270] B. Willis and P. Liu, "Simulation, design and control of a soft robotic arm with integrated bending sensing," in *Proc. 20th Int. Conf. Adv. Robot. (ICAR)*, Dec. 2021, pp. 26–31.
- [271] R. Mengacci, G. Zambella, G. Grioli, D. Caporale, M. G. Catalano, and A. Bicchi, "An open-source ROS-gazebo toolbox for simulating robots with compliant actuators," *Frontiers Robot. AI*, vol. 8, p. 246, Aug. 2021.
- [272] B. Caasenbrood. (2020). *Sorotoki—A Soft Robotics Toolkit for MATLAB*. [Online]. Available: <https://github.com/BJCaasenbrood/SorotokiCode>
- [273] S. Kriegman, C. Cappelle, F. Corucci, A. Bernatskiy, N. Cheney, and J. C. Bongard, "Simulating the evolution of soft and rigid-body robots," in *Proc. Genetic Evol. Comput. Conf. Companion*, Jul. 2017, pp. 1117–1120.
- [274] J. Hiller and H. Lipson, "Dynamic simulation of soft multimaterial 3D-printed objects," *Soft Robot.*, vol. 1, no. 1, pp. 88–101, Mar. 2014.
- [275] J. Collins, S. Chand, A. Vanderkop, and D. Howard, "A review of physics simulators for robotic applications," *IEEE Access*, vol. 9, pp. 51416–51431, 2021.

- [276] J. Pinskiar and D. Howard, "From bioinspiration to computer generation: Developments in autonomous soft robot design," *Adv. Intell. Syst.*, vol. 4, no. 1, Jan. 2022, Art. no. 2100086. [Online]. Available: <https://onlinelibrary.wiley.com/doi/abs/10.1002/aisy.202100086>
- [277] F. Chen and M. Y. Wang, "Design optimization of soft robots: A review of the state of the art," *IEEE Robot. Autom. Mag.*, vol. 27, no. 4, pp. 27–43, Dec. 2020.
- [278] Z. Wang and S. Hirai, "Chamber dimension optimization of a bellows-type soft actuator for food material handling," in *Proc. IEEE Int. Conf. Soft Robot. (RoboSoft)*, Apr. 2018, pp. 382–387.
- [279] P. Ćurković and A. Jambrečić, "Improving structural design of soft actuators using finite element method analysis," *Interdiscip. Descr. Complex Syst.*, vol. 18, no. 4, pp. 501–515, 2020.
- [280] A. Pagoli, F. Chapelle, J.-A. Corrales-Ramon, Y. Mezouar, and Y. Lapusta, "Design and optimization of a dextrous robotic finger," *IEEE Robot. Autom. Mag.*, vol. 27, no. 4, pp. 56–64, Oct. 2020.
- [281] Y. Elsayed, C. Lekakou, T. Geng, and C. M. Saaj, "Design optimisation of soft silicone pneumatic actuators using finite element analysis," in *Proc. IEEE/ASME Int. Conf. Adv. Intell. Mechatronics*, Jul. 2014, pp. 44–49.
- [282] G. Runge, J. Peters, and A. Raatz, "Design optimization of soft pneumatic actuators using genetic algorithms," in *Proc. IEEE Int. Conf. Robot. Biomimetics (ROBIO)*, Macau, China, Dec. 2017, pp. 393–400.
- [283] M. Raeesinezhad, N. Pagliocca, B. Koohbor, and M. Trkov, "Design optimization of a pneumatic soft robotic actuator using model-based optimization and deep reinforcement learning," *Frontiers Robot. AI*, vol. 8, p. 107, May 2021.
- [284] S. Bhagat, H. Banerjee, Z. Ho Tse, and H. Ren, "Deep reinforcement learning for soft, flexible robots: Brief review with impending challenges," *Robotics*, vol. 8, no. 1, p. 4, Jan. 2019.
- [285] K. Chin, T. Hellebrekers, and C. Majidi, "Machine learning for soft robotic sensing and control," *Adv. Intell. Syst.*, vol. 2, no. 6, Jun. 2020, Art. no. 1900171.
- [286] G. Runge and A. Raatz, "A framework for the automated design and modelling of soft robotic systems," *CIRP Ann.*, vol. 66, no. 1, pp. 9–12, 2017.
- [287] X. Zhang and B. Zhu, *Topology Optimization of Compliant Mechanisms*. Cham, Switzerland: Springer, 2018.
- [288] J. Pinskiar and B. Shirinzadeh, "Topology optimization of leaf flexures to maximize in-plane to out-of-plane compliance ratio," *Precis. Eng.*, vol. 55, pp. 397–407, Jan. 2019.
- [289] J. Pinskiar, B. Shirinzadeh, M. Ghafarian, T. K. Das, A. Al-Jodah, and R. Nowell, "Topology optimization of stiffness constrained flexure-hinges for precision and range maximization," *Mechanism Mach. Theory*, vol. 150, Aug. 2020, Art. no. 103874.
- [290] P. Kumar, J. S. Frouws, and M. Langelaar, "Topology optimization of fluidic pressure-loaded structures and compliant mechanisms using the Darcy method," *Struct. Multidisciplinary Optim.*, vol. 61, no. 4, pp. 1637–1655, Apr. 2020.
- [291] P. Kumar and M. Langelaar, "On topology optimization of design-dependent pressure-loaded three-dimensional structures and compliant mechanisms," *Int. J. Numer. Methods. Eng.*, vol. 122, no. 9, pp. 2205–2220, 2021.
- [292] H. Zhang, A. S. Kumar, J. Y. H. Fuh, and M. Y. Wang, "Design and development of a topology-optimized three-dimensional printed soft gripper," *Soft Robot.*, vol. 5, no. 5, pp. 650–661, Oct. 2018.
- [293] C. H. Liu, L. J. Chen, J. C. Chi, and J. Y. Wu, "Topology optimization design and experiment of a soft pneumatic bending actuator for grasping applications," *IEEE Robot. Autom. Lett.*, vol. 7, no. 2, pp. 2086–2093, Apr. 2022.
- [294] S. Chen, F. Chen, Z. Cao, Y. Wang, Y. Miao, G. Gu, and X. Zhu, "Topology optimization of skeleton-reinforced soft pneumatic actuators for desired motions," *IEEE/ASME Trans. Mechatronics*, vol. 26, no. 4, pp. 1745–1753, Aug. 2021.
- [295] E. M. de Souza and E. C. N. Silva, "Topology optimization applied to the design of actuators driven by pressure loads," *Structural Multidisciplinary Optim.*, vol. 61, no. 5, pp. 1763–1786, May 2020.
- [296] B. Caasenbrood, A. Pogromsky, and H. Nijmeijer, "A computational design framework for pressure-driven soft robots through nonlinear topology optimization," in *Proc. 3rd IEEE Int. Conf. Soft Robot. (RoboSoft)*, May 2020, pp. 633–638.
- [297] S. G. Fitzgerald, G. W. Delaney, D. Howard, and F. Maire, "Evolving soft robotic jamming grippers," in *Proc. Genetic Evol. Comput. Conf.*, Jun. 2021, pp. 102–110.
- [298] J. K. Pugh, L. B. Soros, and K. O. Stanley, "Quality diversity: A new frontier for evolutionary computation," *Frontiers Robot. AI*, vol. 3, p. 40, Jul. 2016.
- [299] D. Howard, A. E. Eiben, D. F. Kennedy, J.-B. Mouret, P. Valencia, and D. Winkler, "Evolving embodied intelligence from materials to machines," *Nat. Mach. Intell.*, vol. 1, no. 1, p. 12, 2019.
- [300] R. Pfeifer and J. Bongard, *How the Body Shapes the Way We Think: A New View of Intelligence*. Cambridge, MA, USA: MIT Press, 2006.
- [301] N. Cheney, R. MacCurdy, J. Clune, and H. Lipson, "Unshackling evolution: Evolving soft robots with multiple materials and a powerful generative encoding," *ACM SIGEVOlution*, vol. 7, no. 1, pp. 11–23, Aug. 2014.
- [302] F. Corucci, N. Cheney, F. Giorgio-Serchi, J. Bongard, and C. Laschi, "Evolving soft locomotion in aquatic and terrestrial environments: Effects of material properties and environmental transitions," *Soft Robot.*, vol. 5, no. 4, pp. 475–493, 2018.
- [303] J. Rieffel, D. Knox, S. Smith, and B. Trimmer, "Growing and evolving soft robots," *Artif. Life*, vol. 19, nos. 3–4, pp. 119–140, 2013.
- [304] S. Chand and D. Howard, "Multi-level evolution for robotic design," *Frontiers Robot. AI*, vol. 8, p. 192, Jun. 2021.
- [305] M. Joachimczak, R. Suzuki, and T. Arita, "Improving evolvability of morphologies and controllers of developmental soft-bodied robots with novelty search," *Frontiers Robot. AI*, vol. 2, pp. 1–16, Dec. 2015.
- [306] J. Hiller and H. Lipson, "Automatic design and manufacture of soft robots," *IEEE Trans. Robot.*, vol. 28, no. 2, pp. 457–466, Apr. 2012.
- [307] S. Kriegman, A. M. Nasab, D. Shah, H. Steele, G. Branin, M. Levin, J. Bongard, and R. Kramer-Bottiglio, "Scalable sim-to-real transfer of soft robot designs," in *Proc. 3rd IEEE Int. Conf. Soft Robot. (RoboSoft)*, May 2020, pp. 359–366.
- [308] D. Howard, J. O'Connor, J. Letchford, J. Brett, T. Joseph, S. Lin, D. Furby, and G. W. Delaney, "Getting a grip: In materio evolution of membrane morphology for soft robotic jamming grippers," 2021, *arXiv:2111.01952*.
- [309] S. Joshi and J. Paik, "Pneumatic supply system parameter optimization for soft actuators," *Soft Robot.*, vol. 8, no. 2, pp. 152–163, Apr. 2021.
- [310] T. Jagadeesha, *Pneumatics: Concepts, Design and Applications*. Cambridge, U.K.: Universities Press, 2015.
- [311] B. Wijnen, E. J. Hunt, G. C. Anzalone, and J. M. Pearce, "Open-source syringe pump library," *PLoS ONE*, vol. 9, no. 9, Sep. 2014, Art. no. e107216.
- [312] K. Ikuta, H. Ichikawa, K. Suzuki, and D. Yajima, "Multi-degree of freedom hydraulic pressure driven safety active catheter," in *Proc. IEEE Int. Conf. Robot. Autom. (ICRA)*, May 2006, pp. 4161–4166.
- [313] K. Ikuta, Y. Matsuda, D. Yajima, and Y. Ota, "Pressure pulse drive: A control method for the precise bending of hydraulic active catheters," *IEEE/ASME Trans. Mechatronics*, vol. 17, no. 5, pp. 876–883, Oct. 2012.
- [314] J. R. Lake, K. C. Heyde, and W. C. Ruder, "Low-cost feedback-controlled syringe pressure pumps for microfluidics applications," *PLoS ONE*, vol. 12, no. 4, Apr. 2017, Art. no. e0175089.
- [315] M. S. V. Appaji, G. S. Reddy, S. Arunkumar, and M. Venkatesan, "An 8051 microcontroller based syringe pump control system for surface micromachining," *Proc. Mater. Sci.*, vol. 5, pp. 1791–1800, Jan. 2014.
- [316] M. S. Cubberley and W. A. Hess, "An inexpensive programmable dual-syringe pump for the chemistry laboratory," *J. Chem. Educ.*, vol. 94, no. 1, pp. 72–74, Jan. 2017.
- [317] A. D. Marchese, K. Komorowski, C. D. Onal, and D. Rus, "Design and control of a soft and continuously deformable 2D robotic manipulation system," in *Proc. IEEE Int. Conf. Robot. Autom. (ICRA)*, May 2014, pp. 2189–2196.
- [318] A. D. Marchese and D. Rus, "Design, kinematics, and control of a soft spatial fluidic elastomer manipulator," *Int. J. Robot. Res.*, vol. 35, no. 7, pp. 840–869, Jun. 2016.
- [319] J. W. Booth, J. C. Case, E. L. White, D. S. Shah, and R. Kramer-Bottiglio, "An addressable pneumatic regulator for distributed control of soft robots," in *Proc. IEEE Int. Conf. Soft Robot. (RoboSoft)*, Apr. 2018, pp. 25–30.
- [320] A. Shtarbanov, "FlowIO development platform—The pneumatic 'Raspberry Pi' for soft robotics," in *Proc. Extended Abstr. Conf. Hum. Factors Comput. Syst.*, May 2021, pp. 1–6.
- [321] A. Shrivastava, "Programmable-air," New York Univ., New York, NY, USA, Tech. Rep. US000159, 2019.
- [322] T. R. Young, M. S. Xavier, Y. K. Yong, and A. J. Fleming, "A control and drive system for pneumatic soft robots: PneuSoRD," in *Proc. IEEE/RSJ Int. Conf. Intell. Robots Syst. (IROS)*, Sep. 2021, pp. 2822–2829.

- [367] M. Brancadoro, M. Manti, S. Tognarelli, and M. Cianchetti, "Preliminary experimental study on variable stiffness structures based on fiber jamming for soft robots," in *Proc. IEEE Int. Conf. Soft Robot. (RoboSoft)*, Apr. 2018, pp. 258–263.
- [368] M. Brancadoro, M. Manti, F. Grani, S. Tognarelli, A. Menciassi, and M. Cianchetti, "Toward a variable stiffness surgical manipulator based on fiber jamming transition," *Frontiers Robot. AI*, vol. 6, p. 12, Mar. 2019.
- [369] B. Yang, R. Baines, D. Shah, S. Patiballa, E. Thomas, M. Venkadesan, and R. Kramer-Bottiglio, "Reprogrammable soft actuation and shape-shifting via tensile jamming," *Sci. Adv.*, vol. 7, no. 40, Oct. 2021, Art. no. eabh2073.
- [370] Y. Yang, Y. Zhang, Z. Kan, J. Zeng, and M. Y. Wang, "Hybrid jamming for bioinspired soft robotic fingers," *Soft Robot.*, vol. 7, no. 3, pp. 292–308, Jun. 2020.
- [371] Y. Zhao, Y. Shan, J. Zhang, K. Guo, L. Qi, L. Han, and H. Yu, "A soft continuum robot, with a large variable-stiffness range, based on jamming," *Bioinspiration Biomimetics*, vol. 14, no. 6, Sep. 2019, Art. no. 066007.
- [372] A. Jiang, G. Xynogalas, P. Dasgupta, K. Althoefer, and T. Nanayakkara, "Design of a variable stiffness flexible manipulator with composite granular jamming and membrane coupling," in *Proc. IEEE/RSJ Int. Conf. Intell. Robots Syst.*, Oct. 2012, pp. 2922–2927.
- [373] N. G. Cheng, M. B. Lobovsky, S. J. Keating, A. M. Setapen, K. I. Gero, A. E. Hosoi, and K. D. Iagnemma, "Design and analysis of a robust, low-cost, highly articulated manipulator enabled by jamming of granular media," in *Proc. IEEE Int. Conf. Robot. Autom.*, May 2012, pp. 4328–4333.
- [374] J. Kapadia and M. Yim, "Design and performance of nubbed fluidizing jamming grippers," in *Proc. IEEE Int. Conf. Robot. Autom.*, May 2012, pp. 5301–5306.
- [375] A. Jiang, T. Aste, P. Dasgupta, K. Althoefer, and T. Nanayakkara, "Granular jamming transitions for a robotic mechanism," in *Proc. AIP Conf. Proc.*, 2013, vol. 1542, no. 1, pp. 385–388.
- [376] S. Licht, E. Collins, G. Badlissi, and D. Rizzo, "A partially filled jamming gripper for underwater recovery of objects resting on soft surfaces," in *Proc. IEEE/RSJ Int. Conf. Intell. Robots Syst. (IROS)*, Oct. 2018, pp. 6461–6468.
- [377] K. Tanaka, M. A. Karimi, B.-P. Busque, D. Mulroy, Q. Zhou, R. Batra, A. Srivastava, H. M. Jaeger, and M. Spenke, "Cable-driven jamming of a boundary constrained soft robot," in *Proc. 3rd IEEE Int. Conf. Soft Robot. (RoboSoft)*, May 2020, pp. 852–857.
- [378] J. L. C. Santiago, I. S. Godage, P. Gonthina, and I. D. Walker, "Soft robots and kangaroo tails: Modulating compliance in continuum structures through mechanical layer jamming," *Soft Robot.*, vol. 3, no. 2, pp. 54–63, Jun. 2016.
- [379] Y. Li, Y. Chen, Y. Yang, and Y. Li, "Soft robotic grippers based on particle transmission," *IEEE/ASME Trans. Mechatronics*, vol. 24, no. 3, pp. 969–978, Jun. 2019.
- [380] Y. Jiang, D. Chen, C. Liu, and J. Li, "Chain-like granular jamming: A novel stiffness-programmable mechanism for soft robotics," *Soft Robot.*, vol. 6, no. 1, pp. 118–132, Feb. 2019.
- [381] M. Cianchetti, T. Ranzani, G. Gerboni, I. De Falco, C. Laschi, and A. Menciassi, "STIFF-FLOP surgical manipulator: Mechanical design and experimental characterization of the single module," in *Proc. IEEE/RSJ Int. Conf. Intell. Robots Syst.*, Nov. 2013, pp. 3576–3581.
- [382] W. H. Choi, S. Kim, D. Lee, and D. Shin, "Soft, multi-DoF, variable stiffness mechanism using layer jamming for wearable robots," *IEEE Robot. Autom. Lett.*, vol. 4, no. 3, pp. 2539–2546, Jul. 2019.
- [383] E. Thompson-Bean, O. Steiner, and A. McDaid, "A soft robotic exoskeleton utilizing granular jamming," in *Proc. IEEE Int. Conf. Adv. Intell. Mechatronics (AIM)*, Jul. 2015, pp. 165–170.
- [384] S. Hauser, P. Eckert, A. Tuleu, and A. Ijspeert, "Friction and damping of a compliant foot based on granular jamming for legged robots," in *Proc. 6th IEEE Int. Conf. Biomed. Robot. Biomechatronics (BioRob)*, Jun. 2016, pp. 1160–1165.
- [385] S. Chopra, M. T. Tolley, and N. Gravish, "Granular jamming feet enable improved foot-ground interactions for robot mobility on deformable ground," *IEEE Robot. Autom. Lett.*, vol. 5, no. 3, pp. 3975–3981, Jul. 2020.
- [386] Y. S. Narang, A. Degirmenci, J. J. Vlassak, and R. D. Howe, "Transforming the dynamic response of robotic structures and systems through laminar jamming," *IEEE Robot. Autom. Lett.*, vol. 3, no. 2, pp. 688–695, Apr. 2017.
- [387] C. Tawk, H. Zhou, E. Sariyildiz, M. Panhuis, G. M. Spinks, and G. Alici, "Design, modeling, and control of a 3D printed monolithic soft robotic finger with embedded pneumatic sensing chambers," *IEEE/ASME Trans. Mechatronics*, vol. 26, no. 2, pp. 876–887, Apr. 2020.
- [388] V. Kumar, Z. Xu, and E. Todorov, "Fast, strong and compliant pneumatic actuation for dexterous tendon-driven hands," in *Proc. IEEE Int. Conf. Robot. Autom.*, May 2013, pp. 1512–1519.
- [389] W. McMahan, B. A. Jones, and I. D. Walker, "Design and implementation of a multi-section continuum robot: Air-octor," in *Proc. IEEE/RSJ Int. Conf. Intell. Robots Syst.*, Aug. 2005, pp. 3345–3352.
- [390] Y. Kim and Y. Cha, "Soft pneumatic gripper with a tendon-driven soft origami pump," *Frontiers Bioeng. Biotechnol.*, vol. 8, p. 461, May 2020.
- [391] X. Wang, H. Zhou, H. Kang, W. Au, and C. Chen, "Bio-inspired soft bistable actuator with dual actuations," *Smart Mater. Struct.*, vol. 30, no. 12, Dec. 2021, Art. no. 125001.
- [392] M. M. Dalvand, S. Nahavandi, and R. D. Howe, "High speed vision-based 3D reconstruction of continuum robots," in *Proc. IEEE Int. Conf. Syst., Man, Cybern. (SMC)*, Oct. 2016, pp. 618–623.
- [393] G. Gerboni, A. Diodato, G. Ciuti, M. Cianchetti, and A. Menciassi, "Feedback control of soft robot actuators via commercial flex bend sensors," *IEEE/ASME Trans. Mechatronics*, vol. 22, no. 4, pp. 1881–1888, Aug. 2017.
- [394] R. A. Bilodeau, M. C. Yuen, J. C. Case, T. L. Buckner, and R. Kramer-Bottiglio, "Design for control of a soft bidirectional bending actuator," in *Proc. IEEE/RSJ Int. Conf. Intell. Robots Syst. (IROS)*, Oct. 2018, pp. 1–8.
- [395] S. Ozel, E. H. Skorina, M. Luo, W. Tao, F. Chen, Y. Pan, and C. D. Onal, "A composite soft bending actuation module with integrated curvature sensing," in *Proc. IEEE Int. Conf. Robot. Autom. (ICRA)*, May 2016, pp. 4963–4968.
- [396] O. Azami, D. Morisaki, T. Miyazaki, T. Kanno, and K. Kawashima, "Development of the extension type pneumatic soft actuator with built-in displacement sensor," *Sens. Actuators A, Phys.*, vol. 300, Dec. 2019, Art. no. 111623.
- [397] H. Zhao, K. O'Brien, S. Li, and R. F. Shepherd, "Optoelectronically innervated soft prosthetic hand via stretchable optical waveguides," *Sci. Robot.*, vol. 1, no. 1, Dec. 2016, Art. no. eaai7529.
- [398] H. Wang, M. Totaro, and L. Beccai, "Toward perceptive soft robots: Progress and challenges," *Adv. Sci.*, vol. 5, no. 9, Sep. 2018, Art. no. 1800541.
- [399] R. K. Kramer, C. Majidi, R. Sahai, and R. J. Wood, "Soft curvature sensors for joint angle proprioception," in *Proc. IEEE/RSJ Int. Conf. Intell. Robots Syst.*, Sep. 2011, pp. 1919–1926.
- [400] G. Alici, "Softer is harder: What differentiates soft robotics from hard robotics?" *MRS Adv.*, vol. 3, no. 28, pp. 1557–1568, Jun. 2018.
- [401] G. Soter, A. Conn, H. Hauser, and J. Rossiter, "Bodily aware soft robots: Integration of proprioceptive and exteroceptive sensors," in *Proc. IEEE Int. Conf. Robot. Autom. (ICRA)*, May 2018, pp. 2448–2453.
- [402] N. Lu and D.-H. Kim, "Flexible and stretchable electronics paving the way for soft robotics," *Soft Robot.*, vol. 1, no. 1, pp. 53–62, 2014.
- [403] Z. Wang and S. Hirai, "A 3D printed soft gripper integrated with curvature sensor for studying soft grasping," in *Proc. IEEE/SICE Int. Symp. Syst. Integr. (SII)*, Dec. 2016, pp. 629–633.
- [404] K. Elgeneidy, N. Lohse, and M. Jackson, "Bending angle prediction and control of soft pneumatic actuators with embedded flex sensors—A data-driven approach," *Mechatronics*, vol. 50, pp. 234–247, Apr. 2018.
- [405] M. H. Mohamed, S. H. Wagdy, M. A. Atalla, A. R. Youssef, and S. A. Maged, "A proposed soft pneumatic actuator control based on angle estimation from data-driven model," *Proc. Inst. Mech. Eng. H, J. Eng. Med.*, vol. 234, no. 6, pp. 612–625, Jun. 2020.
- [406] P. H. Nguyen, S. Sridar, W. Zhang, and P. Polygerinos, "Design and control of a 3-chambered fiber reinforced soft actuator with off-the-shelf stretch sensors," *Int. J. Intell. Robot. Appl.*, vol. 1, no. 3, pp. 342–351, Sep. 2017.
- [407] J. C. Yeo, H. K. Yap, W. Xi, Z. Wang, C.-H. Yeow, and C. T. Lim, "Flexible and stretchable strain sensing actuator for wearable soft robotic applications," *Adv. Mater. Technol.*, vol. 1, no. 3, Jun. 2016, Art. no. 1600018.
- [408] X. Gan, J. Wang, Z. Wang, Z. Zheng, M. Lavorgna, A. Ronca, G. Fei, and H. Xia, "Simultaneous realization of conductive segregation network microstructure and minimal surface porous macrostructure by SLS 3D printing," *Mater. Design*, vol. 178, Sep. 2019, Art. no. 107874.

- [409] G. Stano and G. Percoco, “Design, 3D printing and characterization of a soft actuator with embedded strain sensor,” in *Proc. IEEE Int. Symp. Med. Meas. Appl. (MeMeA)*, Jun. 2020, pp. 1–6.
- [410] B. Eijking, R. Sanders, and G. Krijnen, “Development of whisker inspired 3D multi-material printed flexible tactile sensors,” in *Proc. IEEE SENSORS*, Oct. 2017, pp. 1–3.
- [411] S. Mousavi, D. Howard, S. Wu, and C. Wang, “An ultrasensitive 3D printed tactile sensor for soft robotics,” 2018, *arXiv:1810.09236*.
- [412] K. Yoshida, Y. Takishima, Y. Hara, M. Kawakami, and H. Furukawa, “3D printing for gel robotics,” in *Proc. Nano-, Bio-, Info-Tech Sensors, 3D Syst.*, Mar. 2018, Art. no. 1059717.
- [413] G. Gaál, T. A. da Silva, V. Gaál, R. C. Hensel, L. R. Amaral, V. Rodrigues, and A. Riul, “3D printed e-Tongue,” *Frontiers Chem.*, vol. 6, p. 151, May 2018.
- [414] B. Taherkhani, M. B. Azizkhani, J. Kadkhodapour, A. P. Anaraki, and S. Rastigordani, “Highly sensitive, piezoresistive, silicone/carbon fiber-based auxetic sensor for low strain values,” *Sens. Actuators A, Phys.*, vol. 305, Apr. 2020, Art. no. 111939.
- [415] J. Ou, G. Dublon, C.-Y. Cheng, F. Heibeck, K. Willis, and H. Ishii, “Cillia: 3D printed micro-pillar structures for surface texture, actuation and sensing,” in *Proc. Conf. Hum. Factors Comput. Syst.*, May 2016, pp. 5753–5764.
- [416] P. Laszczak, L. Jiang, D. L. Bader, D. Moser, and S. Zahedi, “Development and validation of a 3D-printed interfacial stress sensor for prosthetic applications,” *Med. Eng. Phys.*, vol. 37, no. 1, pp. 132–137, Jan. 2015.
- [417] A. Wickberg, J. B. Mueller, Y. J. Mange, J. Fischer, T. Nann, and M. Wegener, “Three-dimensional micro-printing of temperature sensors based on up-conversion luminescence,” *Appl. Phys. Lett.*, vol. 106, no. 13, Mar. 2015, Art. no. 133103.
- [418] L. Y. W. Loh, U. Gupta, Y. Wang, C. C. Foo, J. Zhu, and W. F. Lu, “3D printed metamaterial capacitive sensing array for universal jamming gripper and human joint wearables,” *Adv. Eng. Mater.*, vol. 23, no. 5, May 2021, Art. no. 2001082.
- [419] B. Li, L. Meng, H. Wang, J. Li, and C. Liu, “Rapid prototyping eddy current sensors using 3D printing,” *Rapid Prototyping J.*, vol. 24, no. 1, pp. 106–113, Jan. 2018.
- [420] N. Jeranč, N. Bednar, and G. Stojanović, “An ink-jet printed eddy current position sensor,” *Sensors*, vol. 13, no. 4, pp. 5205–5219, Apr. 2013.
- [421] S.-Y. Wu, C. Yang, W. Hsu, and L. Lin, “RF wireless LC tank sensors fabricated by 3D additive manufacturing,” in *Proc. 18th Int. Conf. Solid-State Sensors, Actuat. Microsystems (TRANSDUCERS)*, Jun. 2015, pp. 2208–2211.
- [422] S. J. Leigh, C. P. Purcell, D. R. Billson, and D. A. Hutchins, “Using a magnetite/thermoplastic composite in 3D printing of direct replacements for commercially available flow sensors,” *Smart Mater. Struct.*, vol. 23, no. 9, Sep. 2014, Art. no. 095039.
- [423] Y. K. Lin, T. S. Hsieh, L. Tsai, S. H. Wang, and C. C. Chiang, “Using three-dimensional printing technology to produce a novel optical fiber Bragg grating pressure sensor,” *Sensors Mater.*, vol. 28, no. 5, pp. 389–394, 2016.
- [424] B. Igrec, M. Bosiljevac, Z. Sipus, D. Babic, and S. Rudan, “Fiber optic vibration sensor for high-power electric machines realized using 3D printing technology,” in *Proc. Photonic Instrum. Eng.*, vol. 9754, Mar. 2016, Art. no. 975410.
- [425] P. D. Palma, A. Iadicicco, and S. Campopiano, “Curvature sensor based on FBGs embedded in 3D printed patches,” *IEEE Sensors J.*, vol. 21, no. 16, pp. 17868–17874, Aug. 2021.
- [426] C. Tawk, E. Sariyildiz, and G. Alici, “Force control of a 3D printed soft gripper with built-in pneumatic touch sensing chambers,” *Soft Robot.*, Oct. 2021.
- [427] G. R. Sherwood, D. Chronopoulos, A. Marini, and F. Ciampa, “3D-printed phononic crystal waveguide transducers for nonlinear ultrasonic damage detection,” *NDT & E Int.*, vol. 121, Jul. 2021, Art. no. 102456.
- [428] Y. Toshimitsu, K. W. Wong, T. Buchner, and R. Katschmann, “SoPrA: Fabrication & dynamical modeling of a scalable soft continuum robotic arm with integrated proprioceptive sensing,” in *Proc. IEEE/RSJ Int. Conf. Intell. Robots Syst. (IROS)*, Sep. 2021, pp. 653–660.
- [429] E. L. White, M. C. Yuen, J. C. Case, and R. K. Kramer, “Low-cost, facile, and scalable manufacturing of capacitive sensors for soft systems,” *Adv. Mater. Technol.*, vol. 2, no. 9, Sep. 2017, Art. no. 1700072.
- [430] T. H. Yang, J. Shintake, R. Kanno, C. R. Kao, and J. Mizuno, “Low-cost sensor-rich fluidic elastomer actuators embedded with paper electronics,” *Adv. Intell. Syst.*, vol. 2, no. 8, Aug. 2020, Art. no. 2080073.
- [431] A. Frutiger, J. T. Muth, D. M. Vogt, Y. Mengüç, A. Campo, A. D. Valentine, C. J. Walsh, and J. A. Lewis, “Capacitive soft strain sensors via multicore-shell fiber printing,” *Adv. Mater.*, vol. 27, no. 15, pp. 2440–2446, Apr. 2015.
- [432] J. O. Hardin, C. A. Grabowski, M. Lucas, M. F. Durstock, and J. D. Berrigan, “All-printed multilayer high voltage capacitors with integrated processing feedback,” *Additive Manuf.*, vol. 27, pp. 327–333, May 2019.
- [433] S. Mousavi, D. Howard, F. Zhang, J. Leng, and C. H. Wang, “Direct 3D printing of highly anisotropic, flexible, constriction-resistive sensors for multidirectional proprioception in soft robots,” *ACS Appl. Mater. Interfaces*, vol. 12, no. 13, pp. 15631–15643, 2020.
- [434] S. Ozel, N. A. Keskin, D. Khea, and C. D. Onal, “A precise embedded curvature sensor module for soft-bodied robots,” *Sens. Actuators A, Phys.*, vol. 236, pp. 349–356, Dec. 2015.
- [435] M. Bodnicki and J. Grzybowski, *Miniature Transducer of Linear Displacement Based on Miniature Hall Effect Sensors*. Cham, Switzerland: Springer, 2015, pp. 21–26.
- [436] J. van Tiem, J. Groenesteijn, R. Sanders, and G. Krijnen, “3D printed bio-inspired angular acceleration sensor,” in *Proc. IEEE SENSORS*, Nov. 2015, pp. 1–4.
- [437] Y. R. Jeong, J. Kim, Z. Xie, Y. Xue, S. M. Won, G. Lee, S. W. Jin, S. Y. Hong, X. Feng, Y. Huang, J. A. Rogers, and J. S. Ha, “A skin-attachable, stretchable integrated system based on liquid GaInSn for wireless human motion monitoring with multi-site sensing capabilities,” *NPG Asia Mater.*, vol. 9, no. 10, p. e443, Oct. 2017.
- [438] B. Jamil, G. Yoo, Y. Choi, and H. Rodrigue, “Proprioceptive soft pneumatic gripper for extreme environments using hybrid optical fibers,” *IEEE Robot. Autom. Lett.*, vol. 6, no. 4, pp. 8694–8701, Oct. 2021.
- [439] J. Jung, M. Park, D. Kim, and Y.-L. Park, “Optically sensorized elastomer air chamber for proprioceptive sensing of soft pneumatic actuators,” *IEEE Robot. Autom. Lett.*, vol. 5, no. 2, pp. 2333–2340, Apr. 2020.
- [440] D. J. Lorang, D. Tanaka, C. M. Spadaccini, K. A. Rose, N. J. Cherepy, and J. A. Lewis, “Photocurable liquid core-fugitive shell printing of optical waveguides,” *Adv. Mater.*, vol. 23, no. 43, pp. 5055–5058, Nov. 2011.
- [441] C. Tawk, M. Panhuis, G. M. Spinks, and G. Alici, “Soft pneumatic sensing chambers for generic and interactive human–machine interfaces,” *Adv. Intell. Syst.*, vol. 1, no. 1, May 2019, Art. no. 1900002.
- [442] R. Slyper and J. Hodgins, “Prototyping robot appearance, movement, and interactions using flexible 3D printing and air pressure sensors,” in *Proc. 21st IEEE Int. Symp. Robot Hum. Interact. Commun.*, Sep. 2012, pp. 6–11.
- [443] J. Kim, A. Alspach, and K. Yamane, “3D printed soft skin for safe human-robot interaction,” in *Proc. IEEE/RSJ Int. Conf. Intell. Robots Syst. (IROS)*, Sep. 2015, pp. 2419–2425.
- [444] H. Yang, Y. Chen, Y. Sun, and L. Hao, “A novel pneumatic soft sensor for measuring contact force and curvature of a soft gripper,” *Sens. Actuator A Phys.*, vol. 266, pp. 318–327, Oct. 2017.
- [445] H. Choi, P.-G. Jung, K. Jung, and K. Kong, “Design and fabrication of a soft three-axis force sensor based on radially symmetric pneumatic chambers,” in *Proc. IEEE Int. Conf. Robot. Autom. (ICRA)*, May 2017, pp. 5519–5524.
- [446] D. Gong, R. He, J. Yu, and G. Zuo, “A pneumatic tactile sensor for co-operative robots,” *Sensors*, vol. 17, no. 11, p. 2592, 2017.
- [447] Q. Lu, L. He, T. Nanayakkara, and N. Rojas, “Precise in-hand manipulation of soft objects using soft fingertips with tactile sensing and active deformation,” in *Proc. 3rd IEEE Int. Conf. Soft Robot. (RoboSoft)*, May 2020, pp. 52–57.
- [448] H. A. Putra, “Exploring air properties for fMRI-compatible interaction devices,” in *Proc. MATEC Web Conf.*, vol. 215, 2018, Art. no. 01001.
- [449] M. Vázquez, E. Brockmeyer, R. Desai, C. Harrison, and S. E. Hudson, “3D printing pneumatic device controls with variable activation force capabilities,” in *Proc. 33rd Annu. ACM Conf. Hum. Factors Comput. Syst.*, New York, NY, USA, Apr. 2015, pp. 1295–1304.
- [450] J.-B. Chossat and P. B. Shull, “Soft acoustic waveguides for strain, deformation, localization, and twist measurements,” *IEEE Sensors J.*, vol. 21, no. 1, pp. 222–230, Jan. 2021.
- [451] G. Zoller, V. Wall, and O. Brock, “Active acoustic contact sensing for soft pneumatic actuators,” in *Proc. IEEE Int. Conf. Robot. Autom. (ICRA)*, May 2020, pp. 7966–7972.

- [452] G. Zoller, V. Wall, and O. Brock, "Acoustic sensing for soft pneumatic actuators," in *Proc. IEEE/RSJ Int. Conf. Intell. Robots Syst. (IROS)*, Oct. 2018, pp. 6986–6991.
- [453] K. Takaki, Y. Taguchi, S. Nishikawa, R. Niiyama, and Y. Kawahara, "Acoustic length sensor for soft extensible pneumatic actuators with a frequency characteristics model," *IEEE Robot. Autom. Lett.*, vol. 4, no. 4, pp. 4292–4297, Oct. 2019.
- [454] C. P. Tan, S. Nurzaman, J. Y. Loo, and Z. Y. Ding, "Future trends in I&M: Indirect sensing in soft robots using observers/filters," *IEEE Instrum. Meas. Mag.*, vol. 23, no. 1, pp. 42–43, Feb. 2020.
- [455] D. Simon, *Optimal State Estimation: Kalman, H Infinity, and Nonlinear Approaches*. Hoboken, NJ, USA: Wiley, 2006.
- [456] J. Y. Loo, K. C. Kong, C. P. Tan, and S. G. Nurzaman, "Non-linear system identification and state estimation in a pneumatic based soft continuum robot," in *Proc. IEEE Conf. Control Technol. Appl. (CCTA)*, Aug. 2019, pp. 39–46.
- [457] J. Y. Loo, Z. Y. Ding, E. Davies, S. G. Nurzaman, and C. P. Tan, "Curvature and force estimation for a soft finger using an EKF with unknown input optimization," *IFAC-PapersOnLine*, vol. 53, no. 2, pp. 8506–8512, 2020.
- [458] J. Y. Loo, Z. Y. Ding, V. M. Baskaran, S. G. Nurzaman, and C. P. Tan, "Robust multimodal indirect sensing for soft robots via neural network-aided filter-based estimation," *Soft Robot.*, Jun. 2021.
- [459] H. Cheng, D. Li, J. Zhang, Y. Li, and J. Hong, "Nonlinear error feedback positioning control for a pneumatic soft bionic fin via an extended state observer," *IEEE Access*, vol. 8, pp. 12688–12696, 2020.
- [460] A. Ataka, T. Abrar, F. Putzu, H. Godaba, and K. Althoefer, "Observer-based control of inflatable robot with variable stiffness," in *Proc. IEEE/RSJ Int. Conf. Intell. Robots Syst. (IROS)*, Oct. 2020, pp. 8646–8652.
- [461] M. Li, R. Kang, D. T. Branson, and J. S. Dai, "Model-free control for continuum robots based on an adaptive Kalman filter," *IEEE/ASME Trans. Mechatronics*, vol. 23, no. 1, pp. 286–297, Feb. 2017.
- [462] M. S. Xavier, A. J. Fleming, and Y. K. Yong, "Nonlinear estimation and control of bending soft pneumatic actuators using feedback linearization and UKF," *IEEE/ASME Trans. Mechatronics*, early access, Mar. 15, 2022, doi: [10.1109/TMECH.2022.3155790](https://doi.org/10.1109/TMECH.2022.3155790).
- [463] P. Breitman, Y. Matia, and A. D. Gat, "Fluid mechanics of pneumatic soft robots," *Soft Robot.*, vol. 8, no. 5, pp. 519–530, Oct. 2021.
- [464] B. Shih, D. Shah, J. Li, T. G. Thuruthel, Y.-L. Park, F. Iida, Z. Bao, R. Kramer-Bottiglio, and M. T. Tolley, "Electronic skins and machine learning for intelligent soft robots," *Sci. Robot.*, vol. 5, no. 41, Apr. 2020, Art. no. eaaz9239.
- [465] Z. Tang, J. Lu, Z. Wang, W. Chen, and H. Feng, "Design of a new air pressure perception multi-cavity pneumatic-driven earthworm-like soft robot," *Auto. Robots*, vol. 44, no. 2, pp. 267–279, Jan. 2020.
- [466] G. H. Franzini, J. H. Price, J. F. Fuller, and N. Schmidt, "Manta ray robot," M.S. thesis, Worcester Polytech. Inst., Worcester, MA, USA, 2016.
- [467] S. Ibrahim, J. C. Krause, and A. Raatz, "Linear and nonlinear low level control of a soft pneumatic actuator," in *Proc. 2nd IEEE Int. Conf. Soft Robot. (RoboSoft)*, Apr. 2019, pp. 434–440.
- [468] A. H. Khan, Z. Shao, S. Li, Q. Wang, and N. Guan, "Which is the best PID variant for pneumatic soft robots an experimental study," *IEEE/CAA J. Autom. Sinica*, vol. 7, no. 2, pp. 451–460, Mar. 2020.
- [469] G. C. Goodwin, S. F. Graebe, and M. E. Salgado, *Control System Design*, vol. 240. Upper Saddle River, NJ, USA: Prentice-Hall, 2001.
- [470] K. Ogata and Y. Yang, *Modern Control Engineering*, vol. 5. Upper Saddle River, NJ, USA: Prentice-Hall, 2010.
- [471] Z. Zhang, H. Chen, and Z. Zhang, "Configuration synthesis and performance analysis of finger soft actuator," *Appl. Bionics Biomech.*, vol. 2018, pp. 1–14, Aug. 2018.
- [472] J. Realmuto and T. Sanger, "A robotic forearm orthosis using soft fabric-based helical actuators," in *Proc. 2nd IEEE Int. Conf. Soft Robot. (RoboSoft)*, Apr. 2019, pp. 591–596.
- [473] C. Luo, K. Wang, G. Li, S. Yin, L. Yu, and E. Yang, "Development of active soft robotic manipulators for stable grasping under slippery conditions," *IEEE Access*, vol. 7, pp. 97604–97613, 2019.
- [474] J. Zhou, X. Chen, U. Chang, J.-T. Lu, C. C. Y. Leung, Y. Chen, Y. Hu, and Z. Wang, "A soft-robotic approach to anthropomorphic robotic hand dexterity," *IEEE Access*, vol. 7, pp. 101483–101495, 2019.
- [475] J. Yi, X. Chen, C. Song, J. Zhou, Y. Liu, S. Liu, and Z. Wang, "Customizable three-dimensional-printed origami soft robotic joint with effective behavior shaping for safe interactions," *IEEE Trans. Robot.*, vol. 35, no. 1, pp. 114–123, Oct. 2018.
- [476] D. Liang, N. Sun, Y. Wu, G. Liu, and Y. Fang, "Fuzzy-sliding mode control for humanoid arm robots actuated by pneumatic artificial muscles with unidirectional inputs, saturations, and dead zones," *IEEE Trans. Ind. Informat.*, vol. 18, no. 5, pp. 3011–3021, May 2022.
- [477] D. Liang, N. Sun, Y. Wu, Y. Chen, Y. Fang, and L. Liu, "Energy-based motion control for pneumatic artificial muscle actuated robots with experiments," *IEEE Trans. Ind. Electron.*, vol. 69, no. 7, pp. 7295–7306, Jul. 2021.
- [478] E. Franco, A. Garriga Casanovas, and A. Donaire, "Energy shaping control with integral action for soft continuum manipulators," *Mechanism Mach. Theory*, vol. 158, Apr. 2021, Art. no. 104250.
- [479] E. Franco, T. Ayatullah, A. Sugiharto, A. Garriga-Casanovas, and V. Virdyawan, "Nonlinear energy-based control of soft continuum pneumatic manipulators," *Nonlinear Dyn.*, vol. 106, no. 1, pp. 229–253, Sep. 2021.
- [480] D. Ross, M. P. Nemitz, and A. A. Stokes, "Controlling and simulating soft robotic systems: Insights from a thermodynamic perspective," *Soft Robot.*, vol. 3, no. 4, pp. 170–176, Dec. 2016.
- [481] H.-T.-D. Chun, J. O. Roberts, M. E. Sayed, S. Aracri, and A. A. Stokes, "Towards more energy efficient pneumatic soft actuators using a port-Hamiltonian approach," in *Proc. 2nd IEEE Int. Conf. Soft Robot. (RoboSoft)*, Apr. 2019, pp. 277–282.
- [482] S. Ibrahim, J. C. Krause, A. Olbrich, and A. Raatz, "Modeling and reconstruction of state variables for low-level control of soft pneumatic actuators," *Frontiers Robot. AI*, vol. 8, p. 32, Mar. 2021.
- [483] M. S. Xavier, A. J. Fleming, and Y. K. Yong, "Model-based nonlinear feedback controllers for pressure control of soft pneumatic actuators using on/off valves," *Frontiers Robot. AI*, vol. 9, p. 33, Mar. 2022.
- [484] V. Falkenhahn, A. Hildebrandt, R. Neumann, and O. Sawodny, "Dynamic control of the bionic handling assistant," *IEEE/ASME Trans. Mechatronics*, vol. 22, no. 1, pp. 6–17, Feb. 2016.
- [485] D. B. Camarillo, K. E. Loewke, C. R. Carlson, and J. K. Salisbury, "Vision based 3-D shape sensing of flexible manipulators," in *Proc. IEEE Int. Conf. Robot. Autom.*, May 2008, pp. 2940–2947.
- [486] M. W. Hannan and I. D. Walker, "Real-time shape estimation for continuum robots using vision," *Robotica*, vol. 23, no. 5, pp. 645–651, Sep. 2005.
- [487] K. Wu, L. Wu, and H. Ren, "An image based targeting method to guide a tentacle-like curvilinear concentric tube robot," in *Proc. IEEE Int. Conf. Robot. Biomimetics (ROBIO)*, Dec. 2014, pp. 386–391.
- [488] M. C. Yip and D. B. Camarillo, "Model-less feedback control of continuum manipulators in constrained environments," *IEEE Trans. Robot.*, vol. 30, no. 4, pp. 880–889, Aug. 2014.
- [489] Y. Lu, C. Zhang, S. Song, and M. Q.-H. Meng, "Precise motion control of concentric-tube robot based on visual servoing," in *Proc. IEEE Int. Conf. Inf. Autom. (ICIA)*, Jul. 2017, pp. 299–304.
- [490] H. Wang, B. Yang, Y. Liu, W. Chen, X. Liang, and R. Pfeifer, "Visual servoing of soft robot manipulator in constrained environments with an adaptive controller," *IEEE/ASME Trans. Mechatronics*, vol. 22, no. 1, pp. 41–50, Feb. 2017.
- [491] Y. Wang, H. Wang, Z. Liu, and W. Chen, "Visual servo-collision avoidance hybrid task by considering detection and localization of contact for a soft manipulator," *IEEE/ASME Trans. Mechatronics*, vol. 25, no. 3, pp. 1310–1321, Jun. 2020.
- [492] F. Xu, H. Wang, J. Wang, K. W. S. Au, and W. Chen, "Underwater dynamic visual servoing for a soft robot arm with online distortion correction," *IEEE/ASME Trans. Mechatron.*, vol. 24, no. 3, pp. 979–989, Jun. 2019.
- [493] J. Lai, K. Huang, B. Lu, and H. K. Chu, "Toward vision-based adaptive configuring of a bidirectional two-segment soft continuum manipulator," in *Proc. IEEE/ASME Int. Conf. Adv. Intell. Mechatronics (AIM)*, Jul. 2020, pp. 934–939.
- [494] Y. Jin, Y. Wang, X. Chen, Z. Wang, X. Liu, H. Jiang, and X. Chen, "Model-less feedback control for soft manipulators," in *Proc. IEEE/RSJ Int. Conf. Intell. Robots Syst. (IROS)*, Sep. 2017, pp. 2916–2922.
- [495] H. Jiang, X. Liu, X. Chen, Z. Wang, Y. Jin, and X. Chen, "Design and simulation analysis of a soft manipulator based on honeycomb pneumatic networks," in *Proc. IEEE Int. Conf. Robot. Biomimetics (ROBIO)*, Dec. 2016, pp. 350–356.

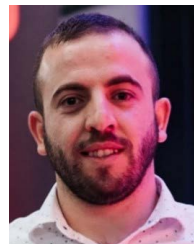
- [584] M. Pan, C. Yuan, X. Liang, T. Dong, T. Liu, J. Zhang, J. Zou, H. Yang, and C. Bowen, "Soft actuators and robotic devices for rehabilitation and assistance," *Adv. Intell. Syst.*, vol. 4, no. 4, Apr. 2022, Art. no. 2100140.
- [585] M. Xiloyannis, R. Alicea, A.-M. Georgarakis, F. L. Haufe, P. Wolf, L. Masia, and R. Riener, "Soft robotic suits: State of the art, core technologies, and open challenges," *IEEE Trans. Robot.*, early access, Jun. 18, 2021, doi: [10.1109/TRO.2021.3084466](https://doi.org/10.1109/TRO.2021.3084466).
- [586] Y. Wang, S. Kokubu, Z. Zhou, X. Guo, Y.-H. Hsueh, and W. Yu, "Designing soft pneumatic actuators for thumb movements," *IEEE Robot. Autom. Lett.*, vol. 6, no. 4, pp. 8450–8457, Oct. 2021.
- [587] Y. Chen, Y. Yang, M. Li, E. Chen, W. Mu, R. Fisher, and R. Yin, "Wearable actuators: An overview," *Textiles*, vol. 1, no. 2, pp. 283–321, Aug. 2021.
- [588] P. H. Nguyen and W. Zhang, "Design and computational modeling of fabric soft pneumatic actuators for wearable assistive devices," *Sci. Rep.*, vol. 10, no. 1, pp. 1–13, Dec. 2020.
- [589] H. K. Yap, J. Hoon Lim, F. Nasrallah, J. C. H. Goh, and R. C. H. Yeow, "A soft exoskeleton for hand assistive and rehabilitation application using pneumatic actuators with variable stiffness," in *Proc. IEEE Int. Conf. Robot. Autom. (ICRA)*, May 2015, pp. 4967–4972.
- [590] C. T. O'Neill, N. S. Phipps, L. Cappello, S. Paganoni, and C. J. Walsh, "A soft wearable robot for the shoulder: Design, characterization, and preliminary testing," in *Proc. Int. Conf. Rehabil. Robot. (ICORR)*, Jul. 2017, pp. 1672–1678.
- [591] H. K. Yap, J. H. Lim, F. Nasrallah, and C.-H. Yeow, "Design and preliminary feasibility study of a soft robotic glove for hand function assistance in stroke survivors," *Frontiers Neurosci.*, vol. 11, p. 547, Oct. 2017.
- [592] C. J. Payne, E. G. Hevia, N. Phipps, A. Atalay, O. Atalay, B. R. Seo, D. J. Mooney, and C. J. Walsh, "Force control of textile-based soft wearable robots for mechanotherapy," in *Proc. IEEE Int. Conf. Robot. Autom. (ICRA)*, May 2018, pp. 5459–5465.
- [593] H. L. Heung, Z. Q. Tang, X. Q. Shi, K. Y. Tong, and Z. Li, "Soft rehabilitation actuator with integrated post-stroke finger spasticity evaluation," *Frontiers Bioengineering Biotechnol.*, vol. 8, p. 111, Feb. 2020.
- [594] B. W. K. Ang and C.-H. Yeow, "Design and modeling of a high force soft actuator for assisted elbow flexion," *IEEE Robot. Autom. Lett.*, vol. 5, no. 2, pp. 3731–3736, Apr. 2020.
- [595] D. Xie, S. Zuo, and J. Liu, "A novel flat modular pneumatic artificial muscle," *Smart Mater. Struct.*, vol. 29, no. 6, Jun. 2020, Art. no. 065013, doi: [10.1088/1361-665X/ab84b9](https://doi.org/10.1088/1361-665X/ab84b9).
- [596] C. Di Natali, A. Sadeghi, A. Mondini, E. Bottenberg, B. Hartigan, A. De Eyto, L. O'Sullivan, E. Rocon, K. Stadler, B. Mazzolai, D. G. Caldwell, and J. Ortiz, "Pneumatic quasi-passive actuation for soft assistive lower limbs exoskeleton," *Frontiers Neurorobotics*, vol. 14, p. 31, Jun. 2020.
- [597] A. Golgouneh, E. Beaudette, H. Woelfle, B. Li, N. Subash, A. J. Redhouse, M. Jones, T. Martin, M. A. Lobo, B. Holschuh, and L. E. Dunne, "Design of a hybrid SMA-pneumatic based wearable upper limb exoskeleton," in *Proc. Int. Symp. Wearable Comput. (ISWC)*, New York, NY, USA, 2021, pp. 179–183.
- [598] L. Gerez, A. Dwivedi, and M. Liarokapis, "A hybrid, soft exoskeleton glove equipped with a telescopic extra thumb and abduction capabilities," in *Proc. IEEE Int. Conf. Robot. Autom. (ICRA)*, May 2020, pp. 9100–9106.
- [599] Y.-S. Seo, S. J. Cho, J.-Y. Lee, C. Park, U. Kim, S. Lee, B. Kim, C. Park, and S.-H. Song, "Human-mimetic soft robot joint for shock absorption through joint dislocation," *Bioinspiration Biomimetics*, vol. 15, no. 1, Nov. 2019, Art. no. 016001.
- [600] D. Singh, C. Tawk, R. Mutlu, E. Sariyildiz, V. Sencadas, and G. Alici, "A 3D printed soft force sensor for soft haptics," in *Proc. 3rd IEEE Int. Conf. Soft Robot. (RoboSoft)*, May 2020, pp. 458–463.
- [601] D. Singh, C. Tawk, R. Mutlu, E. Sariyildiz, and G. Alici, "A 3D printed soft robotic monolithic unit for haptic feedback devices," in *Proc. IEEE/ASME Int. Conf. Adv. Intell. Mechatronics (AIM)*, Jul. 2019, pp. 388–393.
- [602] F. Sebastian, Q. Fu, M. Santello, and P. Polygerinos, "Soft robotic haptic interface with variable stiffness for rehabilitation of neurologically impaired hand function," *Frontiers Robot. AI*, vol. 4, p. 69, Dec. 2017.
- [603] H. A. Sonar, A. P. Gerratt, S. P. Lacour, and J. Paik, "Closed-loop haptic feedback control using a self-sensing soft pneumatic actuator skin," *Soft Robot.*, vol. 7, no. 1, pp. 22–29, Feb. 2020.
- [604] A. Talhan, H. Kim, and S. Jeon, "Tactile ring: Multi-mode finger-worn soft actuator for rich haptic feedback," *IEEE Access*, vol. 8, pp. 957–966, 2020.
- [605] M. Culjat, C. King, M. Franco, J. Bisley, W. Grundfest, and E. Dutton, "Pneumatic balloon actuators for tactile feedback in robotic surgery," *Ind. Robot, Int. J.*, vol. 35, no. 5, pp. 449–455, Aug. 2008.
- [606] L. He, C. Xu, D. Xu, and R. Brill, "PneuHaptic: Delivering haptic cues with a pneumatic armband," in *Proc. ACM Int. Symp. Wearable Comput. (ISWC)*, New York, NY, USA, 2015, pp. 47–48.
- [607] G. Frediani and F. Carpi, "Tactile display of softness on fingertip," *Sci. Rep.*, vol. 10, no. 1, pp. 1–10, Dec. 2020.
- [608] Y.-L. Feng, R. L. Peiris, C. L. Fernando, and K. Minamizawa, "3D printed haptics: Creating pneumatic haptic display based on 3D printed airbags," in *Proc. Int. Conf. Hum. Haptic Sens. Touch Enabled Comput. Appl.*, 2018, pp. 180–192.
- [609] R. B. Scharff, E. L. Doubrovski, W. A. Poelman, P. P. Jonker, C. C. Wang, and J. M. Geraedts, "Towards behavior design of a 3D-printed soft robotic hand," in *Soft Robotics: Trends, Applications and Challenges*. Springer, 2017, pp. 23–29.
- [610] G. Gu, N. Zhang, H. Xu, S. Lin, Y. Yu, G. Chai, L. Ge, H. Yang, Q. Shao, X. Sheng, X. Zhu, and X. Zhao, "A soft neuroprosthetic hand providing simultaneous myoelectric control and tactile feedback," *Nature Biomed. Eng.*, pp. 1–10, Aug. 2021.
- [611] S. Jadhav, V. Kannanda, B. Kang, M. T. Tolley, and J. P. Schulze, "Soft robotic glove for kinesthetic haptic feedback in virtual reality environments," *Electron. Imag.*, vol. 29, no. 3, pp. 19–24, Jan. 2017.
- [612] C. J. Payne, I. Wamala, C. Abah, T. Thalhofer, M. Saeed, D. Bautista-Salinas, M. A. Horvath, N. V. Vasilyev, E. T. Roche, F. A. Pigula, and C. J. Walsh, "An implantable extracardiac soft robotic device for the failing heart: Mechanical coupling and synchronization," *Soft Robot.*, vol. 4, no. 3, pp. 241–250, Sep. 2017.
- [613] M. Y. Saeed, D. Van Story, C. J. Payne, I. Wamala, B. Shin, D. Bautista-Salinas, D. Zurakowski, P. J. del Nido, C. J. Walsh, and N. V. Vasilyev, "Dynamic augmentation of left ventricle and mitral valve function with an implantable soft robotic device," *J. Am. Coll. Cardiol. Basic Trans. Sci.*, vol. 5, no. 3, pp. 229–242, Mar. 2020.
- [614] C. M. Schumacher, M. Loepfe, R. Fuhrer, R. N. Grass, and W. J. Stark, "3D printed lost-wax casted soft silicone monoblocks enable heart-inspired pumping by internal combustion," *RSC Adv.*, vol. 4, no. 31, pp. 16039–16042, 2014.
- [615] B. C. Mac Murray, X. An, S. S. Robinson, I. M. van Meerbeek, K. W. O'Brien, H. Zhao, and R. F. Shepherd, "Poroeleastic foams for simple fabrication of complex soft robots," *Adv. Mater.*, vol. 27, no. 41, pp. 6334–6340, Nov. 2015.
- [616] N. H. Cohrs, A. Petrou, M. Loepfe, M. Yliruka, C. M. Schumacher, A. X. Kohll, C. T. Starck, M. Schmid Daners, M. Meboldt, V. Falk, and W. J. Stark, "A soft total artificial heart-first concept evaluation on a hybrid mock circulation," *Artif. Organs*, vol. 41, no. 10, pp. 948–958, Oct. 2017.
- [617] Y. Dang, Y. Liu, R. Hashem, D. Bhattacharya, J. Allen, M. Stommel, L. K. Cheng, and W. Xu, "SoGut: A soft robotic gastric simulator," *Soft Robot.*, vol. 8, no. 3, pp. 273–283, Jun. 2021.
- [618] M. A. Horvath, L. Hu, T. Mueller, J. Hochstein, L. Rosalia, K. A. Hibbert, C. C. Hardin, and E. T. Roche, "An organosynthetic soft robotic respiratory simulator," *APL Bioeng.*, vol. 4, no. 2, Jun. 2020, Art. no. 026108.
- [619] D. Bhattacharya, S. J. V. Ali, L. K. Cheng, and W. Xu, "RoSE: A robotic soft esophagus for endoprosthetic stent testing," *Soft Robot.*, vol. 8, no. 4, pp. 397–415, Aug. 2021.
- [620] Z. Samadikhoshkho, K. Zareinia, and F. Janabi-Sharifi, "A brief review on robotic grippers classifications," in *Proc. IEEE Can. Conf. Electr. Comput. Eng. (CCECE)*, May 2019, pp. 1–4.
- [621] J.-Y. Lee, J. Eom, S. Y. Yu, and K. Cho, "Customization methodology for conformable grasping posture of soft grippers by stiffness patterning," *Frontiers Robot. AI*, vol. 7, p. 114, Sep. 2020.
- [622] C. Tawk, Y. Gao, R. Mutlu, and G. Alici, "Fully 3D printed monolithic soft gripper with high conformal grasping capability," in *Proc. IEEE/ASME Int. Conf. Adv. Intell. Mechatronics (AIM)*, Jul. 2019, pp. 1139–1144.
- [623] M. Ariyanto, M. Munadi, J. D. Setiawan, D. Mulyanto, and T. Nugroho, "Three-fingered soft robotic gripper based on pneumatic network actuator," in *Proc. 6th Int. Conf. Inf. Technol., Comput. Electr. Eng. (ICITACEE)*, Sep. 2019, pp. 1–5.

- [624] A. K. Nguyen, A. Russell, N. Naclerio, V. Vuong, H. Huang, K. Chui, and E. W. Hawkes, "A tri-stable soft robotic finger capable of pinch and wrap grasps," in *Proc. IEEE Int. Conf. Robot. Autom. (ICRA)*, May 2020, pp. 9028–9034.
- [625] C. Tawk, A. Gillett, M. Panhuis, G. M. Spinks, and G. Alici, "A 3D-printed omni-purpose soft gripper," *IEEE Trans. Robot.*, vol. 35, no. 5, pp. 1268–1275, Oct. 2019.
- [626] M. Hofer, J. Zughäibi, and R. D'Andrea, "Design and control of an inflatable spherical robotic arm for pick and place applications," *Actuators*, vol. 10, no. 11, p. 299, Nov. 2021.
- [627] H.-J. Kim, A. Kawamura, Y. Nishioka, and S. Kawamura, "Mechanical design and control of inflatable robotic arms for high positioning accuracy," *Adv. Robot.*, vol. 32, no. 2, pp. 89–104, Jan. 2018.
- [628] X. Liang, H. Cheong, Y. Sun, J. Guo, C. K. Chui, and C.-H. Yeow, "Design, characterization, and implementation of a two-DOF fabric-based soft robotic arm," *IEEE Robot. Autom. Lett.*, vol. 3, no. 3, pp. 2702–2709, Jul. 2018.
- [629] E. Navas, R. Fernández, D. Sepúlveda, M. Armada, and P. Gonzalez-de-Santos, "Soft grippers for automatic crop harvesting: A review," *Sensors*, vol. 21, no. 8, p. 2689, Apr. 2021.
- [630] Z. Wang, D. S. Chaturanga, and S. Hirai, "3D printed soft gripper for automatic lunch box packing," in *Proc. IEEE Int. Conf. Robot. Biomimetics (ROBIO)*, Dec. 2016, pp. 503–508.
- [631] S. Terryn, J. Brancart, D. Lefeber, G. Van Assche, and B. Vanderborght, "Self-healing soft pneumatic robots," *Sci. Robot.*, vol. 2, no. 9, p. eaan4268, Aug. 2017.
- [632] C. Tawk, R. Mutlu, and G. Alici, "A 3D printed modular soft gripper integrated with metamaterials for conformal grasping," *Frontiers Robot. AI*, vol. 8, p. 429, Jan. 2022.
- [633] S. Abondance, C. B. Teeple, and R. J. Wood, "A dexterous soft robotic hand for delicate in-hand manipulation," *IEEE Robot. Autom. Lett.*, vol. 5, no. 4, pp. 5502–5509, Oct. 2020.
- [634] Y. Hao, Z. Gong, Z. Xie, S. Guan, X. Yang, Z. Ren, T. Wang, and L. Wen, "Universal soft pneumatic robotic gripper with variable effective length," in *Proc. 35th Chin. Control Conf. (CCC)*, Jul. 2016, pp. 6109–6114.
- [635] D. Wang, X. Wu, J. Zhang, and Y. Du, "A pneumatic novel combined soft robotic gripper with high load capacity and large grasping range," *Actuators*, vol. 11, no. 1, p. 3, Dec. 2021.
- [636] Y. Fei, J. Wang, and W. Pang, "A novel fabric-based versatile and stiffness-tunable soft gripper integrating soft pneumatic fingers and wrist," *Soft Robot.*, vol. 6, no. 1, pp. 1–20, 2018.
- [637] P. Glick, S. A. Suresh, D. Ruffatto, M. Cutkosky, M. T. Tolley, and A. Parness, "A soft robotic gripper with gecko-inspired adhesive," *IEEE Robot. Autom. Lett.*, vol. 3, no. 2, pp. 903–910, Apr. 2018.
- [638] C. Tawk, R. Mutlu, and G. Alici, "A3D printed modular soft gripper for conformal grasping," in *Proc. IEEE/ASME Int. Conf. Adv. Intell. Mechatron.*, Jul. 2020, pp. 583–588.
- [639] K. Yu, A. Xin, H. Du, Y. Li, and Q. Wang, "Additive manufacturing of self-healing elastomers," *NPG Asia Mater.*, vol. 11, no. 1, pp. 1–11, Dec. 2019.
- [640] S. Terryn, J. Langenbach, E. Roels, J. Brancart, C. Bakkali-Hassani, Q.-A. Poutrel, A. Georgopoulou, T. G. Thuruthel, A. Safaei, and P. Ferrentino, "A review on self-healing polymers for soft robotics," *Mater. Today*, vol. 47, pp. 187–205, Jul. 2021.
- [641] M. D. Bartlett, M. D. Dickey, and C. Majidi, "Self-healing materials for soft-matter machines and electronics," *NPG Asia Mater.*, vol. 11, no. 1, pp. 1–4, Dec. 2019.
- [642] T. J. Wallin, J. H. Pikul, S. Bodkhe, B. N. Peele, B. C. M. Murray, D. Therriault, B. W. McEnerney, R. P. Dillon, E. P. Giannelis, and R. F. Shepherd, "Click chemistry stereolithography for soft robots that self-heal," *J. Mater. Chem. B*, vol. 5, no. 31, pp. 6249–6255, 2017.
- [643] A. Pena-Francesch, H. Jung, M. C. Demirel, and M. Sitti, "Biosynthetic self-healing materials for soft machines," *Nature Mater.*, vol. 19, no. 11, pp. 1230–1235, Nov. 2020.
- [644] K. Narumi, F. Qin, S. Liu, H.-Y. Cheng, J. Gu, Y. Kawahara, M. Islam, and L. Yao, "Self-healing UI: Mechanically and electrically self-healing materials for sensing and actuation interfaces," in *Proc. 32nd Annu. ACM Symp. User Interface Softw. Technol.*, Oct. 2019, pp. 293–306.
- [645] R. F. Shepherd, A. A. Stokes, R. M. D. Nunes, and G. M. Whitesides, "Soft machines that are resistant to puncture and that self seal," *Adv. Mater.*, vol. 25, no. 46, pp. 6709–6713, Dec. 2013.
- [646] M. Baumgartner, F. Hartmann, M. Drack, D. Preninger, D. Wirthl, R. Gerstmayr, L. Lehner, G. Mao, R. Pruckner, and S. Demchyshyn, "Resilient yet entirely degradable gelatin-based biogels for soft robots and electronics," *Nature Mater.*, vol. 19, no. 10, pp. 1102–1109, Oct. 2020.
- [647] R. A. Bilodeau and R. K. Kramer, "Self-healing and damage resilience for soft robotics: A review," *Frontiers Robot. AI*, vol. 4, p. 48, Oct. 2017.
- [648] M. T. Tolley, R. F. Shepherd, B. Mosadegh, K. C. Galloway, M. Wehner, M. Karpelson, R. J. Wood, and G. M. Whitesides, "A resilient, untethered soft robot," *Soft Robot.*, vol. 1, no. 3, pp. 213–223, Sep. 2014.
- [649] O. D. Yirmibeğözü, T. Oshiro, G. Olson, C. Palmer, and Y. Mengüç, "Evaluation of 3D printed soft robots in radiation environments and comparison with molded counterparts," *Frontiers Robot. AI*, vol. 6, p. 40, May 2019.
- [650] R. V. Martinez, A. C. Glavan, C. Keplinger, A. I. Oyetibo, and G. M. Whitesides, "Soft actuators and robots that are resistant to mechanical damage," *Adv. Funct. Mater.*, vol. 24, no. 20, pp. 3003–3010, May 2014.
- [651] N. S. Usevitch, Z. M. Hammond, M. Schwager, A. M. Okamura, E. W. Hawkes, and S. Follmer, "An untethered isoperimetric soft robot," *Sci. Robot.*, vol. 5, no. 40, Mar. 2020, Art. no. eaaz0492.
- [652] A. A. Amiri Moghadam, S. Alaie, S. D. Nath, M. A. Shaarbaif, J. K. Min, S. Dunham, and B. Mosadegh, "Laser cutting as a rapid method for fabricating thin soft pneumatic actuators and robots," *Soft Robot.*, vol. 5, no. 4, pp. 443–451, Aug. 2018.
- [653] J.-Y. Lee, W.-B. Kim, W.-Y. Choi, and K.-J. Cho, "Soft robotic blocks: Introducing SoBL, a fast-build modularized design block," *IEEE Robot. Autom. Mag.*, vol. 23, no. 3, pp. 30–41, Sep. 2016.
- [654] M. Yim, W. Shen, B. Salemi, D. Rus, M. Moll, H. Lipson, E. Klavins, and G. S. Chirikjian, "Modular self-reconfigurable robot systems [grand challenges of robotics]," *IEEE Robot. Autom. Mag.*, vol. 14, no. 1, pp. 43–52, Mar. 2007.
- [655] C. Zhang, P. Zhu, Y. Lin, Z. Jiao, and J. Zou, "Modular soft robotics: Modular units, connection mechanisms, and applications," *Adv. Intell. Syst.*, vol. 2, no. 6, Jun. 2020, Art. no. 1900166.
- [656] M. A. Skylar-Scott, J. Mueller, C. W. Visser, and J. A. Lewis, "Voxelated soft matter via multimaterial multinozzle 3D printing," *Nature*, vol. 575, no. 7782, pp. 330–335, Nov. 2019.
- [657] R. Nakayama, R. Suzuki, S. Nakamaru, R. Niiyama, Y. Kawahara, and Y. Kakehi, "MorphIO: Entirely soft sensing and actuation modules for programming shape changes through tangible interaction," in *Proc. Designing Interact. Syst. Conf.*, Jun. 2019, pp. 975–986.
- [658] L. Ge, T. Wang, N. Zhang, and G. Gu, "Fabrication of soft pneumatic network actuators with oblique chambers," *J. Visualized Exp.*, no. 138, Aug. 2018, Art. no. e58277.
- [659] G. Gu, D. Wang, L. Ge, and X. Zhu, "Analytical modeling and design of generalized pneu-net soft actuators with three-dimensional deformations," *Soft Robot.*, vol. 8, no. 4, pp. 462–477, Aug. 2021.
- [660] O. Byrne, F. Coulter, M. Glynn, J. F. X. Jones, A. N. Annaidh, E. D. O'Ceirbhail, and D. P. Holland, "Additive manufacture of composite soft pneumatic actuators," *Soft Robot.*, vol. 5, no. 6, pp. 726–736, Dec. 2018.
- [661] Y. Sun, J. Guo, T. M. Miller-Jackson, X. Liang, M. H. Ang, and R. C. H. Yeow, "Design and fabrication of a shape-morphing soft pneumatic actuator: Soft robotic pad," in *Proc. IEEE/RSJ Int. Conf. Intell. Robots Syst. (IROS)*, Sep. 2017, pp. 6214–6220.
- [662] Z. Jiao, C. Ji, J. Zou, H. Yang, and M. Pan, "Vacuum-powered soft pneumatic twisting actuators to empower new capabilities for soft robots," *Adv. Mater. Technol.*, vol. 4, no. 1, Jan. 2019, Art. no. 1800429.
- [663] T. J. Jones, E. Jambon-Puillet, J. Marthelot, and P.-T. Brun, "Bubble casting soft robotics," *Nature*, vol. 599, no. 7884, pp. 229–233, Nov. 2021.
- [664] X.-Y. Guo, W.-B. Li, and W.-M. Zhang, "Rapid actuation for soft pneumatic actuators using dynamic instability mechanism," in *Proc. Int. Conf. Intell. Robot. Appl.*, 2020, pp. 387–397.
- [665] A. Pal, D. Goswami, and R. V. Martinez, "Elastic energy storage enables rapid and programmable actuation in soft machines," *Adv. Funct. Mater.*, vol. 30, no. 1, Jan. 2020, Art. no. 1906603.
- [666] O. Bas, B. Gorissen, S. Luposchainsky, T. Shabab, K. Bertoldi, and D. W. Huttmacher, "Ultrafast, miniature soft actuators," *Multifunctional Mater.*, vol. 4, no. 4, Nov. 2021, Art. no. 045001.
- [667] C. Qiao, L. Liu, and D. Pasini, "Bi-shell valve for fast actuation of soft pneumatic actuators via shell snapping interaction," *Adv. Sci.*, vol. 8, no. 15, Aug. 2021, Art. no. 2100445.
- [668] B. Mazzolai et al., "Roadmap on soft robotics: Multifunctionality, adaptability and growth without borders," *Multifunctional Mater.*, Jan. 2022.

- [669] P. Boyraz, G. Runge, and A. Raatz, "An overview of novel actuators for soft robotics," *Actuators*, vol. 7, no. 3, p. 48, Aug. 2018.
- [670] H. Zhou, A. Mohammadi, D. Oetomo, and G. Alici, "A novel monolithic soft robotic thumb for an anthropomorphic prosthetic hand," *IEEE Robot. Autom. Lett.*, vol. 4, no. 2, pp. 602–609, Apr. 2019.
- [671] Q. He and S. Cai, "Soft pumps for soft robots," *Sci. Robot.*, vol. 6, no. 51, Feb. 2021, Art. no. eabg6640.
- [672] W. Tang, C. Zhang, Y. Zhong, P. Zhu, Y. Hu, Z. Jiao, X. Wei, G. Lu, J. Wang, Y. Liang, Y. Lin, W. Wang, H. Yang, and J. Zou, "Customizing a self-healing soft pump for robot," *Nature Commun.*, vol. 12, no. 1, pp. 1–11, Dec. 2021.
- [673] D. Drotman, S. Jadhav, D. Sharp, C. Chan, and M. T. Tolley, "Electronics-free pneumatic circuits for controlling soft-legged robots," *Sci. Robot.*, vol. 6, no. 51, Feb. 2021, Art. no. eaay2627.
- [674] C. Lee, M. Kim, Y. J. Kim, N. Hong, S. Ryu, H. J. Kim, and S. Kim, "Soft robot review," *Int. J. Control, Autom. Syst.*, vol. 15, no. 1, pp. 3–15, Feb. 2017.
- [675] R. S. Diteesawat, T. Helps, M. Taghavi, and J. Rossiter, "Electropneumatic pumps for soft robotics," *Sci. Robot.*, vol. 6, no. 51, Feb. 2021, Art. no. eabc3721.
- [676] V. Cacucciolo, J. Shintake, Y. Kuwajima, S. Maeda, D. Floreano, and H. Shea, "Stretchable pumps for soft machines," *Nature*, vol. 572, no. 7770, pp. 516–519, Aug. 2019.
- [677] Y. Cheng, K. H. Chan, X.-Q. Wang, T. Ding, T. Li, X. Lu, and G. W. Ho, "Direct-ink-write 3D printing of hydrogels into biomimetic soft robots," *ACS Nano*, vol. 13, no. 11, pp. 13176–13184, Nov. 2019.
- [678] B. Sparrman, S. Kernizan, J. Laucks, S. Tibbits, and C. Guberan, "Liquid printed pneumatics," in *Proc. ACM SIGGRAPH Emerg. Technol.*, New York, NY, USA, 2019, pp. 1–2.
- [679] P. Cai, C. Wang, H. Gao, and X. Chen, "Mechanomaterials: A rational deployment of forces and geometries in programming functional materials," *Adv. Mater.*, vol. 33, no. 46, Nov. 2021, Art. no. 2007977.
- [680] K. K. Kim, I. Ha, M. Kim, J. Choi, P. Won, S. Jo, and S. H. Ko, "A deep-learned skin sensor decoding the epicentral human motions," *Nature Commun.*, vol. 11, no. 1, pp. 1–8, Dec. 2020.
- [681] J.-W. Su, D. Li, Y. Xie, T. Zhou, W. Gao, H. Deng, M. Xin, and J. Lin, "A machine learning workflow for 4D printing: Understand and predict morphing behaviors of printed active structures," *Smart Mater. Struct.*, vol. 30, no. 1, Jan. 2021, Art. no. 015028.
- [682] H. M. Elmoughni, A. F. Yilmaz, K. Ozlem, F. Khalilbayli, L. Cappello, A. T. Atalay, G. Ince, and O. Atalay, "Machine-knitted seamless pneumatic actuators for soft robotics: Design, fabrication, and characterization," *Actuators*, vol. 10, no. 5, p. 94, 2021.
- [683] N. Boddeti, T. Van Truong, V. S. Joseph, T. Stalin, T. Calais, S. Y. Lee, M. L. Dunn, and P. V. Y. Alvarado, "Optimal soft composites for under-actuated soft robots," *Adv. Mater. Technol.*, vol. 6, no. 8, Aug. 2021, Art. no. 2100361.
- [684] P. Abbasi, M. A. Nekoui, M. Zareinejad, P. Abbasi, and Z. Azhang, "Position and force control of a soft pneumatic actuator," *Soft Robot.*, vol. 7, no. 5, pp. 550–563, Oct. 2020.
- [685] A. Shariati, J. Shi, S. Spurgeon, and H. A. Wurdemann, "Dynamic modelling and visco-elastic parameter identification of a fibre-reinforced soft fluidic elastomer manipulator," in *Proc. IEEE/RJS Int. Conf. Intell. Robots Syst. (IROS)*, Sep. 2021, pp. 661–667.
- [686] I. S. Godage, D. T. Branson, E. Guglielmino, and D. G. Caldwell, "Pneumatic muscle actuated continuum arms: Modelling and experimental assessment," in *Proc. IEEE Int. Conf. Robot. Autom.*, May 2012, pp. 4980–4985.
- [687] E. W. Hawkes, C. Majidi, and M. T. Tolley, "Hard questions for soft robotics," *Sci. Robot.*, vol. 6, no. 53, Apr. 2021, Art. no. eabg6049.
- [688] J. J. Monaghan, "Smoothed particle hydrodynamics," *Annu. Rev. Astron. Astrophys.*, vol. 30, no. 1, pp. 543–574, Sep. 1992.
- [689] J. P. Gray, J. J. Monaghan, and R. P. Swift, "SPH elastic dynamics," *Comput. Methods Appl. Mech. Eng.*, vol. 190, nos. 49–50, pp. 6641–6662, Oct. 2001.
- [690] P. W. Cleary, S. M. Harrison, M. D. Sinnott, G. G. Pereira, M. Prakash, R. C. Z. Cohen, M. Rudman, and N. Stokes, "Application of SPH to single and multiphase geophysical, biophysical and industrial fluid flows," *Int. J. Comput. Fluid Dyn.*, vol. 35, nos. 1–2, pp. 22–78, Feb. 2021.
- [691] M. D. Sinnott, P. W. Cleary, J. W. Arkwright, and P. G. Dinning, "Investigating the relationships between peristaltic contraction and fluid transport in the human colon using smoothed particle hydrodynamics," *Comput. Biol. Med.*, vol. 42, no. 4, pp. 492–503, Apr. 2012.
- [692] P. W. Cleary, M. Prakash, J. Ha, and N. Stokes, "Smooth particle hydrodynamics: Status and future potential," *Prog. Comput. Fluid Dyn.*, vol. 7, no. 2, pp. 70–90, 2007.
- [693] S. M. Harrison, R. C. Z. Cohen, P. W. Cleary, S. Barris, and G. Rose, "A coupled biomechanical-smoothed particle hydrodynamics model for predicting the loading on the body during elite platform diving," *Appl. Math. Model.*, vol. 40, nos. 5–6, pp. 3812–3831, Mar. 2016.
- [694] S. M. Harrison, P. W. Cleary, and R. C. Z. Cohen, "Dynamic simulation of flat water kayaking using a coupled biomechanical-smoothed particle hydrodynamics model," *Hum. Movement Sci.*, vol. 64, pp. 252–273, Apr. 2019.
- [695] R. C. Z. Cohen, P. W. Cleary, B. R. Mason, and D. L. Pease, "Studying the effects of asymmetry on freestyle swimming using smoothed particle hydrodynamics," *Comput. Methods Biomechanics Biomed. Eng.*, vol. 23, no. 7, pp. 271–284, May 2020.
- [696] A. Palyanov, S. Khayrulin, and S. D. Larson, "Three-dimensional simulation of the *Caenorhabditis elegans* body and muscle cells in liquid and gel environments for behavioural analysis," *Phil. Trans. Roy. Soc. B, Biol. Sci.*, vol. 373, no. 1758, Oct. 2018, Art. no. 20170376.
- [697] L. Vannozzi, T. Mazzocchi, A. Hasebe, S. Takeoka, T. Fujie, and L. Ricotti, "A coupled FEM-SPH modeling technique to investigate the contractility of biohybrid thin films," *Adv. Biosyst.*, vol. 4, no. 8, Aug. 2020, Art. no. 1900306.



MATHEUS S. XAVIER (Graduate Student Member, IEEE) received the B.S. degree in science and technology and the B.Eng. degree in control and automation engineering from the Federal University of ABC, Brazil, in 2016 and 2017, respectively. He is currently pursuing the Ph.D. degree in electrical engineering with the Precision Mechatronics Laboratory, The University of Newcastle, Australia. He is also an Associate Lecturer at the Department of Electrical and Electronic Engineering, The University of Melbourne, Australia. His research interests include soft robotics, mechatronics design, pneumatic systems, biomedical devices, and nonlinear control.



CHARBEL D. TAWK received the B.E. degree (Hons.) in mechanical engineering from Lebanese American University (LAU), in 2016, and the Ph.D. degree in soft robotics from The University of Wollongong, Australia, and the ARC Centre of Excellence for Electromaterials Science (ACES), in 2019. From 2019 to 2020, he was a Postdoctoral Research Fellow with the University of Wollongong, where he worked on soft prosthetic hands with sensing capabilities, soft wearable devices, and soft dexterous grippers. He is currently an Assistant Professor of mechanical engineering at the University of Wollongong in Dubai. His research interests include soft and smart 3D printed actuators and sensors, soft and smart prosthetic hands, wearable soft robotic devices, and soft human-machine interfaces.



ALI ZOLFAGHARIAN is currently a Senior Lecturer with the School of Engineering, Deakin University, Australia. He has thus far received AUD \$183k research support funds from academic and industrial firms. His recent research outputs in the field of 3D and 4D printing include 69 articles, being editor of two journals, five books, and special issues. He is among the 2% top cited scientists listed by Stanford University and Elsevier (2020), the Alfred Deakin Medallist for Best Doctoral Thesis (2019), and the Alfred Deakin Postdoctoral Fellowship Awardee (2018). He is the Co-Founder of the 4D Printing Society. He is the Co-Editor of the *Smart Materials in Additive Manufacturing* book series published by Elsevier. His 4D Printing and Robotic Materials Laboratory established in Australia, in 2018.



JOSHUA PINSKIER (Member, IEEE) received the Ph.D. degree in mechanical engineering from Monash University, in 2019. He joined the Robotics and Autonomous Systems Group, Material Robotics Team, CSIRO Data61, as a Postdoctoral Fellow, in 2020. He has previously studied mechatronics engineering and commerce at Monash University. His current research interests include soft robotics, topology optimization, computational design, and autonomous manufacturing.



DAVID HOWARD (Member, IEEE) received the B.S. and M.Sc. degrees from the University of Leeds, U.K., in 2005 and 2006, and the Ph.D. degree from the University of the West of England, U.K., in 2011. He has been with the Commonwealth Scientific and Industrial Research Organization, Brisbane, QLD, Australia, since 2013. His research interests include evolutionary algorithms, embodied cognition, soft robotics, and computational design.



TAYLOR YOUNG (Student Member, IEEE) received the B.Eng. degree (Hons.) in electrical engineering from The University of Newcastle, Australia, in 2019, where he is currently pursuing the Ph.D. degree with the Precision Mechatronics Laboratory. His research interests include soft robotics, pneumatic systems, biomedical devices, nonlinear control, and humanoid robots.



JIEWEN LAI (Graduate Student Member, IEEE) received the M.Sc. degree in mechanical and automation engineering from The Chinese University of Hong Kong (CUHK), Hong Kong, in 2017, and the Ph.D. degree in mechanical engineering from The Hong Kong Polytechnic University, in 2021. He is currently a Postdoctoral Fellow with the Department of Electronic Engineering, CUHK. His research interests include soft robots, continuum robots, robot motion planning, and surgical robot systems. He was a recipient of the 2019 IEEE International Conference on Robotics and Biomimetics Best Paper Finalist Award.



SIMON M. HARRISON received the Ph.D. degree in biomechanical engineering from The University of Western Australia, Australia, in 2007. He held a postdoctoral position focused on equine biomechanics at The University of Melbourne, Australia. Since 2011, he has been working as a Research Scientist with the CSIRO Data61's Computational Modeling Group combining mesh-free particle methods with musculoskeletal models in computational

simulations to problems in the areas of human performance, injury, food digestion, and health. Since 2017, he has been leading the Digital Human Initiative, a team with a focus on improving human performance and health using computational simulation and analysis.



YUEN K. YONG (Member, IEEE) received the B.Eng. degree (Hons.) in mechatronic engineering and the Ph.D. degree in mechanical engineering from The University of Adelaide, Australia, in 2001 and 2007, respectively.

Her research interests include miniature robots, biomedical devices, finite-element analysis of smart structures, the design and control of nanopositioning systems, and MEMS. She was a recipient of the 2008 and 2016 IEEE/ASME International

Conference on Advanced Intelligent Mechatronics (AIM) Best Conference Paper Finalist Award, The University of Newcastle Vice-Chancellor's Awards for Research Excellence, and the Pro Vice-Chancellor's Award for Excellence in Research Performance.



MAHDI BODAGHI received the B.Sc., M.Sc., and Ph.D. degrees in mechanical engineering. He is currently a Senior Lecturer with the Department of Engineering, School of Science and Technology, Nottingham Trent University. He has founded and heads the 4D Materials and Printing Laboratory (4DMPL) that hosts a broad portfolio of projects focusing on the electro-thermo-mechanical multiscale behaviors of smart materials, soft robots, and 3D/4D printing technologies. In the recent

12 years, he has been working towards the advancement of state-of-the-art smart materials and additive manufacturing leading him to co-found the 4D Printing Society and to co-edit the book series *Smart Materials in Additive Manufacturing*. His research has led to the publication of over 125 scientific articles in prestigious journals in mechanics, manufacturing, and materials science, as well as the presentation of his work at major international conferences. He has also served as the Chairperson and a member of scientific committees for ten international conferences, as a guest editor for ten journals, as an editorial board member for ten scientific journals, and as a reviewer for over 135 journals. His research awards include the Best Doctoral Thesis Award of 2015, the 2016 CUHK Postdoctoral Fellowship, the Annual Best Paper Award in Mechanics and Material Systems presented by the American Society of Mechanical Engineers, in 2017, the 2018 Horizon Postdoctoral Fellowship Award, and the 2021 *IJPEM-GT* Contribution Award recognized by the Korea Society for Precision Engineering.



ANDREW J. FLEMING (Member, IEEE) received the B.Eng. and Ph.D. degrees in electrical engineering from The University of Newcastle, Australia, in 2000 and 2004, respectively.

He is currently the Director of the Precision Mechatronics Laboratory and the Priority Research Center for Complex Dynamic Systems and Control, The University of Newcastle. He is the coauthor of three books and more than 190 journal and conference papers. He is the

inventor of several patent applications. His research includes soft biomedical devices, micro-robotics, nanofabrication, metrological sensing, and nanopositioning. His research awards include the ATSE Batterham Medal, the IEEE Transactions on Control Systems Technology Outstanding Paper Award, the University of Newcastle Researcher of the Year Award, and the Faculty of Engineering and Built Environment Award for Research Excellence. He received the Newcastle Innovation Rising Star Award for Excellence in Industrial Engagement in 2012.

...